EQUILIBRIUM, KINETICS, AND THERMODYNAMIC STUDIES OF BIOSORPTION OF REACTIVE RED-120 DYE BY BIOMASS OF *Enterobacter* sp. STRAIN MM05

By

YAHUZA SALIHU

Thesis Submitted to the School of Graduate Studies, Universiti Putra Malaysia, in Fulfilment of the Requirement for the Degree of Doctor of Philosophy

August 2023

FBSB 2023 12

DEDICATION

This thesis is dedicated to my late father in the person of Ahmad T. Salihu for his fatherly upbringing, guidance, mentorship, and advice throughout my childhood until his death. How I wish he is alive to witness this remarkable life achievement! May his gentle soul continue to rest in peace and may we meet in Jannatul Firdaus, Ameen ya Hayyu ya Qayyum.

Abstract of thesis presented to Senate of Universiti Putra Malaysia in fulfillment of the requirements for the Degree of Doctor of Philosophy

EQUILIBRIUM, KINETICS, AND THERMODYNAMIC STUDIES OF BIOSORPTION OF REACTIVE RED-120 DYE BY BIOMASS OF *Enterobacter* sp. STRAIN MM05

By

YAHUZA SALIHU

August 2023

Chairman : Professor Mohd Yunus bin Abd. Shukor, PhD
Faculty : Biotechnology and Biomolecular Sciences

Water pollution caused by organic dyes poses a significant global threat to human and marine life. Reactive Red-120 dye is one of the textile dyes that is widely used for dyeing in many countries. The dye and its metabolites have been shown also to be toxic, carcinogenic, and mutagenic. A screening result of several bacteria for the dye sorption has yielded the best isolate, *Enterobacter* sp. strain MM05. Then, the bacterial biomass morphological structure was characterized using Fourier Transform Infrared (FTIR) and Scanning Electron Microscopy (SEM) techniques. The adsorption kinetics, isotherm, and thermodynamic parameters for RR-120 dye adsorption were determined in the study. Twelve (12) different bacterial isolates were screened against RR-120 dye. Of the 12 isolates screened, *Enterobacter* sp. strain MM05 biomass was found to have a higher percentage of dye removal (67.86%). Optimization techniques such as One-factor-at-a-time (OFAT) and Response Surface Methodology (RSM) were used to improve the adsorption process. The OFAT optimum conditions found for the adsorption of the reactive red-120 dye were; 60 min (contact time), 50 ppm (dye concentration), 7.0 (pH), 150 rpm (agitation speed), 1.5ml (adsorbent amount), and 45 °C (temperature). The RSM optimisation provided the most ideal condition for the removal of the RR-120 dye, which increased the percentage removal of the dye to 73%. The models' R^2 was determined to be 0.9563. Different non-linear mathematical models were used to study the adsorption kinetics of the bacterial biomass on RR-120 dye. The dye exhibited a pseudo-second-order kinetics reaction with the lowest *AICc* value of -39.09 and $adjR^2$ that is closest to 1.0 (0.998). Langmuir, Henry Freundlich, BET, Toth, Sips, Fritz-Schlunder IV, and Fritz-Schlunder V were the best-fitting mathematical models for the RR-120 dye in the isotherm studies. Except for the Henry model, all of the nine (8) isotherm models tested on the RR-120 dye provided significant fitting results. The Feundlich model was found to be the best isotherm model after statistical analysis using the corrected Akaike Information Criterion (*AICc*), root-mean-square error (*RMSE*), adjusted coefficient of

determination (*adjR*^{2}), accuracy factor (*AF*), and bias factor (*BF*). The model had the lowest *AICc* value of -51.54. Thermodynamic parameters for the adsorption of reactive red-120 dye were studied at different temperatures (30, 35, 40, 45, and 50 °C), starting with the rate constants derived from the pseudo-second-order kinetic (k_2) and moving on to the isotherm constant (K_L) determined from the Langmuir model. By converting the K_L constant, the dimensionless thermodynamic constant K_C was obtained. The thermodynamic parameters such as standard Gibbs free energy (*Δ*G), enthalpy (*ΔH*), and entropy (*ΔS*) were determined using non-linear regression of the van't Hoff plot. The RR-120 dye adsorption thermodynamic results showed that the reaction was endothermic having the positive *ΔH*° value of 52.91 kJ/mol. However, the result equally showed that the adsorption process was spontaneous and feasible having negative Gibb's free energy. Furthermore, the positive value of the *ΔS*° (301.30 *kJ/mol/K*) indicated the affinity of the bacterial biomass (adsorbent) toward an adsorbate (RR-120 dye). In other word, the positive *ΔS*° value suggested an increased randomness at the solid/liquid interface with the structural changes in the adsorbent and adsorbate. The presence of many functional groups, including hydroxyl, alkyl, and carbonyl, which are essential in the process of dye adsorption, particularly reactive red-120 dye, is revealed by Fourier transform infrared (FTIR) analysis. The heterogeneous, non-porous, smooth, and tightly packed surfaces following the dye adsorption of RR-120 dye are revealed by the analysis of the SEM data on the biomass of *Enterobacter* sp. strain MM05. This finding has concluded that, the biomass of *Enterobacter* sp. strain MM05 is essential in the adsorption of reactive red-120 dye and could be employed in bioremediation processes especially in the removal of azo dyes from the environment.

Keyword: Biosorption, *Enterobacter*, Kinetics, Reactive Red-120, Thermodynamic

SDG: GOAL 3: Good Health and Well-Being, GOAL 6: Clean Water and Sanitation

Abstrak tesis yang dikemukakan kepada Senat Universiti Putra Malaysia sebagai memenuhi keperluan untuk ijazah Doktor Falsafah

KAJIAN KESEIMBANGAN, KINETIK DAN TERMODINAMIK *BIOSORPTION OF REACTIVE RED-120 DYE* OLEH BIOMAS *Enterobacter* sp. *STRAIN MM05*

Oleh

YAHUZA SALIHU

Ogos 2023

Pengerusi : Profesor Mohd Yunus bin Abd Shukor, PhD
Fakulti : Bioteknologi dan Sains Biomolekul

Pencemaran air yang disebabkan oleh pewarna organik menimbulkan ancaman global yang ketara kepada kehidupan manusia dan marin. Pewarna Reaktif Red-120 adalah salah satu pewarna tekstil yang digunakan secara meluas untuk pencelupan di banyak negara. Pewarna dan metabolitnya telah ditunjukkan juga sebagai toksik, karsinogenik, dan mutagenik. Hasil saringan beberapa bakteria untuk penyerapan pewarna telah menghasilkan isolat terbaik, *Enterobacter* sp. terikan MM05. Kemudian, struktur morfologi biojisim bakteria dicirikan menggunakan teknik Fourier Transform Infrared (FTIR) dan Scanning Electron Microscopy (SEM). Kinetik penjerapan, isoterma, dan parameter termodinamik untuk penjerapan pewarna RR-120 telah ditentukan dalam kajian ini. Dua belas (12) pencilan bakteria berbeza telah disaring terhadap pewarna RR-120. Daripada 12 isolat yang disaring, *Enterobacter* sp. biojisim MM05 terikan didapati mempunyai peratusan penyingkiran pewarna yang lebih tinggi (67.86%). Teknik pengoptimuman seperti One-factor-at-a-time (OFAT) dan Response Surface Methodology (RSM) telah digunakan untuk menambah baik proses penjerapan. Keadaan optimum OFAT yang ditemui untuk penjerapan pewarna merah-120 reaktif ialah; 60 min (masa sentuhan), 50 ppm (kepekatan pewarna), 7.0 (pH), 150 rpm (kelajuan pengadukan), 1.5ml (jumlah penjerap), dan 45 °C (suhu). Pengoptimuman RSM menyediakan keadaan paling ideal untuk penyingkiran pewarna RR-120, yang meningkatkan peratusan penyingkiran pewarna kepada 73%. R2 model telah ditentukan untuk menjadi 0.9563. Model matematik bukan linear yang berbeza digunakan untuk mengkaji kinetik penjerapan biojisim bakteria pada pewarna RR-120. Pewarna mempamerkan tindak balas kinetik tertib pseudo kedua dengan nilai AICc terendah -39.09 dan adjR2 yang paling hampir kepada 1.0 (0.998). Langmuir, Henry Freundlich, BET, Toth, Sips, Fritz-Schlunder IV dan Fritz-Schlunder V ialah model matematik yang paling sesuai untuk pewarna RR-120 dalam kajian isoterm. Kecuali model Henry, kesemua sembilan (8) model isoterma yang diuji pada pewarna RR-120 memberikan hasil yang sesuai. Model Feundlich didapati

sebagai model isoterma terbaik selepas analisis statistik menggunakan Kriteria Maklumat Akaike (AICc) yang diperbetulkan, ralat punca-min kuasa dua (RMSE), pekali penentuan terlaras (adjR2), faktor ketepatan (AF), dan bias. faktor (BF). Model tersebut mempunyai nilai AICc terendah iaitu -51.54. Parameter termodinamik untuk penjerapan pewarna merah-120 reaktif telah dikaji pada suhu yang berbeza (30, 35, 40, 45, dan 50 °C), bermula dengan pemalar kadar yang diperoleh daripada kinetik tertib pseudo kedua (k2) dan bergerak. kepada pemalar isoterma (KL) yang ditentukan daripada model Langmuir. Dengan menukar pemalar KL, pemalar termodinamik tak berdimensi KC diperolehi. Parameter termodinamik seperti tenaga bebas Gibbs standard (ΔG), entalpi (ΔH), dan entropi (ΔS) ditentukan menggunakan regresi bukan linear plot van't Hoff. Keputusan termodinamik penjerapan pewarna RR-120 menunjukkan bahawa tindak balas adalah endotermik yang mempunyai nilai ΔH° positif 52.91 kJ/mol. Walau bagaimanapun, keputusan sama menunjukkan bahawa proses penjerapan adalah spontan dan boleh dilaksanakan mempunyai tenaga bebas Gibb negatif. Tambahan pula, nilai positif ΔS° (301.30 kJ/mol/K) menunjukkan pertalian biojisim bakteria (penjerap) terhadap penjerap (pewarna RR-120). Dalam erti kata lain, nilai ΔS° positif mencadangkan peningkatan rawak pada antara muka pepejal/cecair dengan perubahan struktur dalam penjerap dan penjerap. Kehadiran banyak kumpulan berfungsi, termasuk hidroksil, alkil, dan karbonil, yang penting dalam proses penjerapan pewarna, khususnya pewarna merah-120 reaktif, didedahkan oleh analisis Fourier transform inframerah (FTIR). Permukaan heterogen, tidak berliang, licin dan padat berikutan penjerapan pewarna pewarna RR-120 didedahkan melalui analisis data SEM pada biojisim *Enterobacter* sp. terikan MM05. Dapatan ini telah membuat kesimpulan bahawa, biojisim *Enterobacter* sp. terikan MM05 adalah penting dalam penjerapan pewarna merah-120 reaktif dan boleh digunakan dalam proses biopemulihan terutamanya dalam penyingkiran pewarna azo daripada persekitaran.

Kata kunci: Biosorpsi, Enterobacter, Kinetik, Reaktif Merah-120, Termodinamik

SDG: MATLAMAT 3: Kesihatan dan Kesejahteraan yang Baik, MATLAMAT 6: Air Bersih dan Sanitasi

ACKNOWLEDGEMENTS

All praise and gratitude go to Almighty Allah for His many blessings and mercies upon us. This study would not have been feasible without the contributions of a significant number of people, whose names may not be included in this list. With heartfelt gratitude and sincere appreciation, I hereby acknowledge and thank them for their efforts towards the accomplishment of this great task. However, I would like to express my deepest gratitude and appreciation to the following individuals and organizations.

My heartfelt gratitude goes to my supervisor in person of Prof. Dr. Mohd. Yunus Abd. Shukor, for his support, patience, fatherly advice, exceptional mentorship, and guidance throughout the period of my Ph.D. studies and beyond. Also, to my co-supervisors, Dr. Nur Adeela Yasid and Dr. Ahmad Razi Othman for their constructive criticism, scrutiny of the work, fantastic contributions, and guidance. My supervisory team is superb!

I would like to extend my gratitude to my family members which include; my lovely wife (Amina Ibrahim Hassan), my lovely doughter (Maryam Salihu Ahmad), my lovely mother (Hajiya Maryam Ibrahim), my only lovely elder sister (Yaya 'Yarhajja) and my lovely uncle (Yahuza Salihu) for their continuous love, support and prayers throughout my life.

Furthermore, my appreciation goes to the Tertiary Education Trust Fund (Tetfund) Nigeria for the sponsorship of this program. At this juncture, I appreciate the management of Federal University Dutse particularly our indefatigable Vice-Chancellor (Prof. Abdulkarim Sabo Muhammad) for nominating me to enjoy the Tetfund scholarship.

Finally, it is my great pleasure and gratitude I acknowledge the support, guidance and contributions of my laboratory members. On this note, I will like to thank Dr. Motharasan Monagaran for his tireless efforts and kind assistance during the practical.

This thesis was submitted to the Senate of Universiti Putra Malaysia and has been accepted as fulfillment of the requirements for the award of Doctor of Philosophy. The members of the Supervisory Committee were as follows:

Mohd Yunus bin Abd. Shukor, PhD
Professor
Faculty of Biotechnology and Biomolecular Sciences,
Universiti Putra Malaysia
(Chairman)

Nur Adeela binti Yasid, PhD
Senior Lecturer
Faculty Biotechnology and Biomolecular Sciences
Universiti Putra Malaysia
(Member)

Ahmad Razi bin Othman, PhD
Senior Lecturer
Faculty of Engineering and Built Environment
Universiti Kebangsaan Malaysia
(Member)

ZALILAH MOHD SHARIFF, PhD
Professor and Dean
School of Graduate Studies
Universiti Putra Malaysia

Date: 13 March 2025

TABLE OF CONTENTS

LIST OF TABLES

LIST OF FIGURES

LIST OF NOMENCLATURE

A_T	Temkin isotherm equilibrium binding consant
B	Heat of sorption constant
b_B	Baudu constant
b_H	Hill constant
b_K	Khan constant
b_T	Temkin isotherm constant
b_T	Toth equilibrium constant
b_U	Unilin constant
b_{VS}	Vieth-Sladek constant
C_e	Equilibrium adsorbate
C_o	Adsorbate initial concentration
E	mean free energy
k_1	Pseudo-first model constant rate
K_2	energetic constant of the interaction between adsorbed molecules
k_2	Pseudo-second model constant rate
K_{BS}	Brouers-Sotolongo constant
K_D	Dubinin – Radushkevich isotherm constant
K_{DR}	Dubinin-Radushkevich isotherm
K_E	Elovich equilibrium constant
K_F	Freundlich isotherm constant
K_{FS}	Marczewski-Jaroniec isotherm constant
K_H	Henry isotherm constant
K_L/b_L	Langmuir isotherm constant
K_{MJ}	Marczewski-Jaroniec constant

K_{RP}	Radke-Prausnitz constant
q_e	adsorption capacity at equilibrium
q_{mB}	Baudu isotherm adsorption capacity at equilibrium
q_{mBET}	BET isotherm adsorption capacity at equilibrium
q_{mBS}	Brouers-Sotolongo isotherm adsorption capacity
q_{mDR}	theoretical isotherms saturation capacity
q_{mFS}	Fritz-Schlunder-III isotherm adsorption capacity at equilibrium
q_{mFS}	Fritz-Schlunder-IV isotherm adsorption capacity at equilibrium
q_{mFS5}	Fritz-Schlunder-V isotherm adsorption capacity at equilibrium
q_{mK}	Khan isotherm adsorption capacity at equilibrium
q_{mL}	adsorption capacity at equilibrium for Langmuir
q_{mRP}	Radke-Prausnitz isotherm adsorption capacity at equilibrium
q_{mS}	Sips isotherm adsorption capacity at equilibrium
q_{mT}	Toth isotherm adsorption capacity at equilibrium
q_{mU}	Unilin isotherm adsorption capacity at equilibrium
q_{mVS}	Vieth-Sladek isotherm adsorption capacity at equilibrium
q_t	adsorption capacity at time *t*
R	Universal gas constant
R_L	Equilibrium parameter of Langmuir
ΔG	Gibbs free energy change
ΔH	Enthalpy change
ΔS	Entropy change
E	Polanyi potential

LIST OF ABBREVIATONS

Abs	Absorbance
ANOVA	Analysis of variance
BBE	Biomonitoring, Bioremediation and Ecotoxicology Laboratory
BOD	Biological oxygen demand
C.I	Colour index
$CaCl_2$	Calcium chloride
CO_3	Carbonate
COD	Chemical oxygen demand
DB	Disperse blue
dH_2O	Distilled water
DNA	Deoxyribonucleic acid
DO	Disperse orange
DOE	Department of Environment
DV	Disperse violet
EPA	United States Environmental Protection Agency
Eq	Equation
EQA	Environmental Quality Act
et al	and friends
FTIR	Fourier transform-Infrared
H_2O_2	Hydrogen Peroxide
J	Joule
K	Kelvin
K	Potassium
N	Normality

nm	Nanometer
OFAT	One factor at a time
PBD	Plakett Burman Design
ppm	Part per million
RR-120	Reactive red-120
RSM	Response surface methodology
SEM	Scanning electron microscope
SO_3H	Sulfonic acid
SS	Suspended solid
STDEV	Standard deviation
T	Temperature
x g	Gravitational force

CHAPTER 1

INTRODUCTION

1.1 Research Background

Biosorption can be defined as the process through which substances are removed from the solution by biological material. Such substances can be organic, inorganic, gaseous, soluble, or insoluble. It is a physico-chemical process that includes mechanisms such as absorption, adsorption, ion exchange, surface complexation, and precipitation. It is an attribute exhibited by both living and dead biomass (Gadd, 2009). In contrast to biodegradation, biosorption is considered and proven to be a fast and easy to operate method for the removal and detection of pollutants from water, which has efficiency and the possibility of contaminant recovery.

Textile, paper, paint, printing, and cosmetics industries discharge massive amount of wastewater containing synthetic dyes. Most of these dyes are poisonous, carcinogenic, teratogenic, and often cause allergic dermatitis and mutations. They also impart color to wastewater streams, thereby preventing sunlight penetration, eventually decreasing the photosynthesis of aquatic plants (Naskar & Majumder, 2017). Dye effluents originating from textile and dyestuff industries are difficult to treat because of their high alkalinity, Biological Oxygen Demand (BOD), Chemical Oxygen Demand (COD), and total dissolved solids. As a result of the environmental hazards associated with the release of harmful dye effluents, there is an increase in the legislation and regulations of dye usage imposed by regulatory agencies to mitigate its adverse effects on the environment (Srinivasan & Viraraghavan, 2010).

Water pollution caused by organic dyes poses a significant global threat to human and marine life, not only to the climate. These compounds or their metabolites have been shown to also be toxic, carcinogenic, and mutagenic. In addition to their toxic, carcinogenic, and non-biodegradability properties, even the low concentration of dyes (< 50 ppm) found in the water environment is extremely undesirable due to their detrimental effects on the water ecosystem and interference with the photosynthetic activities of aquatic organisms (Baldikova et al., 2019).

A reactive dye can react directly with the fabric, which means that a chemical reaction occurs between the dyes and the molecules of the fabric, effectively incorporating the dyes into the fabric. Reactive Red 120 (RR 120) and Reactive Blue Bezaktiv 150 (RBB 150) are the oldest synthetic dyes that are widely used in many industrial sectors, particularly in the dyeing of clothes and shoes. On the other hand, dyeing procedures that use reactive dyes generate many unfixed dyes, and the wastewater generated as a by-product of this process may impact

the ecosystem through effluent discharges. According to surveys, about 20% of total global production is lost in the dyeing process and is discarded in wastewater (Navaei *et al.,* 2019).

The application of biological processes for the treatment of coloured wastewater has not yet been completely developed. Adsorption is rapidly gaining popularity as a method of treating aqueous wastewater treatment technologies. The most powerful and frequently used adsorbent is activated carbon. Its high costs especially in developed countries prevented its application which necessitated researchers to look for alternative techniques particularly the employment of microorganisms (including their biomass) because of their abundance and low-cost operations and applications (Karthik et al., 2016b).

1.2 Problem Statement

In the 21st century, water quality issues are a major challenge for humanity. Various industries produce large amounts of dye-contaminated aqueous effluent. Most of these dyes are toxic, causing allergies and skin irritation, as well as mutagenic and/or carcinogenic (Fathi & Asfaram, 2011). Because of the release of undesirable dye effluents, the textile industry is responsible for one of the world's major environmental pollution issues (Yaseen & Scholz, 2019). Colour is typically the first contaminant detected in wastewater since even a small amount of synthetic dyes in water (one part per million) has a significant impact on the aesthetic value, transparency, and gas solubility of water bodies (Pereira & Alves, 2012). The color associated with textile dyes not only causes aesthetic damage to water bodies but also prevents light from passing through, resulting in a reduction in the rate of photosynthesis and dissolved oxygen levels, affecting the entire aquatic biota (Lellis *et al*., 2019).

1.3 Significance of the study

The efficiency of biosorption technology in lowering dye concentrations to extremely low levels, as well as the utilization of inexpensive biosorbent materials like bacterial biomass, are two of its major benefits over alternative methods of sorption like chemical or physical (Pereira & Alves, 2012). Amongst the sorption methods, the biological method is proven to be widely used because of its ease, cheaper and eco-friendly. Because biomass is readily available in large quantities at a low cost, it is increasingly being used for wastewater treatment. Microbial biomass is one of the low-cost and efficient biosorbents of dye removal from solutions (Kumar *et al*., 2015).

1.4 Research Hypothesis

In this study, bacterial biomass (*Enterobacter* sp. MM05) was used as a novel eco-friendly biosorbent in the biosorption of reactive red-120 dye. The

employment of microbial biomass in the removal of textile dyes was reported severally in the literature. Response Surface Methodology (RSM) as an experimental design method has been shown to significantly improve adsorption over other methods such as One-Factor-at-a-Time (OFAT) and has been acknowledged by so many researchers. Therefore, this study is not an exception as it has been studied and reported. Usually, kinetic models such as pseudo-first-order, pseudo-second-order, and Elovich are used in the determination of the adsorption mechanism. Similarly, isotherm models like Henry, Langmuir, Freundlich, Brunauer-Emmett-Teller (BET), etc. are used in the characterization of the heterogeneity of adsorbent surfaces which can be mono or multilayers. Therefore, kinetic models were studied and reported in this study. Non-linear regression in place of linear regression was used in the determination of kinetic and isotherm models because of its unbiased nature and provision of smaller residuals. The use of non-linearized regression over linearized one has been reported severally in the literature. The best models can predict the maximum adsorption capacity (qe) whereas the rate constant values can be employed in thermodynamic studies to obtain the values of Gibb's free energy (ΔG), enthalpy (ΔH), and entrofy (ΔS) which are used to describe the nature of adsorption.
Based on the above hypothesis, this study is aimed at screening the biomass of *Enterobacter* sp. MM05 for the biosorption of reactive red-120 dye and the aim could be achieved through the following objectives:

1. To screen the bacterial isolate and biomass for reactive red-120 biosorption

2. To optimize the biosorption conditions using One-Factor-At-a-Time (**OFAT)** and Response Surface Methodology (**RSM).**

3. To characterize the bacterial biomass using FTIR and SEM.

4. To determine the isotherms and **kinetics** of biosorption.

5. To evaluate the effect of thermodynamic parameters on dye biosorption.

CHAPTER 2

LITERATURE REVIEW

2.1 Dyes

Dyes are color-inducing compounds that are widely used in the textile, food, cosmetic, handmade paper, plastic, pharmaceutical, and photographic industries (Chaudhary, 2020). The global colorant market is expected to grow as a result of increased coloring needs in a variety of end-use industries ranging from textiles to coatings. Furthermore, rising demand for high-performance colorants, as well as increased consumer preference for eco-friendly products, are expected to drive global industry demand over the forecast period (Gürses *et al*., 2016a). Color is an important component of our world. They are ubiquitous and serve both functional and aesthetic purposes. Every material is colored, and the molecules that make up that material are very selective about which photon energy they will absorb and which they will not. A red-absorbing object does not appear red. Colors that are not absorbed are visible. The color seen is said to be the complementary color to the color absorbed. For example, if the absorbed color is blue, the observed color will be orange (Chaudhary, 2020).

Dyes have great colorant qualities, are easy to process, and have outstanding color strength, but they have poor solvent and heat stability, as well as low durability and migration. The electrical characteristics of the dye molecule's chromophore determine what color is imparted to the solution. They are utilized to color substrates that are attracted to them (Gürses *et al*., 2016b). The absorption of radiation in the UV and visible regions causes electronic excitation, which causes an electron to shift to a higher energy level. A covalently unsaturated group called Chromophore is responsible for this electromagnetic radiation absorption. Depending on whether or not it absorbs light in the visible region, it may or may not impart color to the substrate (Ed, 2014). Another group that is covalently attached to this molecule is the Auxochrome, which causes a change in both the wavelength and the intensity of the absorption maximum. They are also known as color-enhancing groups because they increase the values of λmax and ϵmax by extending the conjugation by resonance (Gürses *et al*., 2016b).

2.1.1 Classification of Dyes

Because of the remarkable increase in the type and number of dyes, textile dye classification has become critical. These dyes can be classified structurally using the following functional groups: anthraquinone, azo, phthalocyanine, sulfur, indigo, nitro, nitroso, and so on, based on their chemical structures. Table 2.1 shows dyes classification, its substrate and mode of application. Another classification was based on how these colors were applied on a large scale

(Benkhaya *et al*., 2020). Textile dyeing has been a part of human culture for over 4,000 years. Except for the last 150 years, all dyes were derived from natural sources (Ferreira *et al*., 2004). The discovery of Mauveine by William Henry Perkin in 1856, while seeking to find a way to synthesize Quinine, a medication used to treat Malaria, the scourge of many tropical countries, ushered in a major revolution in dyes (Abel, 2012). The table below (**Table 2.1**) shows some classsifications of dyes.

Table 2.1: Dyes classification

Class of Dye	Substrates	Mode of Application	Chemical type and Examples
Reactive	Silk, wool, cotton, and nylon	Under the effect of heat and an alkaline pH, the reactive site on the dye interacts with the functional group on the fiber to covalently bind the dye.	An azo dye. Examples are Reactive red-120 dye and Reactive red-198.
Acidic	Nylon, silk, paper, wool, inks, and leather	With the amount of acidity dependent on the specific dye qualities, the dyes are often applied in acidic circumstances (using formic or acetic acid).	An azo dye including premetallized such anthraquinone, triphenylmethane, azine, xanthene, nitro, and nitroso. Example is acid blue-25 dye.
Basic	Polyacrylonitrile, nylon, paper, polyester, and inks	Because basic dyes have weak migratory qualities at the boil, they are frequently applied with retarders. The high substantivity of the dye for the substrate and the rapid increase in diffusion at high temperatures are to account for this poor migration.	Has a cyanine chemical structure. Example is basic blue-24 dye.
Direct	Rayon, paper, cotton, nylon, and rather.	Applied from additional electrolyte baths with a neutral or slightly alkaline pH.	Azo, stilbene, phthalocyanine, and oxanine. Example is Direct red-2 dye.
Disperse	Plastics, acetate, acrylic, polyester, and polyamide	These dyes are often non-ionic in nature, hardly soluble in water, and applied to hydrophobic fibers from an aqueous dispersion.	Styryl, Nitro, Azo, Anthraquinone, Nitro, and Benzodifuranone. Example is disperse red-8 dye
Vat	Wool, rayon and cotton	Colors that cannot be dissolved in water are first dissolved in sodium hydroxide, then they are drained on fiber and reoxidized.	Indigo and anthraquinone, including polycyclic quinines. Examples are vat blue-5 and acid blue-74 dyes.
Sulfur	Rayon and cotton	Sulfur dyes have specific uses in the dyeing of silk, paper, and some types of leathers, although they are primarily employed to color textile cellulosic materials or mixtures of cellulosic fibers and synthetic fibers.	Uncertain chemical structure. Examples are sulphur black and Leuco sulphur black-1 dyes

(adapted from Ismail & Sakai, 2022)

2.1.2 Reactive Red-120 Dye

Reactive dyes are formed by combining azo-based chromophores with various reactive groups, such as vinyl sulfone, chlorotriazine, trichloropyrimidine, and difluoro chloropyrimidine. They can react directly with fabric, which means that a chemical reaction occurs between the dyes and the fabric molecules, effectively incorporating the dyes into the fabric (Navaei *et al*., 2019) Because of their simple dyeing procedures and good stability during the washing process, reactive azo dyes are widely used in textile dyeing processes. Approximately 20–40% of these dyes are still present in the effluent. Due to their reactivity, toxicity, and stability, discharges of such wastewater into receiving waters can become hazardous to aquatic organisms. Azo dyes are the most dangerous xenobiotic pollutants, causing mutations and cancer (Çelekli *et al*., 2012).

Figure 2.1 shows the structure of Reactive Red-120 (RR-120), one of the azo dyes that is commonly used in the textile industry and poses a potential threat to the aquatic environment because of its poor biodegradability (Bazrafshan *et al*., 2013).

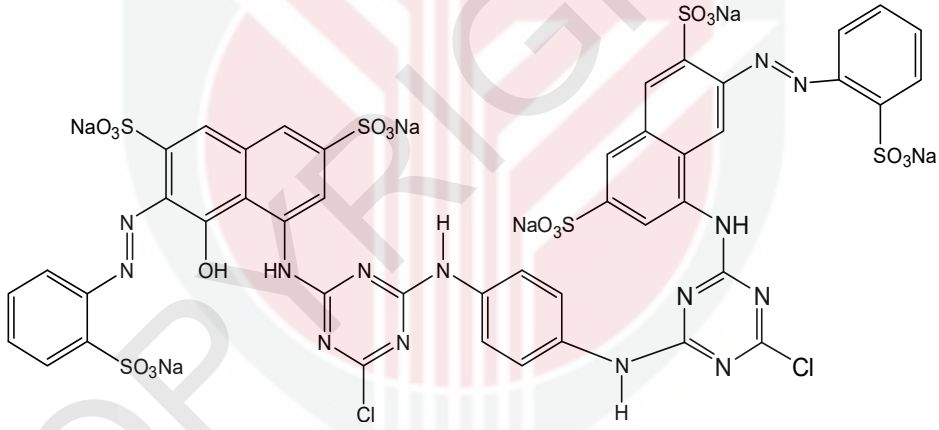

Figure 2.1: Structure of Reactive red-120 Dye (An Azo Dye)

2.2 Global Incidences of Dye Pollution

Dyes are substances that, when applied to a substrate, provide color by altering, at least temporarily, the crystal structure of the colored substances. Such coloring substances are widely used in the textile, pharmaceutical, food, cosmetics, plastics, photographic, and paper industries. The dye manufacturing industry is a small part of the overall chemical industry. (Manzoor & Sharma, 2019). The global production of dyes is nearly 800,000 tons per annum.

A significant portion of the dye is lost to the wastewater stream during the coloration process because it does not adhere to the cloth. During the dyeing process, approximately 10-15% of dyes are released into the air, rendering the effluent highly colored and aesthetically undesirable. Color has a major impact on how people think of water quality. As a result, the removal of color from wastewater is often prioritized over the removal of soluble colorless organic substances. A case of dye pollution occurred in the year 2011 in China when the Jian River turned red as a result of an illegal dye dump from a local chemical plant. Residents and farmers reported the health problems among humans and the death of aquatic organisms such as fishes which were all attributed to dye pollution. An average t-shirt uses 16-20 liters of water during the dyeing process, implying that the global textile industry discharges 40,000 – 50,000 tons of dye into the water system every year. The absorption and reflection of sunlight entering the water is a major environmental problem with dyes. Light absorption reduces algae's photosynthetic activity, which has a significant impact on the food chain because algae are at the bottom of the food chain, impacting all organisms above them. One of the key factors that marine life fails in areas where dyes are discharged is a shortage of algae, but another is the toxicity of the dyes themselves, Trusted Cloth (T.C., 2016).

2.3 Toxicity of Dyes

Dyes are organic compounds that are soluble and are classified into direct, reactive, basic, or acidic (Lellis et al., 2019). Their high solubility in water makes them very difficult to be removed through conventional methods. One of the characteristics of dyes is their ability to impart colors to a given substrate due to the presence of chromophoric groups in their molecular structures (Hassan & Carr, 2018).

The color associated with dyes not only leads to aesthetic damage to the water bodies but prevents the penetration of light through water thereby causing a reduction in the rate of photosynthesis and dissolved oxygen level (Zhou et al., 2013). Moreover, textile dyes act as carcinogenic and mutagenic agents which persist as environmental pollutants and cross the food chains resulting in biomagnification, such that organisms at higher trophic levels show higher levels of contamination compared to their prey (Lellis *et al*., 2019).

Textile dyes and many industrial pollutants are toxic and potentially carcinogenic which cause environmental degradation and various disease in humans and animals (Malik & Grohmann, 2012). The dyes bioaccumulate in sediments and soil and are transported to public water supply systems, due to their susceptibility to being recalcitrant in aerobic environments, particularly in conventional treatment plants (Hassan & Carr, 2018).

The xenobiotic and recalcitrant nature of the dyes harm ecosystem structure and function. Long-term exposures, in particular, have far-reaching consequences for aquatic biota and human health (Benkhaya, *et al.*, 2020).

2.4 Methods of Dye Removal

Nowadays, the public has become more concerned about environmental protection, and general awareness has grown about the potential negative effects of industrial effluents contaminated with various pollutants, including dyes, on the environment. Dyes are primarily used in the textile, food, and pharmaceutical industries, as well as cosmetics, plastics, photographic, and paper industries (Karthik *et al*., 2014). Although industrialization is the most efficient means of achieving economic expansion, it directly or indirectly impacts human health by releasing pollutants into water bodies. Unfortunately, the majority of dyes end up in traditional wastewater treatment processes. Textile plants are the most polluting industrial sector, even though dye effluents seep into water bodies from a variety of sources. Some dyes are highly toxic, mutagenic, and carcinogenic, and they also reduce light penetration and photosynthetic activity, resulting in oxygen deficiency and limiting downstream beneficial uses such as recreation, drinking water, and irrigation (Alqaragully, 2014).

Environmental regulations require businesses to remove the colour from dye-containing effluents before discharging them into the water bodies. Dye removal technologies are classified into three types: physical methods, chemical, and biological (Mohan *et al*., 2004).

2.4.1 Physical method of Dye Removal

The most commonly used physical methods of dye removal are membrane filtration, adsorption, irradiation, electro coagulation, ion exchange, and coagulation-flocculation (Warade *et al*., 2016).

The membrane filtration method can clarify, concentrate, and, most importantly, continuously separate dye from effluent. It has some unique characteristics that other methods do not have, such as resistance to temperature, an adverse chemical environment, and microbial attack. This filtration process is suitable for water recycling within a textile dye plant if the effluent includes low dye concentrations, but it is unable to remove dissolved solid content, making water recycling a challenge. The concentrated residue left over after separation causes disposal difficulties, as well as high capital costs and the possibility of clogging, and membrane replacement is one of its drawbacks. (Warade *et al*., 2016).

Adsorption yields a high-quality product and is a cost-effective process. Its ability to remove almost all impurities with minimal side effects explains its widespread use in tertiary treatment and polishing stages (Choy *et al*., 1999). Many researchers have investigated the use of low-cost materials such as sawdust, waste orange peel, bagasse fly ash, rice husk ash, banana pith, bottom ash, deoiled soya, rice husk, and kaolin. Other researchers used low-cost adsorbents

like bentonite clay, neem leaf powder, powdered activated sludge, perlite, powdered peanut hull, zeolite, and bamboo dust (Warade *et al*., 2016).

A sufficient amount of dissolved oxygen is required in the irradiation method to effectively break down organic substances by radiation. Because dissolved oxygen is rapidly depleted, a constant and adequate supply is required. This has an impact on the cost. A dual-tube bubbling reactor can be used to treat dye-containing effluent. This method demonstrated that some dyes and phenolic molecules can only be effectively oxidized at the laboratory scale (Hosono *et al*., 1993). The possibility of using gamma rays to degrade or decolorize reactive dyes in water was investigated by Olpan and Güven (2002).

The electro coagulation method employs a direct current to generate sacrificial electrode ions, which remove undesirable contaminants via chemical reactions and precipitation or by causing colloidal materials to coalesce and then be removed through the use of electrolytic floatation. In addition to being more shear resistant and easily filterable, electro coagulated sludge contains less bound water (Warade *et al*., 2016).

Ion exchange has not been frequently employed to treat dye-containing effluents, owing to the misconception that ion exchangers cannot handle a wide spectrum of dyes (Slokar & Majcen Le Marechal, 1998). The wastewater is passed through the ion exchange resin until all of the available exchange sites are saturated. This method can remove both cation and anion dyes from dye-containing effluent. The benefits of this method include no adsorbent loss during regeneration, solvent reclamation after use, and the removal of soluble dyes. The cost of this method is its major disadvantage. Organic solvents are expensive, and the ion exchange method is ineffective for dispersing dyes (Warade *et al*., 2016).

One of the most widely used conventional treatment methods is coagulation-flocculation. Polyelectrolytes are commonly utilized as cationic, anionic, and non-anionic coagulant aids. Polyelectrolyte sludge is typically compact and easy to dewater for subsequent treatment and disposal. It entails the addition of ferrous sulfate and ferric chloride, which results in the excellent removal of direct dyes from wastewaters. The ideal coagulant concentration is determined by the dye's static charge in the solute, and removing the coagulation sludge is a challenge (Nigam *et al*., 2000). Large amounts of sludge are produced, which results in significant disposal expenses (Gähr *et al*, 1994).

2.4.2 Chemical Method of Dye Removal

Advanced Oxidation process: One of the traditional methods used for de-colorization is the advanced oxidation method. It is based on a mechanism involving the generation of hydroxyl radicals (as oxidizing agents), which when

attacked by chromogenic groups produces organic peroxide radicals, which eventually transform into CO_2, H_20, and inorganic salts (Antoniadis *et al*., 2010).

The Use of Hydrogen Peroxide H_20_2: Because of its commercial availability and low cost, hydrogen peroxide has risen to prominence among oxidizing agents. It can be used directly in the oxidation process or conjunction with catalysts or UV radiation (Galindo *et al*., 2000; Lu, 2000). Hydrogen peroxide readily reacts with hydrated electrons from the water radiolysis reaction, resulting in the formation of the hydroxide radical. The degree of degradation caused by the addition of H_2O_2 increases as the amount of hydroxide radical formed degrades the dye chromophore more efficiently (Salem et al., 2014). However, significant disadvantages to its utilization have been discovered, such as its inability to oxidize some organic contaminants. It has been discovered that the removal efficiency for Methylene Blue dye with this reagent is 86% (Zhang et al., 2017). According to reports, the hydrogen peroxide reagent is also effective at removing Rhodamine –B dye with a 99% efficiency (Thao *et al*., 2017).

The use of Fenton's Reagent: Fenton's reagent is a mixture of hydrogen peroxide and ferrous ion (Fe^{+2}). It is one of the advanced oxidation processes that has been investigated for the removal of various dyes (Chen et al., 2002; Khataee et al., 2009; Ma et al., 2005). The efficiency of this process is determined by the amount of hydrogen peroxide and ferrous ions present, as well as the pH factor. The oxidation method employing Fenton's reagent completely degrades the contaminants, breaking them down into harmless compounds such as carbon (iv) oxide, water, and inorganic salts (Masomboon *et al*., 2011). Furthermore, this method is simple to implement, completely reacts with organic compounds, is a low-cost treatment, and does not generate any toxic compounds during the reaction. However, its applications have been limited as excess ferric hydroxide sludge generation remains a disposal problem (Neyens & Baeyens, 2003).

Ozonization process: Ozone can oxidise chlorinated hydrocarbons, phenols, and some other hydrocarbons. There are two steps in the reaction mechanism. Step 1 involves a reaction that takes place at a pH of 5-6, where ozone is present in the form of O_3 and selectively reacts with the double bonds of dye molecules. Step 2 involves a reaction that occurs at a higher pH value, i.e. above 8 pH, where ozone readily decomposes, generating hydroxyl radicals that react non-selectively with organic compounds (Sharma *et al*., 2018). The removal of dyes from textile effluents has been proven to be successful using ozonization (Tosik, 2005). According to some research, reactive dyes show a high degree of degradation with ozone, whereas basic dyes show moderate results and disperse dyes show poor results (Aplin & Waite, 2000). The application of ozone in its gaseous state with no sludge generation is a key advantage of this technique, making it an excellent instrument for decolorization. However, the high cost and short half-life of the ozonization process are its disadvantages (Aplin & Waite, 2000; Sharma *et al*., 2018). The ozonization method was found to have a nearly 98 percent removal efficiency for Rhodamine-B dye (Thao *et al*., 2017).

2.4.3 Biological Method of Dye Removal

When compared to other physical and chemical processes, biological treatment has been the most cost-effective alternative method. To treat industrial effluents, biodegradation technologies such as fungal decolorization, microbial degradation, adsorption by (live or dead) microbial biomass, or bioremediation systems have been widely used. Anaerobic biological treatment methods use bacteria (such as *Bacteroides sp*., *Eubacterium sp*., and *Clostridium sp.)* to decolorize azo dye solutions by cleaving the azo bond and producing aromatic amines as a by-product. Many dyes from various classes have been described as being oxidatively decolorized by aerobic bacteria, with azo dyes proving to be the most recalcitrant (Lokesh & R, 2014). Dye-degrading fungi are used in bioreactors to decolorize and degrade azo dyes (Maier *et al*., 2004).

Biologically based methods for the degradation of industrial textile effluents have been used successfully. When compared to other techniques, biological degradation (i.e., bioremediation) is more cost-effective, environmentally friendly, and produces less sludge. Because the breakdown of the bond (i.e., the chromophoric group), causes the degradation of synthetic dyes to a comparatively less toxic inorganic compound, which then aids in the removal of color (Babu *et al*., 2015). The azo dyes are catabolized in two steps: first, the dyes are broken down to form amines by breaking down the azo bonds, and then the aromatic amines are catabolized to small nontoxic molecules in an aerobic environment. The techniques are being developed to take advantage of bacteria's ability to survive in both aerobic and anaerobic conditions to completely degrade the azo bonds formed within the dyes (Bhatia *et al*., 2017).

Electro-coagulation method: This process entails the development of coagulants within the reactor site without the assistance of any outside source. The formation of coagulants is followed by the oxidation of sacrificial anodic electrodes such as aluminum, iron, stainless steel, and other metals, which results in the formation of hydroxyl species, which helps to neutralize the electrostatic charge of solids while also speeding up the agglomeration process. Contaminants, colloidal particles, metal ions, and dyes are all effectively removed with this method (Demirhan, 2020).

Solvent Extraction Method: Solvent extraction has a high potential for removing dye from textile wastewater. The basic principle entails the distribution of a solute in a specific ratio between two immiscible solvents, or the mixing of a known amount of dye phase in an aqueous phase and solvent phases. The liquid-liquid extraction technique was used to remove Methylene Blue dye from this method (Muthuraman *et al*., 2009). Crystal violet dye extraction efficiency was found to be around 90% using this method (Sharma *et al*., 2018). The extraction of Malachite Green dye using a solvent extraction method was also tested, and it was discovered that this method extracted 98.67% of the dye (Sharma *et al*., 2018). Some of the advantages associated with this technique that make it another effective method of treatment are its ease of operation and high purity. The process is more advantageous because solvent and dye recovery are both possible in this dye extraction process (Muthuraman *et al*., 2009).

Use of Surfactants in Solvent Extraction: The solvent extraction method with surfactants has also been used to remove dyes. Encapsulation of dye in a Reverse micelle from the aqueous phase with solvent phase separation results in dye separation from water. By using a liquid-liquid extraction process, reverse micelles have also achieved successful results in protein extraction and enzyme extraction (Krei & Hustedt, 1992; Srinivas *et al*., 2002). Reverse micelle dye removal allows for solvent and dye recovery via back extraction using counter ionic surfactants. For the extraction of Methylene blue and Malachite green dyes, anionic surfactants such as Sodium Dodecylbenzene Sulfonate (SDBS) and Sodium bis (2- ethyl) Sulfosuccinate (AOT) have been reported (Sharma *et al*., 2018).

2.5 Biosorption

The term sorption encompasses both absorption and adsorption. Adsorption is the physical attachment of molecules/ions on the surface of a solid material by bonding, whereas absorption is the incorporation of a substance in one form into another. The adsorbate is the material that is adsorbed at the interface, and the adsorbent is the solid surface on which the adsorption occurs (Rani & Sharma, 2021).

The primary advantages of biosorption over traditional treatment methods include; economical, efficient, decreased biological sludge, best in the use of industrial waste, reuse of biosorbents, do not need additional requirements (for example, nutrients) and the possibility of recovering contaminants for future use (in the case of metals).

A diverse range of naturally occurring biomaterials have been employed as biosorbents for pollutant removal. Different organisms, such as bacteria, cyanobacteria, algae (including microalgae, macroalgae, and seaweeds), fungi, and lichens, have been shown to have a high potential for contaminant removal among the various biosorbents. When compared to living cells as biosorbents, dead biomass is generally used as a biosorbent because of its various properties such as long storage time, no limitation by environmental conditions and adsorbate concentration, and no nutrient requirement (Rani & Sharma, 2021).

Despite significant progress in understanding the complex phenomenon and the volume of publications in this sector, marketing biosorption technologies is still a developing global market (Fomina & Gadd, 2014). In the early 1990s, commercialized biosorbents such as Algasorb^{TM}, AMT-BIOCLAIM^{TM} (MRA), and Bio-fix were marketed. The biosorption approach has proven to be significant due to its ability to adhere to contaminants on various biological materials. Because different sorbents have different biological resources, the biosorption mechanism varies.

The table below (**Table 2.2**) shows an examples of some commercialized biosorption techniques:

Table 2.2: Examples of some commercialized Biosorption Techniques

Commercialized Biosorbent	Family of Biosorbent	State of cell Free/ Immobolized	Company	Affinity	Application Equipment
AlgaSORB™	*C. vulgaris*	Immobolized on silica	Biorecovery systems	Metallic cations and metallic oxoanions	Two columns operating in series or in parallel.
B.V. SORBEX	*S. natans, A. nodosum, Halimeda opuntia, Palmyra pamata, Chondrus crispus,* and *C. vulgaris*	Powder or granules	B.V. SORBEX Inc.	Specific to toxic heavy metals	Fixed bed system, fluid bed system and completely mixed tanks.
AMT-BIOCLAIM™	Bacillus treated with caustic soda	Immobolized in extruded beads polyethyleneimine and glutaraldehyde		Suitable for accumulation of gold, cadmium and zinc from cyanide solutions.	Fixed bed canisters or fluid- bed reactor system
BIO-FIX®	Sphagnum, peat moss, algae, yeast, bacteria and aquatic flora.	Immobolized in polysulfone	U.S. Bureau of Mines (Golden Colarado)	Selective for toxic heavy metals	
MetaGeneR				Remove heavy metal from electroplating and mining waste streams.	
RAHCO Bio-Beads	Variety of sources including peat moss	Immobolized within an organic polymer.		Remove heavy metal from electroplating and mining waste streams.	

2.5.1 Factors affecting Dye Biosorption

Because dyes have a wide range of chemical structures, their ability to interact with microorganisms is influenced by a variety of parameters, including chemical structure, wastewater or dye solution properties, and biomass structural specialization (Argun *et al*., 2017). Factors that affect the dye biosorption are pH, temperature, biosorbent dosage, agitation speed, ionic strength and initial dye concentration.

2.5.1.1 pH

The solution pH is usually a major factor in biosorption, and it appears to influence the solution chemistry of metals/dyes as well as the activity of the biomass's functional groups. Metal ion speciation and biosorption availability are strongly influenced by pH. At higher solution pH, the solubility of metal complexes decreases sufficiently to allow precipitation, which may complicate the sorption process. The activity of binding sites can also be altered by adjusting the pH. For example, during the biosorption of metal ions by bacterial biomass, pH 3 to 6 is favorable for biosorption due to negatively charged carboxyl groups (pKa=3–5), which are responsible for binding metal cations via ion exchange mechanism (Yan & Viraraghavan, 2001). When it comes to dye biosorption, different dye classes require different pH ranges. Basic dyes, for example, require alkaline or neutral conditions for optimal biosorption, whereas reactive dyes require strong acidic conditions (Mahony *et al*., 2002; Farah *et al*., 2007).

2.5.1.2 Temperature

Within the range of 20 to 35 °C, temperature appears to have a minor impact on biosorption (Veglio' & Beolchini, 1997). Higher temperatures normally improve sorption due to the solute's increased surface activity and kinetic energy; nevertheless, higher temperatures might cause physical damage to the biosorbent. Increased temperature has been found to limit the biosorption capacity of biomass due to the exothermic nature of various adsorption processes. Biosorption should always be conducted or evaluated at room temperature, as this is the easiest setting to reproduce (Mameri *et al*., 1999).

2.5.1.3 Biosorbent Dosage

Biosorption is influenced by the size of the biosorbent. Smaller particles have a greater surface area, which aids biosorption and reduces equilibration time. Simultaneously, a biosorption particle must be tough enough to endure the pressures and harsh conditions encountered during regeneration cycles. As a result, preparatory experiments are required to determine the appropriate size of a biosorbent. If a biosorbent is available in powdered form, such as industrial

waste, measures should be made to improve mechanical strength, such as granulation, so that it may be used in biosorption columns effectively (Volesky & Prasetyo, 1994).

2.5.1.4 Agitation Speed

Due to increased turbulence and a decrease in the thickness of the liquid boundary layer, the diffusion rate of a solute from the bulk liquid to the liquid boundary layer around particles increases as the agitation rate is increased (Evans *et al*., 2002). The external diffusion coefficient increases in value under certain circumstances. Finally, as the agitation rate increases, the boundary layer thins out, increasing the rate at which a solute diffuses across the boundary layer (Shen & Duvnjak, 2005).

2.5.1.5 Ionic Strength

The adsorption of a salute to the biomass surface is influenced by ionic strength. The influence of ionic strength can be attributed to ion competition, changes in metal activity, or the electrical double layer's characteristics. Due to electrostatic interaction, when two phases, such as a biomass surface and a solute in an aqueous solution, come into contact, they are bound to be surrounded by an electrical double layer. As a result, adsorption reduces as ionic strength rises. Some inorganic ions, such as chloride, can form complexes with metal ions and so interfere with sorption (Dönmez & Aksu, 2002).

2.5.1.6 Initial Dye Concentration

The initial dye concentration appears to affect biosorption, with a higher concentration resulting in a high dye uptake. This is because, at lower initial dye concentrations, the initial mole of dye to available surface area ratio is low; as a result, fractional sorption becomes independent of initial concentration. However, at higher concentrations, the sites available for sorption become fewer in comparison to the moles of dye present, and thus the removal of solute is strongly dependent on the initial dye concentration. It is always necessary to determine a biosorbent's maximum saturation potential, for which experiments should be carried out at the highest possible initial dye concentration (Yuh Shan Ho, 2006).

2.6 Bioadsorbent

A biological treatment, particularly biosorption using nonliving biomass, is a relatively low-cost method of removing dyes from wastewater. The effective removal of dyes from the effluent is dependent on the unique surface chemistry

of microorganisms with the presence of different functional groups in the cell wall solute concentration (Karthik *et al*., 2016) such as alcohol, aldehydes, ketones, carboxylic, ether, and phenolic, which give biosorbents a high affinity for dye and make them an appealing material for dye removal (Siddiqui *et al*., 2018). Biological materials such as chitin, peat, chitosan, yeast, and fungal biomass are commonly utilized in the sorption of dye from solutions via the chelation and complexion mechanisms (Almeida & Corso, 2019).

A good dye adsorbent must have several desirable properties, including a large surface area, high adsorption capacity, large porosity, easy availability, stability, feasibility, compatibility, environmental-friendly, ease of regeneration, and the ability to remove a wide range of dyes (Nasar & Mashkoor, 2019). To achieve high dye adsorption, the pore volume of the adsorbents and the functional groups of the dyes must be optimized. The presence of a large pore volume allows most dye molecules to bind to the adsorbent (Hassan & Carr, 2021). Adsorption capacity is increased by increased surface area, porosity, and low ash content. The surface functional groups (hydroxyl, carboxyl, etc.) of biomass-based adsorbents play an important role in determining the hydrophobicity or hydrophilicity of biochar as well as its adsorptive mechanism (Law *et al*., 2022).

To remove dye molecules, a variety of microbes including bacteria, fungi, yeast, and algae have been studied (Karthik *et al.*, 2014). Aside from the high dye sorption capacity, the dye removal performance can be improved by combining the biosorption and biodegradation processes by living cells. pH, biosorbent dose, initial dye concentration, temperature, and contact time are all factors that influence biomass biosorption capacities. Recently, the potential of biosorbents derived from bacterial, fungal, algal, yeasts, forest biomasses, and agricultural and industrial wastes for treating dye-containing simulated and field samples has been investigated (Singh & Singh, 2017).

2.6.1 Microbial Bioadsorbent

Due to their immunity to toxic wastes, their independence from a steady supply of nutrients, and their regenerative and recyclable nature, biosorption using dead microbial cells offers significant advantages for water purification. No putrefaction will occur if dead cells are kept at room temperature for long periods of time. They require minimal effort to maintain and can quickly recover from damage. In addition, studies have shown that dead cells can accumulate pollutants such as dyes at the same rate as living or dormant cells (Hu, 1996; Aksu, 2005). Contaminants are bound to the surface of microorganisms via chemical interactions, similar to a chemical ion exchange material, and separated from the liquid stream via biosorption (Zaharia *et al*., 2020). Microbial cells (bacteria, fungi, and algae), industrial and agricultural wastes, and other polysaccharide materials are the most common biosorbents used to remove dyes and metals (Sylloscolus, 2016). Free microbial biosorbents frequently have low density, small size, low mechanical stability, and elasticity (difficult desorption, separation, and regeneration), which could be overcome by biomass immobilization (allowing for continuous biosorbent processes) on suitable carriers (Velkova *et al*., 2018).

Because of the presence of various functional groups on the microbial surface, microbial biomass has been shown to effectively remove soluble toxic organic substances as dyes via biosorption. Complexation, chelation, precipitation, and ionic interactions can all be used by biosorption to bind dyes from a waste solution (Lellis *et al*., 2019; Zaharia *et al*., 2020). Eukaryotic cells, particularly fungi and yeasts, were utilized to remove azo dyes from the color of textile effluent via the cell wall, which is thought to be the principal site of biosorption. The initial dye concentration, aqueous solution pH, temperature, and biomass dosage all have a role in biosorption (Zaharia *et al*., 2020).

2.6.2 Bacterial Biomass as Bioadsorbent

Bacterial roles in bioremediation applications can be based on the adsorption of contaminants from aqueous media via various mechanisms using dead biomasses (Roy *et al*., 2018). Because of their small size, ubiquity, and ability to grow in a variety of environments, they make excellent adsorbents (Shin *et al*., 2020). Bacterial species have been shown to be particularly successful at adsorbing reactive dyes from wastewater under ideal environmental conditions (Oya *et al*., 2015 ; Nasar & Mashkoor, 2019; Zabłocka-Godlewska *et al*., 2018). The rates of bacterial dye decolorization vary depending on the type of bacteria, dye reactivity, and operational parameters such as temperature, pH, co-substrate, electron donor, and dissolved oxygen concentration. Extremophiles can be used to effectively treat textile dyes. For example, haloalkaliphilic bacteria grown from textile wastewater removed 87% of reactive black and 85% of reactive red dyes (Seyedi *et al*., 2020).

At an initial concentration of 2000 mg/L, a bacterial strain (*Bacillus catenulatus* JB-022) isolated from polluted ponds and soils for cationic dye biosorption removed 58% of the cationic basic blue dye. According to the Langmuir adsorption isotherm, the maximum sorption capacity for basic blue dye was found to be 139.74 mg/g. Carboxyl and phosphonate groups on adsorbent surfaces can act as potential surface functional groups capable of binding to cationic pollutants (Flores-Gallegos *et al*., 2015). Several functional groups on the *Penaeus indicus* biomass surface were probably involved in Acid Blue 25 dye binding, but amino groups and alpha-chitin were by far the most important (Kousha *et al*., 2015). *Bacillus subtilis* was immobilized in calcium alginate beads and used to remove methylene blue dye in batch and continuous reactors. The kinetic study in the batch and continuous contactors resulted in greater than 90% removal (Upendar *et al*., 2016).

Various biocomposites have been reported to improve dye removal performance (Hu *et al*., 2019; Chen *et al*., 2020) By joining with electrospun polycaprolactone and polylactic acid nanofibrous polymeric webs, a bacterial strain (*Clavibacter michiganensis*) was studied for the removal of a reactive dye (Sarioglu *et al*., 2017). With reusable and improvable properties, the biocomposite was a promising material for the treatment of textile dyes. Furthermore, for methylene blue dye treatment, electrospun nanofibrous-encapsulated bacterial cells were

used (Saravanan *et al*., 2021). A design of a paper-like multifunctional purifier with a biomass-based structure was reported in another research, with improved adsorption capabilities toward anionic dyes by embedding polyethyleneimine generated from ammonium compounds onto the substrate of bacterial cellulose, including methyl orange, congo red, and methyl red (Hu et al., 2019). Because of differences in bacterial cell wall compositions, biosorption fidelity is dependent not only on the kind of ions but also on the type of bacteria. The metal-binding capacity of the bacterial cell wall was determined by the presence of various anionic functional groups in gram-negative bacteria with phospholipids, peptidoglycan, lipopolysaccharides, and teichoic acids in gram-positive bacteria with peptidoglycan. Ion binding is another property of extracellular polysaccharides (Roy & Saha, 2021). The figure below (**Figure 2.2**) shows the keyword mapping for SCOPUS 2010-2020 based on the co-occurrence of author keywords in scopus published documents (Keywords: biosorption AND dye AND bacteria).

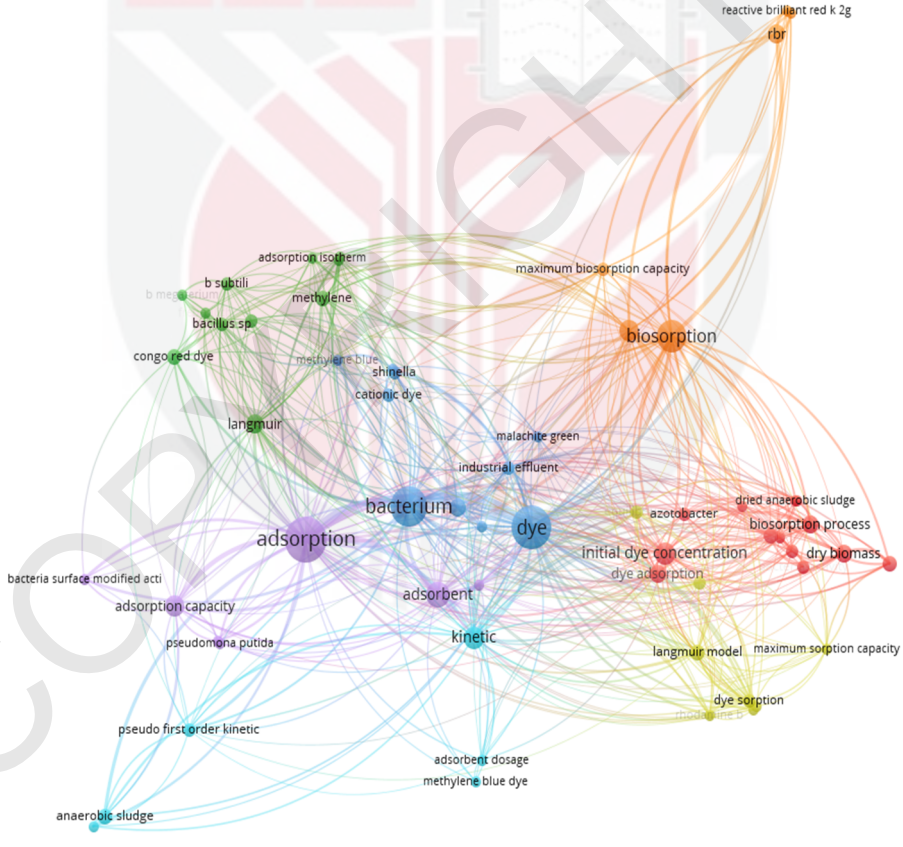

Figure 2.2: Keyword mapping for SCOPUS 2010-2020 based on the co-occurrence of author keywords in SCOPUS published documents. (Keywords: biosorption AND dye AND bacteria).

2.7 Principles and theory of Adsorption Process

Adsorption is the process of adsorptive (gas or liquid) molecules binding to a solid surface. In reality, however, adsorption is carried out in a column packed with porous sorbents as a batch or continuous process. Mass transfer effects are unavoidable in such situations. The entire adsorption process includes mass transfer and consists of three phases (Tan & Hameed, 2017a):

1. The movement of adsorptive from the bulk phase to the external surface of an adsorbent is known as **film diffusion** (external diffusion).

2. The movement of adsorptive from the exterior surface into the pores is known as **pore diffusion** [intraparticle diffusion (IPD)].

3. **The surface reaction** is the adhesion of adsorptive to the sorbent's interior surface.

The adsorptive is met with resistance at each phase. Total resistance, which is the sum of the three-component resistances in series, determines the overall adsorption rate (as determined through experiment) (Viswanathan & Farooq, 2000). The adsorption rate is increased when the resistance of any component is reduced. When contrasted to the first and second steps, the third step is usually very quick, and hence presents less resistance. When one step dominates the total resistance to the point where lowering the other two just slightly enhances the adsorptive uptake rate, the step is referred to as a sole-rate controlling step. Many factors influence transport resistance, including adsorbent and adsorptive kinds, properties, and operating circumstances. During the adsorption process, the rate-controlling step can change (Plazinski & Rudzinski, 2010). When the adsorbent is 80% saturated, the control mechanism for dye adsorption on pine sawdust flips from surface reaction to IPD (Władysław Rudzinski & Plazinski, 2008). Between adsorbent and adsorbate, two types of interactions are possible: physical and chemical (Tan & Hameed, 2017a); the former is referred to as physisorption, whereas the latter is referred to as chemisorption. Physisorption is the outcome of attractive forces between sorbent and adsorbate molecules, whereas chemisorption involves the transfer or sharing of electrons between adsorbent and adsorbate species, resulting in a stronger connection (Vithanage *et al*., 2016). As a general rule, isosteric heat of adsorption between 5 and 40 kJ/mol implies physisorption as the primary adsorption mechanism, while one between 40 and 125 kJ/mol shows chemisorption as the main adsorption mode (Kara *et al*., 2003; Zhou *et al*., 2014).

An adsorbent's monolayer capacity refers to its ability to hold a single layer of adsorbed species on its surface. When the adsorptive concentration is high, subsequent layers often stack onto the original monolayer due to intermolecular interaction, resulting in multilayer adsorption, which is physical in origin (Zhou *et al*., 2014).

Adsorption equilibrium and kinetics are heavily influenced by the heterogeneity of the adsorbent surface. Heterogeneous adsorbents have multiple types of adsorption sites that can bind the adsorbate, each with its adsorption heat. Surprisingly, the Langmuir isotherm, which is based on homogeneous surface sites, can explain a wide range of adsorption systems, including many with heterogeneous surface properties (Foo & Hameed, 2010).

The equilibrium and kinetic studies are the two main components of adsorption research. Thermodynamics governs the adsorbent's ability to achieve equilibrium in terms of adsorptive loading. The adsorption mechanism influences the rate of adsorptive absorption. A broad variety of equilibrium isotherms exist for representing the equilibrium uptake of any target adsorptive, indicating that adsorption equilibrium has matured. Adsorption kinetics theory, on the other hand, is progressing far more slowly, despite its importance in actual applications of a given sorbent. The kinetic isotherm, which is produced empirically by recording the adsorbed amount against time, is the foundation for kinetics research. Kinetic studies are used to create a model that describes the adsorption rate (Tan & Hameed, 2017a).

2.7.1 Kinetics Models in Batch Adsorption

A kinetic isotherm is a plot of uptake vs. time that depicts adsorption kinetics. Because the shape of this figure represents the underlying kinetics of the process, it is the foundation of all kinetics investigations. Material parameters like adsorbent and adsorbate types, as well as experimental parameters like temperature and pH, influence the kinetics (Regti *et al*., 2017; Slimani *et al.*, 2011). To acquire kinetic data, a batch experiment is usually used. It's critical to maintain consistent experimental conditions during batch adsorption.

The intrinsic kinetics, or chemical kinetics on the adsorbent surface in the absence of transport constraints, should be revealed by the kinetic isotherm. Batch operation is a popular way to investigate intrinsic kinetics. Applying (i) a high agitation speed (reduced film thickness) and (ii) a small particle size (reduced pore diffusion) can easily reduce or eliminate mass transfer effects (Froment, 1975).

The adsorptive uptake per unit mass of adsorbent, q (mg/g) is given by:

$$q = (C_O - C)V / m \quad (2.1)$$

Where;
C_O =initial concentration of adsorptive in the bulk liquid (mg/l)
C =concentration of adsorptive in the bulk liquid at time t (mg/l)
V=volume of the bulk solution (l) and
m=mass of adsorbent (g)

2.7.1.1 Pseudo-First-Order (PFO) Kinetics

Largergren proposed the pseudo-first-order (PFO) equation for adsorption of oxalic and malonic acid onto charcoal in 1898. Its differential form is as follows:

$$dq/dt=k_1 (qe-q) \quad (2.2)$$

Where;
q= adsorption capacity (mg/g)
t=time (min) and
k_1= rate constant (1/min)

After integrating with the initial conditions of q=0 when t=0, **equation 3.2** becomes;

$$q=qe (1-exp (-kt)) \quad (2.3)$$

The linearized form of the above equation is;

$$ln (qe/(qe-q)=k_1t \quad (2.4)$$

For systems that satisfy this model, plotting ln ((qe-q)/qe) vs. t yields a straight line passing through the origin with a slope of k_1.

The rate constant k_1 is determined by the conditions of the process. It has been noted that it decreases when the initial bulk concentration rises (Chinoune *et al*., 2016; Zarezadeh-Mehrizi & Badiei, 2014), which may be translated as follows: The timescale for the process to reach equilibrium is $1/k_1$; if the initial concentration (C_0) is higher, a longer period (smaller k_1) is required. According to certain studies, k_1 is either an increasing function of C_0 or independent of C_O (Biswas & Mishra, 2015; Yousef *et al*., 2011). The experimental conditions, such as pH and temperature, are likely to alter the k1 value. Because these two factors influence equilibrium behavior (isotherms), it would be impossible to isolate their impacts on the k1 value empirically. Small particle size is correlated with big k1 values, as expected (Vincent *et al*., 2014).

The validity of the PFO model for long adsorption has been argued when the system is close to equilibrium (Plazinski *et al.,* 2009*;* Wladyslaw Rudzinski *&* Plazinski, 2007*)*. The model has also been demonstrated to be only valid at the beginning of the adsorption process (Ho & McKay, 1999).

The rate-controlling mechanism is influenced by the experimental settings as well as the amount of surface covered (adsorption time). As a result, a model's

validity is restricted to a specific operating range of the supposed mechanism in which it was generated or interpreted (Tan & Hameed, 2017a).

A modified PFO equation is written as follows:

$$dq/dt=k_1\ qe/q\ (qe-q) \quad (2.5)$$

The linearized form becomes:

$$q/qe+\ln (qe-q) = \ln (qe) - k_1 t \quad (2.6)$$

2.7.1.2 Pseudo-Second-Order (PSO) Kinetics

The pseudo-second-order kinetic equation has been frequently utilized in the study of adsorption kinetics to characterize the time development of adsorption in non-equilibrium situations (Liu, 2008). The equation is as follows:

$$dq/dt = k_2\ (qe-q)^2 \quad (2.7)$$

Where:
k_2= pseudo-second-order (PSO) rate constant

When **equation 2.7** is integrated with the initial conditions of q =0 and t =0, the linearized form of the equation becomes:

$$t/q = 1/k_2 qe^2 + t/qe \quad (2.8)$$

The initial adsorption rate is $k_2 qe^2$. For PSO-compliant kinetics, a plot of t/q v s t yields a straight line. 1/qe is the slope, while $1/k_2 qe^2$ is the intercept. Other linearized forms exist, though they are less commonly employed (Yuh Shan Ho, 2006b).

PSO can model most environmental kinetic adsorption well, suggesting its superiority over other models. The constant k_2 is a time scale factor that decreases with rising C_0 in the same way that PFO does (El Haddad *et al*., 2013; Setiabudi *et al*., 2016).

Because of the challenges that come from the impact on equilibrium isotherm shapes, the effects of pH and temperature on k_2 have not been well investigated. Due to the lower IPD resistance, a smaller particle size results in a higher k_2 value (Vincent *et al*., 2014).

Based on pore diffusion and the Langmuir surface reaction, an adsorption–diffusion model was devised If the following conditions are met, their model gives an excellent fit to PSO kinetics: The conditions are as follows:

i. Reaction control, nonlinear (saturated) adsorption, and

ii. A sufficient amount of adsorbent to adsorb half of the adsorptive in the bulk phase. They claimed that, at least over a given time range, those PSO kinetics that could not be predicted by their model are governed by an unknown mechanism.

2.7.1.3 Elovich Equation

To describe the adsorption of carbon monoxide (CO) on manganese dioxide ($Mn0_2$), Roginsky and Zeldovich proposed the term in 1934 (Tan & Hameed, 2017a). The equation is expressed as:

$$dq/dt = \alpha \exp(-\beta q) \quad (2.9)$$

When integrated, the equation becomes:

$$q = 1/\beta \ln(1 + \alpha\beta t) \quad (2.10)$$

The linearized form becomes:

$$Q = 1/\beta \ln(\alpha\beta) + 1/\beta \ln t \quad (2.11)$$

A straight line should appear on the plot of q vs. ln t if the Elovich equation is followed. The slope is 1/β, while the intercept is [ln (αβ)]/β.

Where:
α= initial adsorption rate (mg/g)
β= desorption constant

The Elovich equation ignores desorption and is well-known for accurately describing chemisorption (Kumar & Bandyopadhyay, 2006). It's physically flawed since it predicts infinite q over large periods. As a result, it's appropriate for kinetics far from equilibrium in which desorption isn't possible due to a lack of surface coverage.

Many attempts have been made to develop a theoretical foundation for the Elovich equation, with the majority of these publications assuming significant heterogeneity at the adsorbent surface (Piasecki & Rudziński, 2007). This model

has been used to simulate liquid-phase kinetics. The Elovich equation was found to be the best fit for lead adsorption onto activated carbon (Largitte & Pasquier, 2016). Dye adsorption on eggshell biocomposite beads was discovered to follow Elovich kinetics (Elkady *et al*., 2011). The constants α and β rise with increasing initial dye concentration, as expected from their physical definitions. When the temperature of the bulk solution was raised, the observed values of α increased, but β decreased (Shehata *et al*., 2010).

2.7.2 Equilibrium Isotherms study in Biosorption

The equilibrium relations between the concentration of the adsorbate on the solid phase and its concentration in the liquid phase are known as isotherms. Langmuir, Freundlich, and Tempkin isotherms were used to analyze the equilibrium biosorption data. It is necessary to analyze such isotherms to produce an equation that accurately captures the results and can be used for design purposes. The Langmuir isotherm model assumes that adsorption energies on adsorbent surfaces are homogeneous. Furthermore, the Langmuir equation is predicated on the assumption of monolayer coverage of the adsorbate at the adsorbent's outer surface, where all sorption sites are identical (Çolak *et al*., 2009). The Langmuir equation (Marbawi *et al*., 2019) is as follows:

$$q_e = \frac{q_{mL} b_L C_e}{1 + b_L C_e} \tag{2.12}$$

Where:
q_e= equilibrium dye concentration on the adsorbent (mg g^{-1})
C_e= equilibrium dye concentration in solution (mg l^{-1})
qmL= the adsorbent monolayer capacity (mg g^{-1})
bL= Langmuir constant

The equation for the Freundlich isotherm model is as follows:

$$q_e = K_F C_e^{\frac{1}{n_F}} \tag{2.13}$$

Where:
q_e= equilibrium dye concentration on the adsorbent (mg g^{-1})
C_e= equilibrium dye concentration in solution (mg l^{-1})
K_F= Freundlich constant

Although it can be mathematically determined for an adsorption model in which the heat of adsorption varies exponentially with surface coverage, the Freundlich equation was first developed on a purely empirical basis for adsorption processes happening on gas–solid interfaces (Çolak *et al*., 2009; Cherdchoo *et al*., 2019).

BET isotherm was developed in1938, which is one of the most successful isotherm models for expressing adsorption phenomena (Brunauer *et al*., 1938). The BET equation has a solid theoretical foundation and provides a good understanding of the nature of adsorption phenomena. Among the adsorption parameters that can be determined using this isotherm model are multilayer adsorption behavior, monolayer adsorption capacity, and heat of adsorption at various adsorption layers. Because of these powerful characteristics, the BET isotherm model has found widespread use in determining the surface area and pore size distribution of adsorbents and catalysts (Ebadi *et al*., 2009). The model equation is as follows:

$$q_e = \frac{q_{mBET}\alpha_{BET}C_e}{(1-\beta_{BET}C_e)(1-\beta_{BET}C_e+\alpha_{BET}C_e)} \quad (2.14)$$

Where:
q_e= equilibrium dye concentration on the adsorbent (mg g^{-1})
C_e= equilibrium dye concentration in solution (mg l^{-1})
α and β are the BET constants

Table 2.3 below shows the studies of isotherms and kinetics of some microbial adsorbents:

Table 2.3: Isotherms and kinetic studies of some microbial adsorbents

Microbial Adsorbent	Adsorbate (dye)	Isotherm	Kinetic	Adsorption capacity (mg/g)	Type of regression	Reference
Rhodopseudomonas sp. (Bacteria)	Astrazone red	Freundlich and Langmuir	Not reported	Not reported	Non-linear	Abdullah *et al*., (2021)
Aspergillus carbonarius and *Penicillium glabrum* (fungi)	Congo red	Langmuir	Pseudo-second- order	99.01 for Aspergillus carbonarius and 101.01 for Penicillium glabrum	Non-linear	Bouras *et al*., (2017)
\Rhodococcus erythropolis (bacteria)	Crystal violet	Langmuir	Pseudo-second- order	289.8	Non-linear	Canizo *et al*., (2019)
Saccharomyces cerevisiae (fungi)	Astrazone blue	Langmuir		70	Non-linear	Farah *et al*., (2007)
Phanerochaete chrysosporium (fungi)	Remazol brilliant blue R	Langmuir	Pseudo second- order	101.06	Non-linear	Iqbal & Saeed, (2007)
Penicillium restrictum (fungi)	Reactive black 5		Pseudo-second-order	98.33		Iscen *et al*., (2007)
Trichoderma harzianum (fungi)	Acid yellow 12	Freundlich	Pseudo second- order	78.39		Karthik *et al*., (2019)
Trichoderma harzianum (fungi)	Reactive black B	Freundlich	Pseudo second-order	97.42		Karthik *et al*., (2019)
Escherichia coli (bacteria)	Reactive Yellow 2			335.16		Kim *et al*., (2016)
Chlamydomonas variabilis (microalga)	Methylene blue	Freundlich and Langmuir	Pseudo-second-order	115	Non-linear	Moghazy (2019)

2.8 Thermodynamic studies in Biosorption

A large number of studies published in various newspapers have currently enriched the field of biosorption. Large-scale research has been conducted to understand isotherms and kinetics in adsorption better. Adsorption studies can only be useful and meaningful if it covers the structure and dynamics of its various components separately and in interaction with one another. In this regard, a thorough investigation of thermodynamic biosorption is required (Ayawei *et al*., 2017). Adsorption thermodynamic properties are measured as their value for a two-phase system because adsorption occurs at the interface between two bulk phases, which are solid and fluid. As a result, different perspectives can be taken when applying thermodynamic principles to adsorption equilibrium (Lee, 2015).

The thermodynamic parameters are used to distinguish physical from chemical biosorption processes. The physical biosorption process is characterized by a weak physical reaction, whereas the chemical biosorption process is characterized by a stronger reaction (Tran *et al*., 2016a). As a result, the response is either a physical (physisorption) or a chemical (chemisorption) process, or a combination of both mechanisms (comprehensive adsorption) (Kuipa & Kuipa, 2015). The impact of temperature on the rate of chemical reaction in biosorption has been thoroughly established, and the van't Hoff law has been used to calculate it. According to the law, a 10-kelvin increase in temperature doubles the reaction time by 2 to 4 times. The reaction time reduces as the temperature rises. As a result, at various temperatures, the entire reaction rate may be evaluated experimentally (Chen *et al*., 2021).

Several studies have found that increasing the temperature causes a decrease in the biosorption process, and the process is called an exothermic ($-\Delta H$) reaction because heat in the form of energy is released into the environment (Cherfi, 2014). Endothermic reactions, on the other hand, gain energy from the environment in the form of heat ($+\Delta H$) (Velkova *et al*., 2018). The total energy released in the bond-breaking process is less than the total energy absorbed in the bond formation process between the sorbate and the adsorbent in the endothermic process. The Gibbs free energy (ΔG) is utilized to determine the biosorption process' spontaneity (Yahuza *et al*., 2020b). A higher negative value ($-\Delta G$) at a given temperature implies a favorable spontaneous biosorption process, whereas a non-spontaneous non-desirable reaction process represents a positive Gibbs free energy change ($+\Delta G$). This also shows the sort of reaction, whether it's physisorption or chemisorption (Venkata *et al*., 2002). The degree of randomness of the sorbate in the reaction solution is represented by the entropy change (ΔS). A negative entropy value ($-\Delta S$) suggests an associative interaction, whereas a positive value ($+\Delta S$) indicates a dissociative reaction (Kiran *et al*., 2006; Imran Din *et al*., 2013).

In thermodynamic study, activation energy is a significant factor in determining the rate of a temperature-dependent process. The activation energy (E_a) is the

amount of energy necessary to start a chemical reaction. In the process of adsorption, it is defined as the energy required by the adsorbate ion or molecule to coalesce with the functional groups on the adsorbent surface. Despite the fact that it is thermodynamically feasible, it is the minimum energy required for a certain adsorbent-adsorbent interaction. Its unit is $kJmol^{-1}$. The activation energy for the adsorption of an adsorbate molecule onto an adsorbent surface in an adsorption process can be computed using the Arrhenius equation based on experimental observations of the adsorption rate constant over a wide temperature range (Teng & Hsieh, 1999; Sarkar *et al*., 2003) as follows:

$$\ln k = \ln A - \frac{E_a}{RT} \tag{2.15}$$

Where:
k=Adsorption rate constant
A= Frequency factor (constant)
E_a= Activation Energy ($kJmol^{-1}$)
R=Gas constant (8.314 $J.mol^{-1}k^{-1}$)
T=Temperature (K)

The activation energy value indicates the several forms of adsorption that might happen in a process, such as physical and chemical adsorption. Because physisorption requires little energy, equilibrium is usually reached rapidly, and the reaction is reversible. The activation energy for physisorption is usually less than 4.2 kJ mol^{-1} since the forces driving it are minimal. Chemisorption is more specific and has far stronger pressures than physisorption. As a result, the chemisorption activation energy equals the heat of chemical processes. Less broadly, there are two types of chemicals: activated and non-activated. Chemisorption-inactivation means that the Arrhenius equation (high E_a) rate depends on the final energy activation temperature, which varies between 8.4 and 83.7 kJ / mol. Chemisorption, on the other hand, occurs very quickly in some processes, indicating that the energy of activation is nearly zero (Tan & Hameed, 2017; Tran *et al*., 2017). **Table 2.4** below shows the thermodynamic studies of dye biosorption using some microbial adsorbents:

Table 2.4: Thermodynamic Studies of Dye Biosorption using some microbial Adsorbents

Microbial biomass (adsorbent)	Adsorbate (dye)	Temperature (K)	*ΔG* (kj/mol)	*ΔH* (kj/mol)	*ΔS* (j/mol)	Nature of adsorption	Reference
Cephalasporium aphidicola	Acid red -57	293	-22.38	-13.08	32.26	Spontaneous, exothermic and there is an increase in the degree of randomness at the solid-liquid interface during the adsorption Non-spontaneous, endothermic and there is an increase in the randomness at the solid-liquid interface during the adsorption	Kiran *et al*., (2006)
		303	-22.90				
		313	-23.38				
		323	-23.35				
Penicillium restrictum		298	2.25	9.70	24.83	Spontaneous, endothermic and there is an increase in the randomness at the solid-liquid interface during the adsorption	
		313	2.05				
		323	1.59				
Aspergillus foetidus	Reactive orange-122	303	-12.2	12.2	80.4	Spontaneous, exothermic, and decrease in the degree of randomness at the solid-liquid interface during the adsorption Spontaneous, exothermic, and decrease in the degree of randomness at the solid-liquid interface during the adsorption	(Ahammad, S. Z.; Gomes, J.; Sreekrishnan, 2008) Patel & Suresh, (2008) Atar *et al*., (2008) Çolak *et al*., (2009) Karthik *et al*., (2019)
		323					
Bacillus macerans	Reactive black-5	298	-4.72	-22.90	-0.061 - 273.62	Spontaneous, exothermic, and decrease in the degree of randomness at the solid-liquid interface during the adsorption	
		308	-3.91				
		318	-3.25				
		328	-2.09	-107.72	-81.50		
Paenibacillus macerans	Basic blue- 41	298	-25.62	-50.07	108.5		
		308	-24.81	26.90			
Trichoderma harzianum (fungi)		318	-21.65				
		328	-12.79				
		298	-25.87				

	Acid blue 225	308	-25.43				
	Acid blue 062	318	-23.50				
	Acid Yellow 12	328	-21.87				
		298	-5.51				
		303	-6.05				
		310	-6.81				
		313	-7.14				
	Methylene blue	298	-5354.24	-35.04	-100.07		
		303	-4637.15				
		313	-3723.05				
Streptomyces fradiae (bacteria)						Spontaneous, exothermic, and decrease in the degree of randomness in the adsorption	Velkova *et al*., (2018)
	Congo red	298	-2320.17	-17.47	-50.94		
		303	-1996.15				
		313	-1491.06				
		293	-3.05				
Aspergillus carbonarius (fungi)		298	-2.61				
Penicillium glabrum (fungi)	Congo red	303	-1.50	48.42	154	Spontaneous, endothermic, and increase in the degree of randomness of the adsorption	Bouras *et al*., (2017)
		293	-2.99	74.3	243		
		298	-1.31				
			-0.57				
		298	-26.13				
Rhodococcus erythropolis (bacteria)	Crystal violet	308	-26.98	-13.08	40	Spontaneous, exothermic, and increase in the degree of adsorption randomness	Canizo *et al*., (2019)
		318	-27.25				
		328	-27.50				
		298	-2.750				
Trichoderma harzianum (fungi)	Reactive black B	303	-3.478	-42.53	151	Spontaneous, exothermic, and increase in the degree of adsorption randomness	Karthik *et al*., (2019)
		308	-4.499				
		313	-5.551				
		293	-3.53				
Sargassum hemiphyllum (macroalga)	Methylene blue	303	-3.85	7.46	37.45	Spontaneous, exothermic, and increase in the degree of randomness	Liang *et al*., (2017)
		313	-429				

Several equations, as shown below can be used to determine thermodynamic parameters. The most widely used equations for estimating thermodynamic parameters are the Gibbs free energy and Van't Hoff equations. Because the use of multiple isotherm models will raise deviation in $\Delta H°$, Clausius – Clapeyron equation is rarely employed instead of van't Hoff expression (Milonjić, 2007; Tan & Hameed, 2017; Tran *et al*., 2017). **Table 2.5** below shows the modeling equations used in thermodynamic studies:

Table 2.4: Modeling Equations in Thermodynamic studies

Expression	Equation
Van't Hoff	$\ln(K_C) = \frac{\Delta S°}{R} - \frac{\Delta H°}{RT}$
Gibb's free energy	$\Delta G° = -RTlnK_C$
Clausius – Clapeyron	$\Delta H° = R\frac{T_1T_2}{T_2 - T_1}\left(\frac{lnC_{0,1}}{lnC_{0,2}}\right)$

2.8.1 Biosorption Thermodynamics using Dimensionless Langmuir Constant

The Van't Hoff equation's Langmuir isotherm constant (K_C) was computed for neutral species, dilute, and concentrated ionic solutions. These assumptions could be attributed to the successful use of K_C as the thermodynamic equilibrium constant for a non-ionic or dilute solution of an ionic solute expressed in $molL^{-1}$. Otherwise, the necessary K_C modifications, as listed by several authors, should be used to adopt K_C as the equilibrium constant. (Milonjić, 2007; Zhou & Zhou, 2014; Tan & Hameed, 2017; Tran *et al*., 2017). Concerns about the inaccurate estimation of the equilibrium constant in various publications, according to the above-mentioned authors, should be addressed. The adsorption thermodynamics can be explored with a more accurate estimate of the equilibrium constant and a more relevant conclusion.

The Langmuir equation (**Equation 2.16**) was developed first from a kinetic study and then from a thermodynamic perspective (Liu *et al*., 2018). The accurate estimation of the thermodynamic parameters, K_C is directly dependent on the proper characterization of the equilibrium constant between two phases.

Equations 2.16 and 2.17 below should be used to convert derived K_C values from the Langmuir model to the dimensionless form (Zhou & Zhou, 2014).

$$K_C = MW \times 55.5 \times 1000 \times K_L \quad (2.16)$$

Where:
MW= Molecular weight of the adsorbate used
55.5= Number of moles of pure water per liter
K_L= Langmuir constant

Equation 14 below describes the relationship between dimensional K_L and the unitless equilibrium constant of K_C:

$$K_C \approx \frac{K_L\left(\frac{L}{mol}\right) \times C^{\circ}\left(\frac{mol}{L}\right)}{\gamma} \quad (2.17)$$

Where:
C^o= Adsorbate selected standard (C^o=1molL^{-1})
γ (dimensionless) = Activity coefficient of adsorbate in solution (Nguyen *et al*., 2020).

2.8.2 The use of Non-linear Regression in Thermodynamics study

The transformation of the model into linearized equations, from which the parameters are associated with the slope and intercept of a straight line, is a popular alternative to non-linear regression. According to several authors, non-linear regression is more appropriate than linear regression (Milonjić, 2007; Tan & Hameed, 2017; Tran *et al*., 2017). However, the number of literature papers that continue to employ this regression method should be questioned because the linear transformation significantly modifies error distribution, either for the better or for the worse, bringing statistical bias into experimental data analysis. It is unclear in many of the investigations whether the parameters produced through linearization are consistent with those obtained using non-linear regression or are dependable to any extent (Milonjić, 2007; Kumar *et al*., 2008; Tan & Hameed, 2017; Tran *et al*., 2017).

CHAPTER 3

MATERIALS AND METHODS

3.1 Experimental Design

Figure 3.1 depicts the overall research design for the bioadsorption of Reactive red-120 dye (RR-120) using bacterial biomass. The design includes bacterial biomass screening, optimization using one-factor-at-a-time (OFAT) and response surface methodology (RSM), kinetic and isotherm modeling, thermodynamic studies, and bacterial biomass characterization.

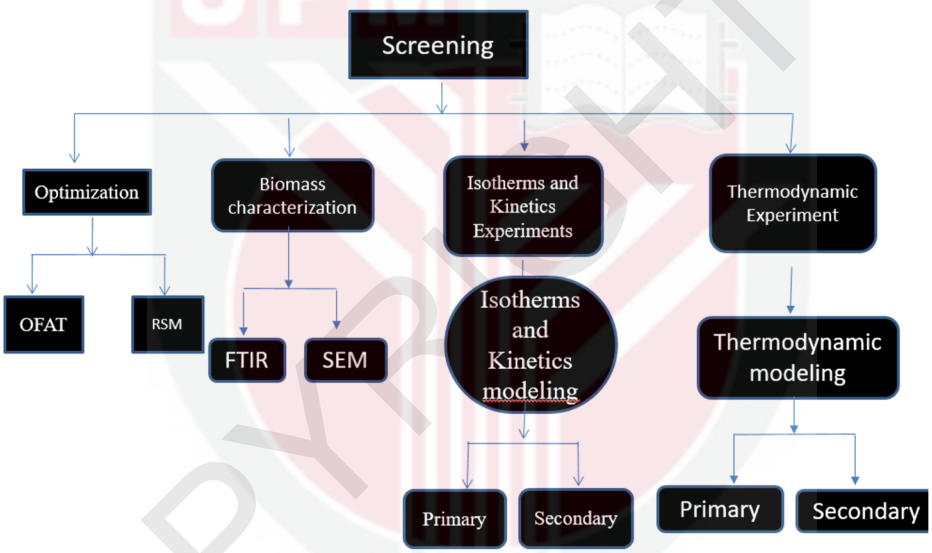

Figure 3.1: The research design for the bioadsorption of reactive red-120 dye

3.2 Reagents, Chemicals, and Equipment

The reagents used were all of the highest analytical quality. The reactive red-120 dye used in this study was purchased from Sigma Aldrich Co., U.S.A. The Appendix contains a list of all the chemicals, reagents, and equipment used in this study. Dissolving 1000 mg of the dye salt in 100 mL of deionized water yielded a dye stock solution of 1000 ppm for RR-120 dye. All dye concentrations for the experiment were reconstituted using deionized water from the dye stock solution (1000 ppm). Using a pH meter, the pH of the solution was adjusted with either 0.5 N HCl or 0.1 mol NaOH.

The maximum peak of absorption spectra from a spectrophotometer was used to standardize dye absorbance for reactive red-120 dye (scanned from 400 to 800 nm, visible range). The best absorbance peak for reactive red-120 dye was between A520 and A535 nm (S. K. Das et al., 2012).

3.3 Preparation of Bacterial Growth Medium

The cultured medium used in the experiment is listed and prepared as follows;

3.3.1 Nutrient Broth (NB)

The Nutrient Broth (Oxoid, Thermo Fisher (Heysham), Ireland) was prepared by dissolving 18 g of media in 1 L of distilled water (dH2O), autoclaved for 20 minutes at 121 °C, and stored in a chiller at 4 °C. The general compositions in (g/L) of the NB are; 3.0 beef extract, 10.0 peptone, and 5 NaCl.

3.3.2 Preparation of Glycerol stock solution

A single colony of each bacterial strain was inoculated into 10 mL of nutrient broth and incubated at 10 °C for 24 hours at 150 rpm. Bacterial glycerol stock was prepared in 20% (v/v) glycerol by transferring 600 µL of overnight culture into a sterile 1.5 mL Eppendorf tube containing 400 µL of 20% sterile glycerol. The stock was then stored at -80 °C for future use. Therefore, sterile glycerol was used for long-term bacteria preservation (Gorman & Adley, 2004).

3.4 Bacterial Source

Twelve (12) distinct pure bacterial cultures (Isolate 1, Isolate 2, Isolate 4, Isolate 5.1, Isolate 5.2, Isolate 7, Isolate 8, Isolate 29, Isolate 30, Isolate 34XR, IsolateXW, and Isolate 52) were obtained from the Bioremediation, Biomonitoring & Ecotoxicology Laboratory (BBE), Faculty of Biotechnology and Biomolecular Sciences, Universiti Putra Malaysia. These bacterial isolates were originally isolated from the Juru river banks in Pulau Penang, Malaysia (Manogaran *et al*., 2021). This area has been reported to have high levels of dye pollution originating from nearby textile and pigment industries (Izuan *et al*., 2015). As a result, regular sub-culturing was performed under aseptic laboratory conditions utilizing Nutrient Broth (NB) as a growth medium to maintain the purity of each isolate. In this regard, a pure colony method was followed.

3.4.1 Bacterial Biomass Harvesting

Each of the twelve (12) isolates' biomass was harvested and screened for reactive red-120 dye adsorption. A day-old culture of the isolates with about 1 OD_{600} absorbance was centrifuged for 10 minutes at 10,000 rpm (Canizo *et al*., 2019). The supernatant from each isolate was discarded, and the pellets were washed twice with Tris Buffer at pH 7.0. The pellets were then inactivated in a water bath at 60 °C for 1 hour to kill the bacterial cells. The pellets were then subjected to reactive red-120 dye adsorption experiments (Liu *et al*., 2011; Huang *et al*., 2013; Sylloscolus, 2016).

3.4.2 Screening of Bacterial Biomass

A volume of 10 mL of reactive red-120 dye was mixed with 0.22 g of each of the 12 inactivated bacterial biomass in 50 mL flasks. The flasks were labelled appropriately and incubated at 25 °C and 150 rpm. Two (2) mL aliquots were taken at regular intervals of 5 minutes for each flask, centrifuged at 10,000 rpm for 10 minutes, and examined with a spectrophotometer (RR-120 OD535nm) to monitor each bacterial biomass adsorption potential (Liu *et al*., 2011; Cheng *et al*., 2020). This procedure was repeated until the absorbance peak for each flask set became uniform. All experiments were carried out in triplicate. The formula below was used to calculate the percentage adsorption:

$$Dye\ adsorption\ percentage\ (\%)\ \frac{A-B}{A} X\ 100 \qquad (3.1)$$

Where:
A= Absorbance before incubation
B= Absorbance after incubation

Isolate having the highest percentage absorption of reactive red-120 dye was selected for further studies.

3.5 Optimization of Reactive red-120 dye adsorption using One-Factor-at-a Time (OFAT)

According to the screening results, Isolate 2 has the highest adsorption percentage on reactive red-120 dye. Manogaran *et al*. (2020) identified and characterized this isolate as *Enterobacter sp*. strain MM05. Therefore, using the isolate *Enterobacter* sp. strain MM05, the OFAT approach was used to optimize the conditions for the adsorption of reactive red-120 dye. The effects of contact time dye concentration, pH, agitation speed, adsorbent size, and temperature were all optimized using the OFAT technique. Each parameter was examined one after the other while keeping the previously optimized parameters constant. All experiments were performed in triplicate.

3.5.1 Effect of pH

The chemistry of the solution is influenced by the pH. Therefore, the pH range investigated for reactive red-120 dye adsorption was 5.0-8.5. (5.0, 5.5, 6.0, 6.5, 7.0, 7.5, 8.0 and 8.5). (Liu *et al*., 2011; Velkova *et al*., 2018).

3.5.2 Effect of Contact Time

A batch adsorption experiment was set up to optimize the effect of contact time on the adsorption of reactive red-120 dye at different time intervals (0, 5, 10, 15, 20, 25, 30, 60, and 90 minutes). At each time interval, an aliquot of the reaction mixture was placed in an Eppendorf tube and centrifuged at 10000 rpm for 10 minutes. The supernatant was then examined with a spectrophotometer at a specific wavelength (RR-120 535 nm). A graph was used to plot the percentage adsorption (Abdelhamid, 2014; Rizzi *et al*., 2014).

3.5.3 Effect of Dye Concentration

To test the effect of increasing dye concentration on the amount of dye adsorption, different concentrations of reactive red-120 dye were prepared (5, 10, 20, 30, 40, 50, 100, and 150 ppm). The absorbance was measured, and the percentage of adsorption was calculated and plotted (Liu *et al*., 2011).

3.5.4 Effect of Adsorbent Dosage

One of the most essential criteria in dye adsorption is the adsorbent dose. It refers to the amount of adsorbent utilized per unit volume of the treated solution (Rápó and Tonk, 2021). The amount of adsorption is heavily influenced by the biosorbent dosage. The volumes used were 0.5, 0.75, 1, 1.25, and 1.5 ml (Rizzi *et al*., 2014; Sylloscolus, 2016).

3.5.5 Effect of Temperature

Temperature effects on reactive red-120 dye adsorption were observed at 25, 30, 35, 40, 45, 50, and 55 °C (Sarim *et al*., 2019; Abdullah *et al*., 2021).

3.5.6 Effect of Agitation speed

The rate of dye adsorption is affected by increasing the agitation speed. This parameter was examined on reactive red-120 dye adsorption at 0, 75, 100, 125, 150, 175, and 200 rpm, respectively. The results were appropriately recorded (Park *et al*., 2010; Hamzeh *et al*., 2012).

3.6 Optimization of Reactive red-120 dye adsorption using Response Surface Methodology (RSM)

Unlike the OFAT, the response surface approach uses a small number of experiments to optimize and study relationships between numerous bioprocess factors (Das & Mishra, 2017; Gopalakrishnan *et al.,* 2020). The RSM is a collection of statistical and mathematical methods that determines the relationship between response and independent variables. The RSM has successfully optimised several parameters in bioremediation processes (Lim *et al*., 2013; Manogaran *et al*., 2021).

The Plackett-Burman design (PBD) and the three-level full factorial design were used in the Response Surface Methodology (RSM) approach. The PBD optimization aimed to find the important parameter(s) for reactive red-120 dye adsorption. To improve the adsorption capacity of the dye by the biosorbent, the significant parameter(s) obtained from the PBD optimization were further optimized using the Three-level full factorial approach (Singh *et al*., 2011; Canizo *et al*., 2019). The experimental design and statistical analysis for this optimization technique were analyzed using Design-Expert 6.0.8 software (Das & Mishra, 2017).

3.6.1 Screening using Plackett-Burman Design (PBD)

According to the software, six independent parameters impacting the adsorption of reactive red-120 dye were evaluated, resulting in a total of 12 unique experimental runs. The 6 significant parameters from the OFAT optimization were used to predict these experiments. The adsorption % was given as the response in the PBD, and each parameter has a high (+1) and low (-1) value. The software was used for the analysis of variance (ANOVA), and the parameters with $p<0.05$ were found to be significant and were further optimized using the three-level- full factorial design (Roy *et al*., 2018; Sivashankar *et al*., 2020). The PBD experimental range and level design for reactive red-120 dye adsorption are presented in **Table 3.1** below:

Table 3.1: Experimental range and level of independent variables tested using the PBD for Reactive red-120 dye

Factors	Variables	Unit	Low level (-1)	High level (+1)
A	Dye concentration	ppm	40	100
B	Contact time	minutes	30	70
C	pH		6	8.5
D	Agitation rate	rpm	100	150
E	Temperature	°C	30	45
F	Adsorbent size	ml	0.5	1.5

3.6.2 Optimization using Three-level Full Factorial Design

Following the PBD optimization, two parameters were determined to be significant and were subjected to three-level full factorial design optimization. The dye concentration and adsorbent amount were significant parameters**.** The high and low levels of the significant parameters were 100ppm and 40ppm (reactive red-120 dye concentration) and 1.5ml and 0.5ml (*Enterobacter* sp MM05 biomass amount). A three-level full factorial design was used to investigate the effect of multiple process variables on the percentage dye removal efficiency (Farooq *et al*., 2017). A total of 20 experimental runs were carried out. All experiments were conducted in triplicate. Each experimental run's adsorption percentage was calculated and recorded as a response variable. The final response predicted by the software was further validated using an experiment (Lim *et al*., 2013).

Validation of Experiment

The predicted adsorption response by the Design-Expert software was validated using the three-level full factorial design results. The values of the most significant parameters were used to validate the experimental results. As a result, the actual percentage adsorption of reactive red-120 dye by *Enterobacter* sp. MM05 was determined and compared to the predicted value.

3.7 Adsorption Kinetics Experiments

A batch kinetics experiment for reactive red-120 dye adsorption was carried out at different dye concentrations based on the results obtained from OFAT and RSM under optimal conditions. The concentrations were 10ppm, 20ppm, 30ppm, 40ppm, 50ppm, 100ppm and 150ppm. The supernatant was examined at various time intervals using a spectrophotometer set to a specific wavelength (RR-120 535nm). Absorbances were recorded and plotted using a graph. For the reactive red-120 dye adsorption kinetics modeling, some previously validated adsorption kinetics models were used (Çelekli *et al*., 2019). The following formula was used to calculate the amount of adsorption at time t, qt (mg/g):

$$q_t = \frac{(C_0 - C_t)}{W} V \qquad (3.2)$$

The pseudo-first-order model (Lagergren, 1898), pseudo-second-order model (Ho & McKay, 1999), and Elovich model (Cope, 1972) were used in this study as adsorption kinetics models. Because linear regression can cause error distortion, the nonlinear forms of these models are better suited for modeling the kinetics of adsorption in the liquid phase than their linear forms.

3.7.1 Pseudo-first-order Kinetics model

The difference between the saturation concentration and the amount of solid adsorption with time is proportional to the rate of change in adsorbate adsorption with time, as shown in the model (Lagergren &Svenska, 1898) It is usually stated as follows:

$$q_t = q_e(1 - e^{-k_1 t}) \tag{3.3}$$

The slope (qe- qt) vs t can be used to calculate the values of k_1 and qe.

3.7.2 Pseudo-second-order kinetics model

The adsorption capacity onto a solid phase is the basis for the pseudo-second-order kinetic model and (Cope, 1972) and Blanchard *et al*. (1984) were the first to propose the nonlinear form of PSO. It is expressed as follows:

$$q_t = \frac{k_t q e^2 t}{1 + k_2 q_e t} \tag{3.4}$$

The slope and intercept of the t/qt vs. t plot yield the values qe and k_2, respectively.

3.7.3 Elovich kinetics model

The Elovich equation is suitable for describing the kinetics of adsorption on heterogeneous solids. It was initially designed to simulate carbon monoxide adsorption on manganese dioxide. The Elovich model (Cope, 1972) is expressed as follows:

$$\frac{dq}{dt} = a \exp(-\beta q_t) \tag{3.5}$$

Where:
α= the initial sorption rate (mg/g min)
β= the extent of surface coverage and
a=activation energy for chemisorption (g/mg)

3.8 Biosorption Isotherm Model

The isotherm describes the relationship between the amount of dye adsorbed and the dye concentration remaining in a solution at a constant temperature under specified conditions. Following a batch adsorption experiment at various

dye concentrations (10, 20, 30, 40, 50, 100, and 150 ppm), isotherm models such as Langmuir, Freundlich, and BET were used to determine the best isotherm model for the adsorption of reactive red-120 dye (Nguyen *et al.*, 2016; Velkova *et al*., 2018; Sarim *et al*., 2019).

Below is the Langmuir equation:

$$q_e = \frac{q_{mL} b_L C_e}{1 + b_L C_e} \tag{3.6}$$

Where:
qe= equilibrium dye of the adsorbent (*mg/g*)
q_{mL}= monolayer capacity of the adsorbent (*mg/g*)
C_e= equilibrium dye of the sorbate (*mg/L*)
b_L= Langmuir constant

The Freundlich isotherm model, on the other hand, describes the sorbent surface as a non-uniform system with varying sites of different affinities (Velkova *et al*., 2018). The equation is as follows:

$$q_e = K_F C_e^{\frac{1}{n_F}} \tag{3.7}$$

Where:
qe= equilibrium dye of the adsorbent (*mg/g*)
C_e= equilibrium dye of the sorbate (*mg/L*)
K_F= Freudlich constant

The BET isotherm describes multilayer adsorption at the adsorbent surface using the Langmuir equation for each layer (Gadd, 2009 ; Asgher, 2012). Another assumption is that a layer does not have to be completed before the next layer can be built. The equation is as follows:

$$q_e = \frac{q_{mBET} \alpha_{BET} C_e}{(1 - \beta_{BET} C_e)(1 - \beta_{BET} C_e + \alpha_{BET} C_e)} \tag{3.8}$$

The choice of a Kinetic or an isotherm model for biosorption data is primarily determined by the goodness of curve fitting, which is typically assessed using statistical analysis (Gadd, 2009). Curve-Expert software was used to fit all curves.

3.9 Biosorption Thermodynamic studies

The effect of temperature on the adsorption of reactive red-120 dye was investigated using batch adsorption experiments at various temperatures (30, 35, 40, 45, and 50 °C). In thermodynamic batch adsorption studies, dye concentrations of 10, 20, 30, 50, and 100 mg/L were used. The results were

processed according to previous literature by determining the thermodynamics parameters (Tran et al., 2016; Monte *et al*., 2017; Shukor, 2020). Gibbs free energy change (*ΔG*), enthalpy change (*ΔH*), and entropy change (*ΔS*) were the thermodynamic parameters. The equations for thermodynamic studies are as follows:

$$\Delta G° = -RT\ ln\ KL \tag{3.9}$$

$$\Delta G° = \Delta H - T\Delta S° \tag{3.10}$$

$$K_C \approx \frac{K_L\left(\frac{L}{mol}\right) \times C^{\circ}\left(\frac{mol}{L}\right)}{\gamma} \tag{3.11}$$

$$lnK_C = \frac{-\Delta H^{\circ}}{R} \times \frac{1}{T} + \frac{\Delta S^{\circ}}{R} \tag{3.12}$$

R=Universal gas constant=0.00831Kj/mol x K

The van't Hoff equation was used to calculate the adsorption thermodynamics parameters (*ΔG°, ΔH°,* and *ΔS°*) using thermodynamic laws. The free energy change (*ΔG*) is nearly zero when adsorption reaches equilibrium. Equation (**3.11**) becomes (**3.12**) which is commonly used to calculate *ΔG°* (standard Gibbs energy change).

The Langmuir equation (**Equation 3.11**) was derived first from a kinetic analysis and then from a thermodynamic evaluation. The proper study of the equilibrium constant between two phases, K_C, is directly dependent on the accurate determination of thermodynamic parameters (Tran *et al*., 2016).

$$q_e = \frac{q_{mL} K_L C_e}{1 + K_L C_e} \tag{3.13}$$

3.10 Biosorbent Characterization

Biosorbent properties such as physical and biochemical properties must be investigated to identify the characteristics of the adsorbent surface (bacterial biomass). A Fourier Transform Infrared Spectroscopy (FTIR) and a scanning electron microscope (SEM) experiment were used to investigate the surface behavior of the biosorbent.

3.10.1 Fourier Transform Infrared Spectroscopy (FTIR)

Fourier-transform infrared (FTIR) spectroscopy is a powerful analytical technique that can be used to identify and characterize bacterial biomass. The technique is based on the principle that different molecules absorb light at different frequencies, which can be used to identify them. By detecting the absorption of infrared radiation by the chemical bonds in the sample, FTIR spectroscopy can be used to assess the composition of bacterial biomass (Michael *et al*., 1994).

To identify the functional group, Fourier transform infrared (FTIR) analysis was used to characterize the structure of the bacterial biosorbent (*Enterobacter sp.* MM05). Bacterial biomass treated with reactive red-120 dye and untreated biomass was harvested, washed, and oven-dried at 60ºC for 48 hours. The biomass was ground and sieved to a small size before being sent for FTIR analysis (Huang *et al*., 2013; Sheshdeh *et al*., 2014; Sudha *et al*., 2018). The measurements were taken between 400-4000 cm-1 to detect the functional groups and types of existing bonds in the dyes. FTIR spectroscopy investigations with attenuated total reflectance (ATR) were carried out using Bruker Optics Korea Co., Ltd.'s VERTEX 80v equipment. Adsorption occurs in the infrared (IR) region as a result of the rotational and vibrational displacement of molecular groups and the chemical bond of a molecule. The dry mixture was compressed and then homogeneously ground with potassium bromide (KBr) to produce a thin and fine pellet, which was then scanned using absorption spectra ranging from 400 to 4000 cm^{-1}.

3.10.2 Scanning Electron Microscopy (SEM)

Scanning electron microscopy (SEM) is an efficient method for characterizing bacterial biomass. It gives high-resolution images of the surfaces of bacterial cells, which can be utilized to investigate the morphology, size, and shape of the cells. SEM can also be used to investigate the distribution of bacteria in a sample as well as the interactions between bacteria and other materials (Ayeni *et al*., 2020).

The surface morphology investigation was performed using a field emission scanning electron microscope (FESEM, LEO1455) with operating data, 20.0 kV, 13.0 mm working distance, and accelerating capacity. Before placing the samples on the plate-stub, FE-SEM samples were cut into minute pieces following the protocol. An SEM-Coating System Machine was used to connect samples to the sample container and coat them in gold before scanning. Several SEM micrographs were obtained with a magnification and size range of 500 - 5000x.

3.11 Statistical and Error Function Analysis

Experiments were conducted in triplicate to ensure accuracy. The experimental errors were represented as standard deviations in an error bar format, corresponding to three distinct determinations. A one-way ANOVA (with a 95% confidence interval) was used to examine the difference between variables, with *a p*-value <0.05 considered statistically significant. The kinetic and isotherm models were determined using the Bayesian Information Criterion (BIC), the Akaike Information Criterion (AICc), the Hannan-Criterion Quinn's (HQ), the Bias Factor (BF), the Root Mean-Square Error (RMSE), the Accuracy Factor (AF), and the adjusted Determination Coefficient (R^2).

The root mean square error (RMSE) was determined by Motulsky and Ransnas (1987), and it was predicted that a smaller number of parameters would result in a lower RMSE value than a larger number of parameters. The letter *n* represents

the number of experimental data points. The letters Ob_i and Pd_i represent the experimental and predicted data, respectively, while the letter p represents the number of parameters.

$$RMSE = \sqrt{\frac{\sum_{i=1}^{n}(Pd_i - Ob_i)^2}{n-p}} \tag{3.14}$$

Because the coefficient of determination, or R^2, does not account for the number of parameters in models, the modified R^2 is used to address this problem. The variance of the y-entire variable is represented by the symbol s^2_y, and the residual mean square (RMS) is a measure of that variance (Equation 29 and 30).

$$Adjusted\left(R^2\right) = 1 - \frac{RMS}{s_Y^2} \tag{3.15}$$

$$Adjusted\left(R^2\right) = 1 - \frac{\left(1-R^2\right)(n-1)}{(n-p-1)} \tag{3.16}$$

The Akaike Information Criterion (AIC) is an information theory-based criterion that addresses the trade-off between model fit and model complexity (Akaike, 1974). It is used to analyze data with fewer or more parameters (Korner-Nievergelt *et al.,* 2015*)*. AICc is calculated as follows, as shown in **equation 3.1**

$$AICc = 2p + n\ln\left(\frac{RSS}{n}\right) + 2(p+1) + \frac{2(p+1)(p+2)}{n-p-2} \tag{3.17}$$

Where p represents the number of parameters and n represents the number of data points. The model with the lowest AICc value is more likely to be correct. Accuracy Factor (AF) and Bias Factor (BF) are statistical evaluations of models derived from the Ross's work to test the goodness-of-fit of the models and were calculated as follows:

$$\text{Bias factor} = 10^{\left(\sum_{i=1}^{n}\log\frac{(Pd_i/Ob_i)}{n}\right)} \tag{3.18}$$

$$\text{Accuracy factor} = 10^{\left(\sum_{i=1}^{n}\log\frac{|(Pd_i/Ob_i)|}{n}\right)} \tag{3.19}$$

3.12 Fitting of the Data

The kinetics and isotherm nonlinear data were fitted using CurveExpert Professional software, Version 2.6, using Marquardt nonlinear regression.

CHAPTER 4

RESULTS AND DISCUSSION

4.1 Screening for Dyes and Bacterial biomass

The source of the bacterial isolates was the Juru river banks in Pulau Penang, Malaysia (Manogaran *et al*., 2021). The screening results of the twelve (12) different bacterial isolates against the reactive red-120 dye are shown in Figure 4.1. The adsorption percentages of the reactive red-120 dye vary between isolates as follows; Isolate 34XR (62.50%), Isolate 34XW (57.14%), Isolate 52 (37.5%), Isolate 2 (67.86%), Isolate 1 (35.71%), Isolate 29 (19.64%), Isolate 7 (41.07%), Isolate 8 (12.5%), Isolate 4 (28.57%), Isolate 5.2 (50.00%), Isolate 30 (1.79%) and Isolate 5.1 (60.71%). Among the other eleven (11) isolates, Isolate 2 had the highest adsorption percentage of 67.86%. However, all isolates demonstrated the ability to adsorb the reactive red-120 dye from the solution. It has been reported that most of these isolates can either decolorize or proliferate when exposed to reactive red-120 dye (Manogaran *et al*., 2021). Furthermore, several previous studies have reported the potential of bacterial biomass in the adsorption of various dyes (Vijayaraghavan & Yun, 2007; Cheng *et al.,* 2020).
In a study conducted by Wang *et al.* (2009), *Enterbacter* sp. was used to decolorize reactive black 5 dye with the maximum decolourization efficiency of 92.56%. The bacterial isolate (Isolate 2) employed in the adsorption of reactive red-120 dye was recently identified and characterized by Manogaran *et al*., (2021). The isolate was a bacterium that is Gram- negative, oxidase-negative, indole-negative, methyl red-negative and Voges-Proskauer-positive that is rod-shaped and live in water, sewage, soil, plants, human and animal faeces. The characterization of the isolate was done using 16S-ribosomal RNA sequencing technique with the gene sequence of 1,439bp linear DNA and accession number: MW031860.1 GI: 1908125037 (Manogaran *et al*., 2021). Bacteria are such groups of microorganisms that are ubiquitous and can be used as inexpensive biosorbent in the removal of pollutants such as dyes and heavy metals. A recent study carried out by (Hasyimah *et al.*, 2021) reported the potentiality of the dead cells of filamentous bacterium (*Aureispira sp*.) in the biosorption of congo red dye and some heavy metals.

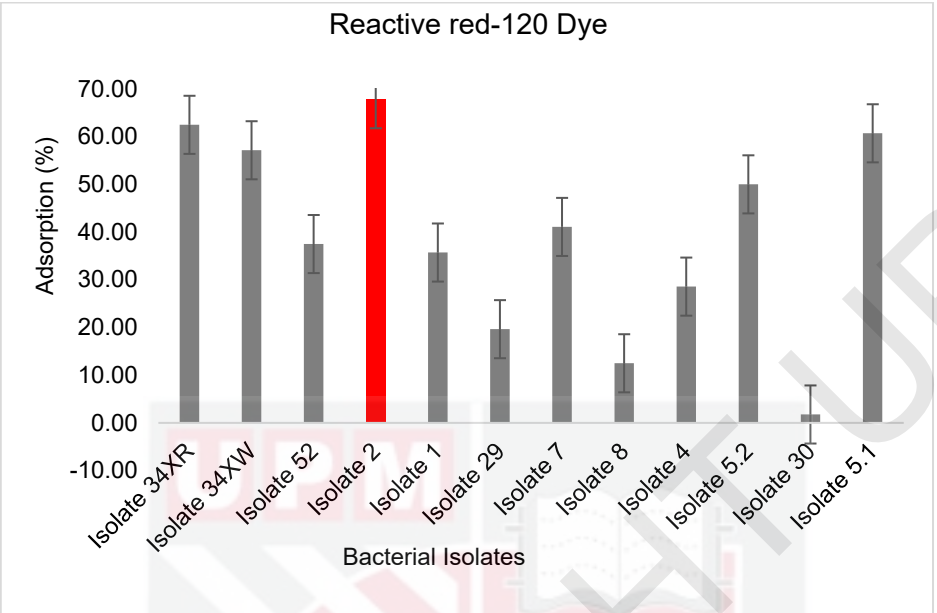

Figure 4.1: Screening result of the adsorption percentage of twelve (12) different bacterial isolates against reactive red-120 dye

4.2 Optimization of Reactive red-120 dye adsorption using One-factor-at-a-time (OFAT) method

The One-Factor-At-A Time (OFAT) method is a fundamental approach that has been widely used in scientific and engineering research. The method is carried out by varying one-factor level at a time while keeping the other factor levels constant (Yuangyai & Nembhard, 2014). The technique was used to investigate the effect of various environmental factors on the adsorption of reactive red-120 dye. The optimum adsorption capacity of 42.14% was obtained at 50ppm.

4.2.1 Initial Dye Concentration Effect

Dye removal becomes more dependent on the initial dye concentration as the number of adsorption sites decreases at increasing concentrations (Santos & Boaventura, 2008). The effect of initial dye concentration on the adsorption of reactive red-120 by the biomass of *Enterobacter sp* MMO5 was investigated using a batch experiment at different concentrations of reactive red-120 dye (5 to 150ppm) as shown in **Figure 4.2.** The percentage adsorption decreases as the concentration of reactive red-120 dye increases. As the surface saturation of the binding site on the biosorbent increased with dye concentration, the adsorption potential decreased (Velkova *et al*., 2018).

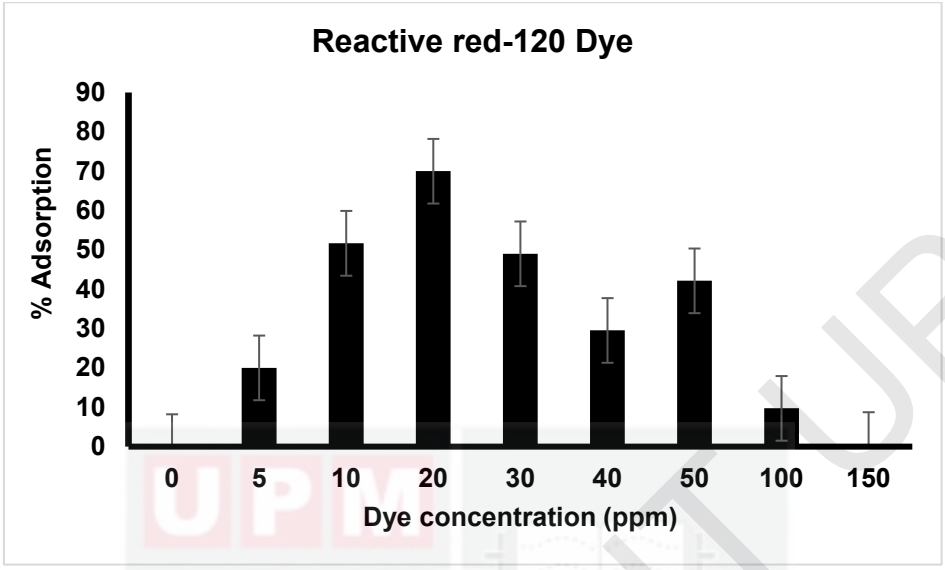

Figure 4.2: Effect of dye concentration on reactive red-120 dye adsorption by the biomass of *Enterobacter* sp. MM05

4.2.2 Effect of pH

The chemistry of the dye solution and the activity of the functional groups in the biosorbent are both affected by the pH, which impacts how structurally stable dye molecules are (Cheruiyot *et al*., 2019). The structures of the dyes and the adsorbent have an impact on the interaction between the adsorbate and adsorbent in the dye removal process. Additionally, two main categories can be distinguished: basic (cationic) and acidic (anionic) dyes. These two categories greatly complicate the process of determining pH in dye adsorption studies. When the surface charge is dependent on variations in the solution, the adsorbent charge is initially amphoteric (Tran *et al*., 2020). As shown in **Figure 4.3**, the percentage adsorption capacity is higher at pH 6.5 (47.77%) and lower at pH 7.5 (30.45%). The percentage of dye removal, however, significantly declines as the pH of the solution rises further to 8.5.

At low pH levels, the surface of the biosorbent is typically positively charged, which inhibits the biosorption of cationic species. However, as the pH of the solution rises, the surface of the biosorbent changes to a negatively charged state, which results in electrostatic interactions between the oppositely charged sorbate and sorbent (Huang *et al*., 2017; Velkova *et al*., 2018). Adsorption of basic dyes increases as the pH of the solution rises, whereas adsorption of acidic dyes decreases as the pH of the solution rises (Velkova *et al*., 2018). Reactive red-120 dye is an acidic azo dye that is proven to exhibit that character. Numerous studies have shown that regardless of the bacteria, fungi, algae, or yeast, the optimal pH for the majority of biosorbents appears to be slightly acidic

to neutral pH (4-7) (Huang et al., 2017; Ribas *et al*., 2020). Liu and Wang, (2008) have reported that the biosorption ability of dyes and metal cations increases linearly with increasing pH of the biosorption system, but not linearly with increasing pH of the biosorption system.

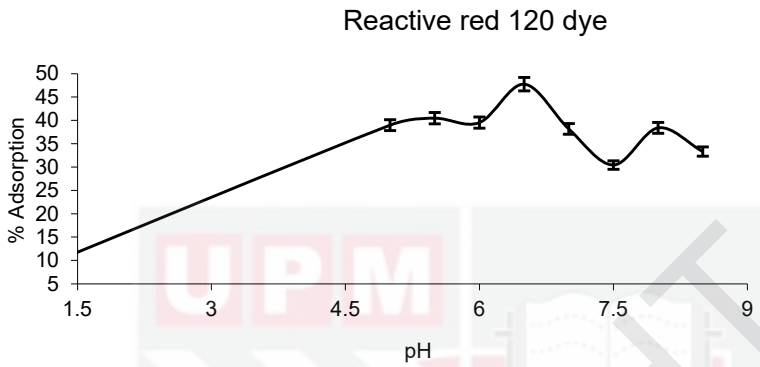

Figure 4.3: Effect of pH on the Adsorption of Reactive red-120 dye by the biomass of *Enterobacter* sp. MM05

4.2.3 Temperature Effect

Figure 4.4 depicts the effect of temperature on the adsorption of reactive red-120 dye at 25, 30, 35, 40, 45, 50, and 55 °C (Liu *et al.,* 2018). The supernatants were analysed as previously described in **Chaper 3**. The dye removal efficiency was optimum at temperatures ranging from 40 to 45 °C (31-51%). Several studies have shown that dye adsorption increases with increasing temperature due to the faster rate of diffusion provided by higher temperatures. As shown in **Figure 4.4** below, as temperature increases, the adsorption percentage increases, and the optimum temperature is attained at 45ºC. This is as a result of chemical reaction that has taken place between the adsorbate (reactive red-120 dye) and adsorbent (*Enterobacter sp.* MM05 biomass). In contrast to this finding, an increase in temperature lead to the decrease of adsorption capacity especially in physical adsorption as a result of the increase in the kinetic energy of the molecule. As reported by Bayramoglu and Yilmaz (2018) in their research finding, the solubility and chemical potential of the adsorbate are related to temperature as higher temperature facilitates the adsorption of pollutants on adsorbent because the mobility of substance interacts more effectively with the functional groups which enhances the rate of protonation and deprotonation on the adsorbent.

Similarly, in a research finding reported by Sheshdeh *et al*. (2014), an increase in temperature increases the adsorption percentage in the biosorption of Basic-red dye by nickel oxide nanoparticles.

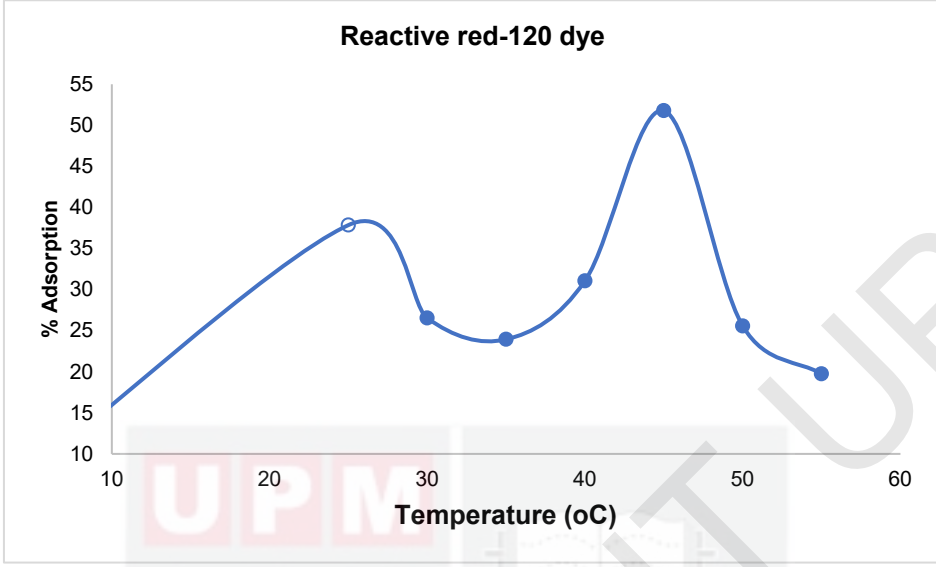

Figure 4.4: Effect of Temperature on the Adsorption of Reactive red-120 dye by the biomass of *Enterobacter* sp. MM05

4.2.4 Effect of Agitation Speed

The rate of agitation is an important parameter in adsorption. It affects the solute distribution in the bulk solution as well as the formation of the exterior boundary film. In general, the degree of agitation affects the rate of dye adsorption and adsorption increases as the stirring rate increases. The agitation rate reduced boundary layer resistance and increased system mobility. (Zhu *et al*., 2010). The effects of agitation rate on the adsorption of reactive red-120 dye by *Enterobacter sp.* MM05 were studied from 0 to 200 rpm as shown in **Figure 4.5.** Based on this finding, the adsorption capacity is higher at 150rpm and lower at 200rpm (**Figure 4.5**). Therefore, the adsorption capacity increases from 0 to 150rpm and decreases as the speed increases.

Similar studies conducted by Shroff and Vaidya, (2011) demonstrated how the rate of sorbent/sorbate agitation (60–210 rpm) affected the adsorption of Ni (II). At higher agitation speeds, the sorption capacity decreased while the removal efficiency increased to 150 rpm (15.83 mg/g). The reason is that agitation encourages proper interaction between metal ions and biomass binding sites. This lessens the thickness of the exterior mass transfer barrier surrounding the adsorbent particles, facilitating the transport of sorbate ions to the sorbent sites. Contrary to this finding, Mahmoud *et al*. (2017) reported the maximum removal efficiency (80.8%) at an agitation speed of 250rpm. This could be attributed to the dispersal of the adsorbent particle. Furthermore, in a research conducted by Long *et a*l. (2017) ,it was found that the agitation speed of 120rpm was enough to guarantee the availability of every surface combining site needed for *B. cereus*

to adsorb S_r (II) ions to their maximum potential. The mass transfer resistance around the adsorbent particles can be reduced with appropriate agitation, making it easier for the metal ions and binding sites to make contact. Lower biosorption at a slower rotation speed was likely caused by insufficient contact with the adsorbent particles, which caused the particles to stick together.

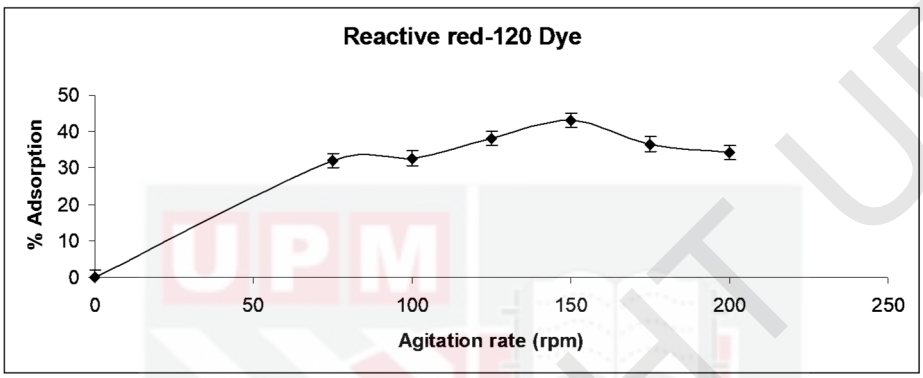

Figure 4.5: Effect of Agitation Speed on the Adsorption of Reactive red-120 by the biomass of *Enterobacter* sp. Strain MM05

4.2.5 Effect of Contact Time

As shown in **Fig. 4.6**, the time significantly impacts the adsorption of reactive red-120 dye. The dye adsorption was quite rapid in the first 30 minutes, then gradually increased as the contact time was increased. There was no discernible variation in adsorbed dye after 60 minutes of contact time. Based on this finding, the equilibrium time in batch adsorption experiments was set at 60 minutes (Mohammadi *et al*., 2011). Adsorption capacity generally increases with increasing time until it reaches an equilibrium where no more dye can be adsorbed from the solution. The amount of the dye adsorbed represents the maximum dye adsorption capacity of the adsorbent (bacterial biomass) and the equilibrium time is the time necessary to reach the state of equilibrium (Chatterjee *et al*., 2010). To study the effect of contact time on the adsorption of reactive red-120 dye by the biomass of *Enterobacter sp.* MM05, an experiment was conducted at different intervals (5, 10, 15, 20, 25, 30, 60 and 90 minutes) and the highest adsorption capacity was obtained at 60 minutes (1 hour). This finding is in agreement with the study conducted by Mohammadi *et al*. (2011), where they found the equilibrium time of the adsorption at 60 minutes.

In contrast to this finding, Huang *et al*. (2016) have found the optimum adsorption capacity of 98% on the biosorption of reactive black 5 dye by the biomass of Aspergillus versicolor at 420 minutes (7 hours). This could be attributed to the composition of the biomass as fungi are eukaryotes while bacteria are prokaryotes.

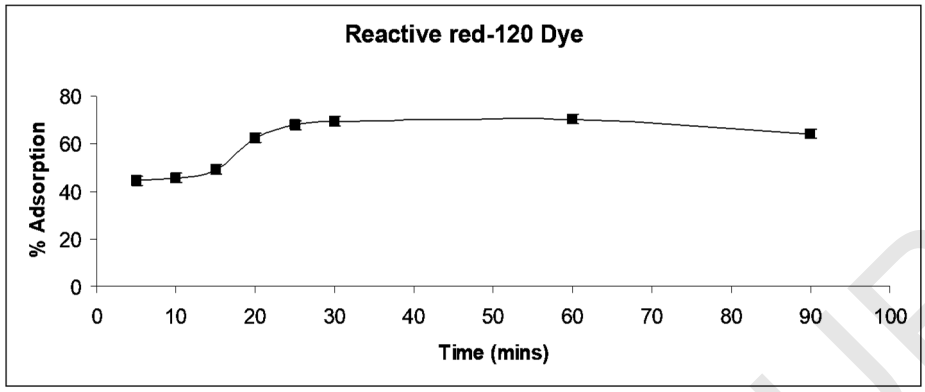

Figure 4.6: Effect of Contact Time on the Adsorption of Reactive red-120 dye by the biomass of *Enterobacter* sp. Strain MM05

4.2.6 Adsorbent dosage effect

The percentatge of adsorption is heavily influenced by the dosage of the biosorbent. As the amount of biosorbent increased, the adsorption efficiency of the biomass increased, resulting to an increase in adsorption percentage, as shown in **Figure 4.7**. (Rizzi *et al*., 2014). The adsorbent amounts used are as follows: 0.5ml, 0.75ml, 1.0ml, 1.25ml and 1.5ml. As reported by Mane *et al*. (2008), the greater the surface area, the greater the availability of adsorption sites.

In a related research conducted by Sulak and Yatmaz (2012), it was observed that the uptake of increased with increased biosorbent dosage from 0.25 to 3.0g with removal efficiency of 93%. Increased percentage of removal may be attributed to an increase in adsorbent surface areas and, as a result, more active functional groups, resulting in the availability of more adsorbent surfaces. Because unsaturated adsorption sites were present throughout the adsorption process, increasing the amount of biosorbent had a negative effect on the sample's absorbance capacity. A research on the removal of cationic dyes from aqueous solution using an alternative adsorbent reported that the removal of those dyes increased with decrease in particle size which may be attributed to the fact that smaller particles yield large surface areas (Santhi *et al*., 2016).

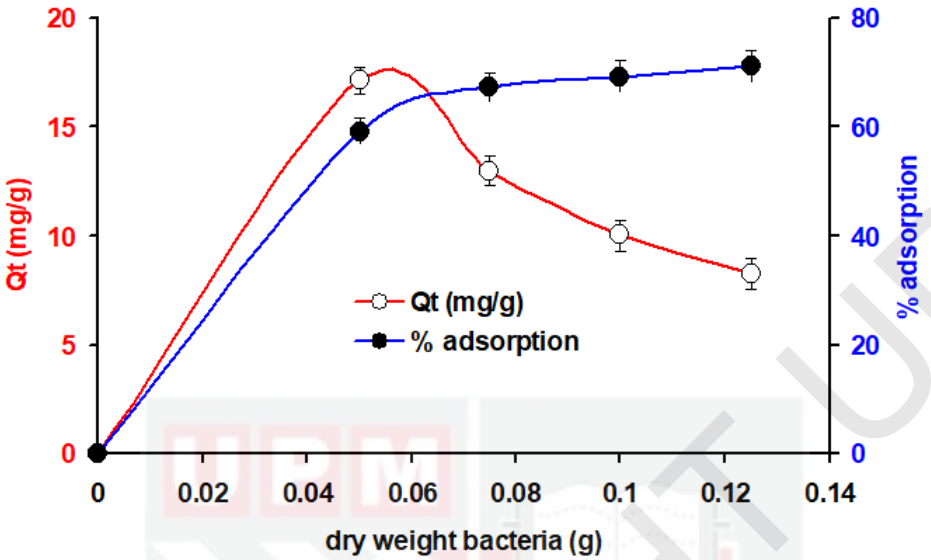

Figure 4.7: Effect of Adsorbent dosage on the adsorption of Reactive red-120 Dye by the biomass of *Enterobacter* sp. MM05

4.2.7 OFAT Results Summary

The optimal conditions for the reactive red-120 dye adsorption optimization using one factor at a time by the biomass of *Enterobacter sp*. strain MM05 are listed in **Table 4.1**. The parameters that were optimized were; temperature, contact time, dye concentration, pH, agitation speed, and adsorbent amount. The optimum conditions adsorption were as follows; 60 minutes (contact time), 50 ppm (dye concentration), 6.5 (pH), 150 rpm (agitation speed), 1.5 ml (adsorbent amount), and 45°C (temperature).

The effectiveness with which an azo dye decolorizes is highly dependent on the type of nutrients and the quantity of the inoculum used, according to several pieces of literature that reported different optimization condition ranges for dye adsorption parameters. They used a one-factor-at-a-time approach to investigate the effect of various parameters on dye removal (Lim *et al.*, 2014; Sharma *et al*., 2016; Manogaran *et al*., 2021). A study conducted by Mawad *et al*. (2021), reported the optimum conditions of pH, temperature, adsorbent dosage, contact time and initial dye concentration of which environmental conditions played a significant role in adsorption process. Similarly, Nath *et al*. (2015) reported the optimum conditions of contact time (360 minutes), temperature (30^{o}C), biomass concentration (0.5 g/L) and initial dye concentration (100mg/L) in the adsorption process. As many researchers reported the impact of environmental factors in enhancing the adsorption process, this finding as well is not an exception. **Table 4.1** below, shows a summary of OFAT parameters and their optimum conditions.

Table 4.1: OFAT Parameters and their Optimum Conditions

	Parameter	Optimum conditions
1.	Dye concentration	50ppm
2.	Temperature	45°C
3.	pH	7.5
4.	Adsorbent amount	1.5ml
5.	Agitation speed	150rpm
6.	Contact Time	60minutes

4.3 Optimization of Reactive red-120 dye adsorption using Response Surface Methodology (RSM)

The optimal conditions of the adsorption of reactive red-120 dye were further determined using the Plackett Burman Design and Three-level Full Factorial Design.

4.3.1 Screening using Plackett Burman Design (PBD)

A Plackett-Burman design is a popular type of screening design developed by R.L. Plackett and J.P. Burman in 1946. It was designed to enhance the quality control process so that intelligent decisions could be made by studying the effects of design parameters on the system state (Vanaja & Rani, 2007). In this study, the software, Design Expert 6.0.8 was used to select and screen the significant variables that influence the adsorption of reactive red-120 dye. The variables that showed significant impacts on the dye adsorption process were selected. They include; pH, temperature, adsorbent dosage, agitation speed, concentration, and contact time. There were a total of 12 separate tests carried out in the PBD using the stated variables, as shown in **Table 4.2** below. The ranges used for each independent variable used were based on the ranges used in OFAT.

Several researchers have reported the utilization of PBD as an alternative method for experimental design in for optimization. Karlapudi *et al*.(2018) in their research finding, reported the use PBD in their work, where the PBD was chosen to screen the important fermentation process components in relation to their effects. Furthermore, Ameenudeen *et al*. (2021) reported the employment of PBD in their research finding. Manogaran et al. (2018) reported the use of PBD in the optimization of culture composition in a study on glyphosate degradation by *Burkholderia vietnamiensis* strain AQ512. Both the experimental design and the statistical analysis of the data collected in this study were carried out using Design Expert software version 6.0.8. According to the design matrix for screening significant variables, run 6 had the lowest RR-120 dye adsorption (7.34%), while run 11 had the highest (57.36%).

Table 4.2: PBD and Reactive red-120 Dye Adsorption Percentage in 12 Experimental Runs

Run	A: Dye conc. (ppm)	B: Contact Time (mins)	C: pH	D: Agitation (rpm)	E: Temperature (°C)	F: Adsorbent size (ml)	% Adsorption
1	100	20	8	100	45	1.5	24.80
2	100	20	4	150	25	0.5	9.22
3	40	5	4	100	25	0.5	20.93
4	40	20	8	150	25	1.5	46.67
5	100	5	8	150	25	1.5	26.59
6	100	20	4	150	45	0.5	7.34
7	100	5	8	100	25	0.5	10.98
8	40	5	4	150	45	1.5	47.67
9	40	5	8	150	45	0.5	21.25
10	100	5	4	100	45	1.5	28.04
11	40	20	4	100	25	1.5	57.36
12	40	20	8	100	45	0.5	25.00

Table **4.3** displays the analysis of variance (ANOVA) and regression analysis of the first-order model. The initial dye concentration (A) and adsorbent amount (F) were discovered to be significant. As a result, they were further investigated using the Three-level Full Factorial Design.

Table 4.3: Analysis of Variance (ANOVA) from PBD for Reactive red-120 Dye Adsorption

Source	Sum of Squares	*df*	Mean Square	*F*-Value	Prob > F	
Model	2275.48	6	379.25	3.81	0.0818	not significant
A	651.07	1	651.07	6.54	0.0508	
B	37.14	1	37.14	0.37	0.5681	
C	142.07	1	142.07	1.43	0.2858	
D	67.17	1	67.17	0.67	0.4488	
E	453.5	1	453.50	4.56	0.0859	
F	924.53	1	924.53	9.29	0.0285	
Residual	497.76	5	99.55			
Cor Total	2773.24	11				
Std. Dev.	10.03748		R-Squared	0.9654		
Mean	20.1375		Adj R-Squared	0.9545		
C.V.	49.84471757		Pred R-Squared	0.9234		
PRESS	234.63		Adeq Precision	15.5400		

In their research finding, Venkataraghavan *et al*. (2020) employed PBD to optimize the adsorption of dye effluents and significant factors responsible for the adsorption were; time, pH and dye concentration. The predicted and experimental values were found to be in agreement and the coefficient of determination value (0.9935) and adjusted coefficient determination value (0.9818) indicated that the model was significant. For this, they employed Box-Behnken (BB) design for further optimization. In contrast, this finding showed that only two factors were significant (adsorbent amount and dye concentration). Therefore, a Three-level full factorial was used to further optimize the adsorption. **Figure 4.8** below shows the similarity plot between the actual and predicted adsorption values for the reactive red-120 dye adsorption using the biomass of *Enterobacter sp*. Strain MM05 in PBD:

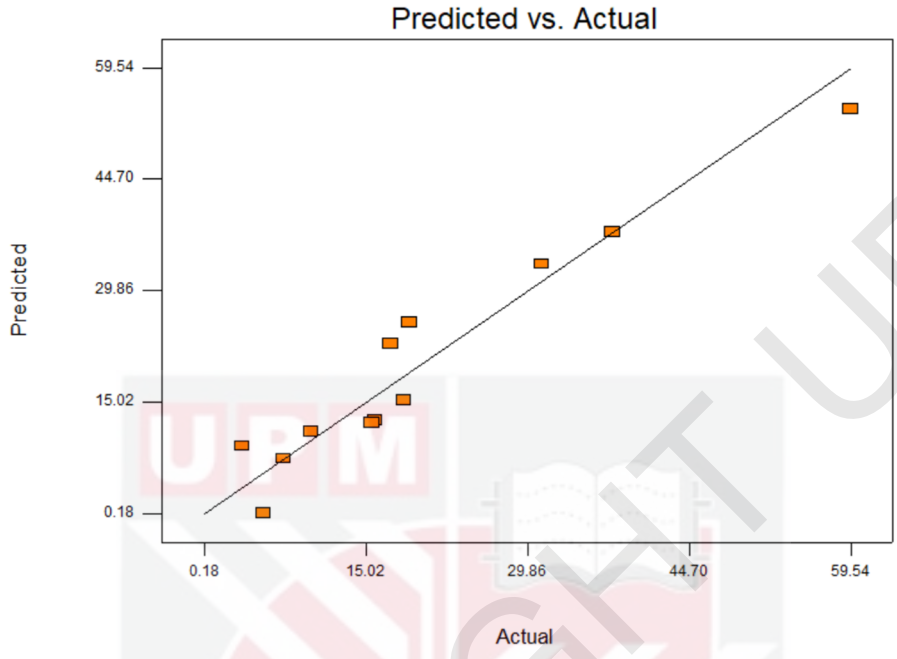

Figure 4.8: PBD similarity plot of actual and predicted adsorption values for Reactive red-120 dye adsorption by *Enterobacter* sp. MM05

4.3.2 Adsorption optimization for reactive red-120 dye using a Three-level Full Factorial Design

A Three-level Full Factorial Design is an experimental design with two or more factors, each with discrete possible levels, and whose experimental units take on all possible combinations of these levels across all such factors. A researcher can use this factorial design to investigate the effects of each factor on the response variable, as well as the effects of factor interactions on the response variable (Dahbi *et al*., 2016). Using this factorial design, the significant parameters identified in PBD (dye concentration and adsorbent amount) were further optimized. About 13 runs of experiments for the two factors that were significant in PBD (dye concentration and adsorbent amount) at low and high levels were conducted. The highest adsorption capacity (72.65%) of the reactive red-120 dye was recorded in run 3. The coefficient of determination is used to estimate a model's accuracy (R^2). The R^2 value is always between 0 and 1, and its order of magnitude indicates the model's goodness between the predicted and model experimental response variable values (Zhang, 2016). The model's R^2 value was found to be 0.9563 which was close to 1. It shows that there was 95.63% model's behaviour that could be interpreted for the dye adsorption while the model cannot explain the only 4.37% of the full variance. It also revealed that the regression model explained the majority of the data variation.

Additionally, the model's relevance was shown by the relatively high adjusted and predicted R^2 values of 0.9325 and 0.8763 (**Table 4.4**) respectively which demonstrates a strong correlation between the actual and predicted values. The model, therefore, provided a wealth of information regarding the relationship between the response variable and the independent variables. Similar results for the second-order RSM experiments based on Box Behnken and three-level full factorial designs have been reported by other researchers (Salar-García *et al*., 2019; Sivashankar *et al*., 2020 ; Solomon *et al*., 2020). A sufficient degree of precision was used to test the signal-to-noise ratio, which was found to be 14.94 indicating a good signal. The value emphasized the model's significance to the process. In their research finding, Manogaran *et al*. (2018), reported an adequate precision value of 31.14 for statistically optimizing culture composition for glyphosate mineralization by the bacterium *Burkholderia vietnamiesis* strain AQ5-12.

The significance of model parameters is typically determined using the *F*-value or *P*-value. As reported by Hassanzadeh-Tabrizi and Taheri-Nassaj (2011), the higher the size of the *F*-value and correspondingly lesser the "prob > *F*" value, the most essential is the corresponding coefficient. According to the quadratic regression model, the models were highly significant. As shown in **Table 4.5**, the model's *F*-value for the reactive red-120 dye adsorption was found to be 15.98 with a very low probability value of 0.001. Similarly, the model's F-value of this magnitude had a 0.01% chance of occurring due to noise. The 0.0500 values for 'Prob > *F*' indicate that the model terms were significant. Only A and B models were significant for adsorption of Reactive red-120 dye by *Enterobacter sp*. strain MM05 biomass in this case. The lack of fit *F*- and *P*-values of the model were 0.26 and 0.16 respectively which showed that the lack of fit was not significant, indicating that the models were sound without any noise. The model *F*-value slumps precipitously, raising the associated *p*-value slightly above acceptable levels for significance (Anderson and Whitcomb, 2019). **Table 4.4** below shows an experimental plan and result for the optimization of reactive red-120 dye adsorption using three-level full factorial design.

Table 4.4: Experimental plan and Result for the optimization of Reactive red-120 dye Adsorption using Three-level Full Factorial Design

Run	A: Dye concentration (ppm)	B: Adsorbent amount (ml)	Actual value (%)	Predicted value (%)
1	100	1	20.28	26.66
2	70	1	41.92	39.65
3	40	1.5	72.65	73.49
4	70	1	43.43	40.65
5	70	0.5	3.54	4.12
6	70	1	38.13	37.65
7	70	1	43.43	41.47
8	70	1.5	52.27	51.99
9	100	1.5	41.57	41.01
10	100	0.5	8.63	9.01
11	40	1	55.56	57.15
12	70	1	43.43	44.67
13	40	0.5	39.74	38.63

Table 4.5: RSM Analysis of Variance (ANOVA) for the Three-level Full Factorial Design of the Reactive red-120 dye Adsorption

Source	Sum of Squares	*df*	Mean Square	*F*-Value	Prob > *F*	
Model	3872.05	5	774.41	15.98	0.0010	significant
A	1583.30	1	1583.30	32.67	0.0007	
B	2187.91	1	2187.91	45.14	0.0003	
A2	76.38	1	76.38	1.58	0.2497	
B2	62.46	1	62.46	1.29	0.2936	
AB	0.00	1	0.00	0.00	0.9986	
Residual	339.28	7	48.47			
Lack of Fit	233.68	3	77.89	0.26	0.1615	not significant
Pure Error	105.60	4	26.40			
Cor Total	4211.34	12				
Std. Dev.	6.96		R-Squared	0.9563		
Mean	37.88		Adj R-Squared	0.9325		
C.V.	18.38		Pred R-Squared	0.8763		
PRESS	2047.23		Adeq Precision	14.94		

In their research finding titled ,Jadhav *et al*. (2013) employed the Three-level full factorial design for the optimization. They reported that the predicted values were found to be in good correlation with the actual values (R^2= 0. 9997 and predicted R^2= 0. 9984), indicating that the used model was also suitable for optimization. In contrast, the Taguchi technique, machine learning, and artificial neural networks (ANNs) are a few of the different optimization techniques that are available in the literature.

The similarities between the actual and predicted values from the three-level full factorial design for reactive red-120 dye adsorption are shown in **Figure 4.9** below. The predicted model value and the actual value were highly correlated. **Equations 3.4 and 3.5** described these in terms of the actual and coded factors.

$$Y= 47.00-1.36A+76.21B+0.006A^2-19.02B^2+0.004AB \quad (3.4)$$

$$Y=37.65-16.24A+19.10B+5.26A^2-4.76B^2+0.006AB \quad (3.5)$$

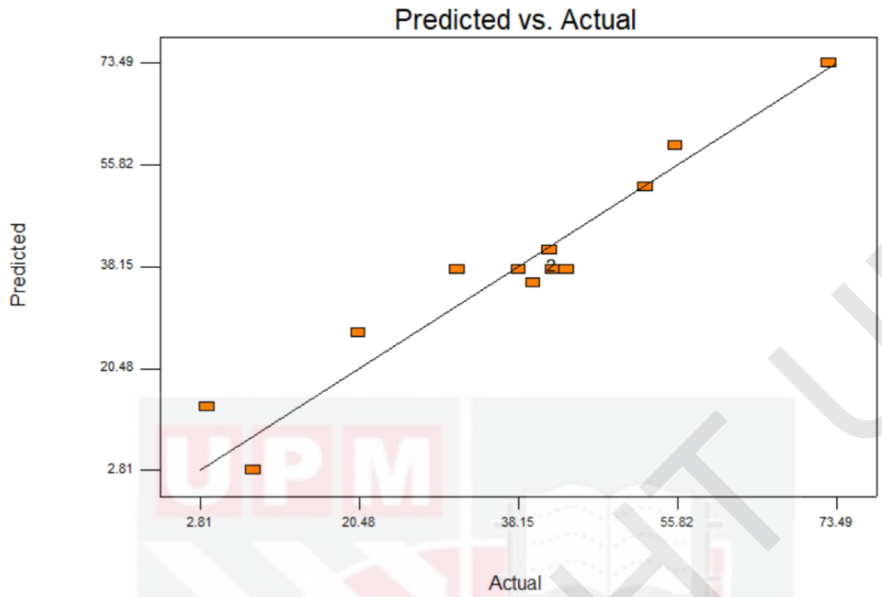

Figure 4.9: Experimental and predicted factors for optimal Reactive red-120 dye adsorption responses

4.3.3 Reactive red-120 dye adsorption 3D response surface plot

The three-dimensional (3D) response surface plots of the dependent variable as a function of two independent factors can provide information on their connections. Furthermore, they can aid in comprehending both the main and interaction effects of these two independent variables (Singh *et al.*, 2011). In order to better understand the effects of the independent factors and their interactions on the dependent variable, 3D response surface plots for the dignified responses were made using the quadratic model. Plots of the 3D response surfaces demonstrate how the three different process parameters affect the response parameter.

Each plot shows the outcome of the interaction between two important independent factors while keeping the other two components under examination constant. The contour of the plot is related to the mutual interaction of the three independent components and their impact on percentage removal. The 3D response surfaces and contour plots of the model of the interactions between significant independent variables (A) dye concentration and (B) Adsorbent amount towards dependent variable (percentage removal) of RR-120 dye from experimental design are shown in **Figure 4.10**.

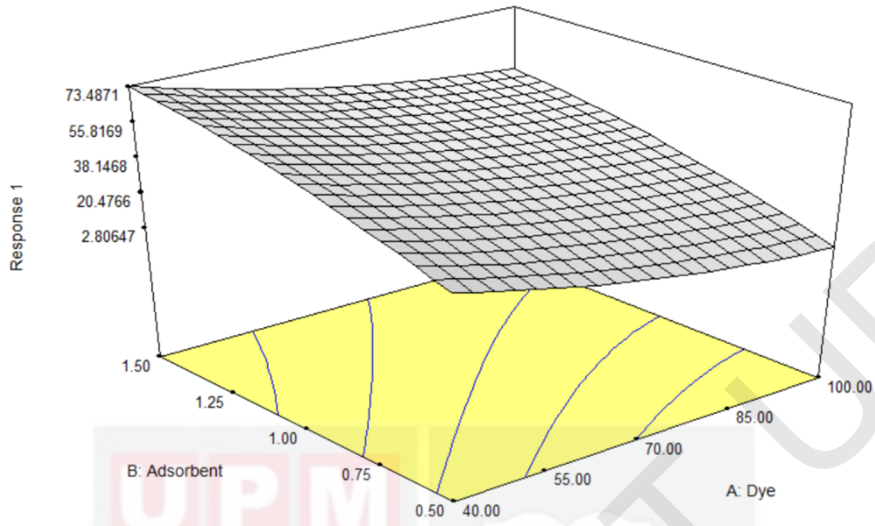

Figure 4.10: Three-Dimensional Response surface plots for Reactive red-120 dye adsorption demonstrating the interactive effects of (A) dye concentration and (B) adsorbent dosage

Several researchers have reported Three-dimensional surface plots on dye adsorption using the three-level full factorial design. In their research finding ,Ashrafi *et al*. (2016) reported the use of three-level factors (pH, initial concentration and adsorbent dosage) in the adsorption optimization and showed the 3D surface plots of the dye adsorption. Similarly, Das and Mishra (2017), have reported the use of 3D surface plots in the their finding. Contrary to this finding, many researchers have employed the use of 3D plots in optimization process using Central Composite Design (CCD) (Sharma *et al.*, 2017; Ahmad *et al*., 2020; Manzar *et al*., 2021).

4.3.4 Validation of RSM

The Three-level Full Factorial Design-RSM result was used to validate the quadratic models. The optimal conditions for reactive red-120 dye adsorption were 48.8 ppm RR-120 dye concentration and 1.38 ml of adsorbent. All other parameters were kept constant based on OFAT because they were not significant in the PBD analysis. RSM therefore, predicted a 37.66% adsorption rate. In order to confirm the outcome predicted by the Three-level full factorial design, an experiment was then conducted using the optimal parameters previously identified. Table 4.5 shows the comparison between the predicted results generated by RSM and those obtained experimentally (41.44%) illustrating no statistically significant difference in adsorption percentage between experimental and predicted values after the t-test (p>0.05).

Many researchers discovered that the observed and predicted values were remarkably similar, implying that RSM was successful

Table 4.6: Comparison of RSM-predicted generated adsorption and experimental results for Reactive red-120 dye

Factors	Name	Predicted levels	Experimental levels
A	Dye conc. (ppm)	48.8	48.8
B	Adsorbent amount (ml)	1.38	1.38
		Predicted	**Experimental**
Response (%)		37.66	41.44

4.4 Determination of Adsorption Kinetic models for Reactive red-120 Dye

The kinetics of an adsorption process crucially describes the rate and mechanism of a reaction. It is reliant on how the adsorbate and adsorbent interact. Given that the best biosorbent for use in adsorption studies must have a rapid and high adsorption capacity rate, the adsorption rate aids in this decision-making (Eris & Azizian, 2017). Additionally, it gives the adsorption process the time it needs to reach equilibrium. As a result, kinetic modeling is essential for research and system development for pollutant removal (Tan & Hameed, 2017). Several models, such as mass transfer and chemical reaction, can be used to express the controlling mechanism of the adsorption process (Miyah *et al*., 2017).

In this study, the adsorption kinetics of reactive red-120 dye were investigated using a batch kinetics experiment at various dye concentrations (10, 20, 30, 40, 50, 100, and 150 mg/L) for about 90 minutes. The analysis of the kinetic studies was done using contact time-dependent of low and high dye concentrations. Based on the OFAT results, all other parameters were kept constant. The pseudo-first-order and pseudo-second-order equations were used to analyze and fit the adsorption data for the reactive red-120 dye using nonlinear kinetic regression. Since the nonlinear regression was performed on the same abscissa as the linear regression plot, it was chosen for kinetic model fitting because it allowed for more precise calculations (Popoola, 2019; Basirun & Shukor, 2021). These are the most commonly used adsorption kinetic models. The models were documented as simple, robust, and capable of fitting experimental biotechnology data and supporting assumptions. It provides a numerical method for fitting adsorption curves, illustrating how biotechnologists approximate adsorption kinetics graphically. The process and adsorption rate could be explained by either the pseudo-first-order or pseudo-second-order models (Neag *et al*., 2019; Paredes-Quevedo *et al*., 2021). However, when compared to the 1st order kinetic model, the 2nd order kinetic model could estimate the adsorption pattern for the entire adsorption period. In many adsorption systems studied, first-order kinetic systems do not fit well across the entire adsorption period and are only applicable to the very early stages of the adsorption process (Moussout *et al*., 2018). Furthermore, the pseudo-second-order equation validates chemisorption as a rate control step in the adsorption process based on the sorption capacity of the solid phase (Aljeboree *et al*., 2017).

Table 4.7: Statistical Analyses of Reactive red-120 dye Adsorption using Kinetic Models

Model	Parameter	SSE	MSE	RMSE	R^2	adR^2	AICc	BIC	HQC	AF	BF
Pseudo-1st order	2	1.036	0.148	0.385	0.923	0.897	-4.660	-15.065	-16.311	1.084	0.938
Pseudo-2nd order	2	0.023	0.003	0.057	0.999	0.998	-39.091	-49.497	-50.743	1.025	1.014

Note:

RMSE	Root mean Square Error
p	no of parameters
adR^2	Adjusted Coefficient of determination
BF	Bias factor
AF	Accuracy factor
AICc	Adjusted Akaike Information Criterion
BIC	Bayesian Information Criterion
HQC	Hannan–Quinn information criterion

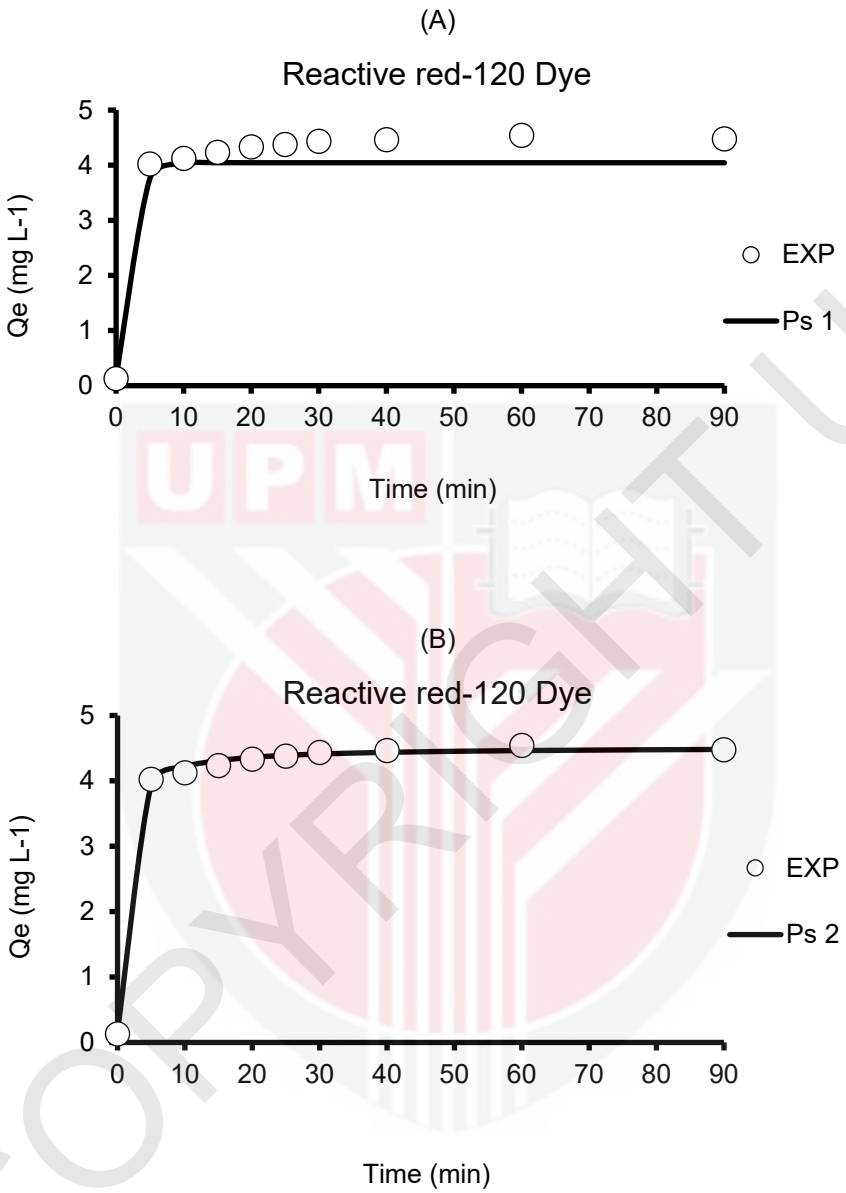

Figure 4.11: Adsorption profile of *Enterobacter* sp. strain MM05 biomass fitted to (A) Pseudo-first order kinetic model and (B) Pseudo-second order kinetic model for Reactive red-120 Dye

Based on the graphs above (**Figure 4.11**) and the table of the error function analysis (**Table 4.7**), the adsorption of reactive red-120 dye by the biomass of *Enterobacter sp*. MM05 is governed by pseudo-second order kinetics model. The finding suggested that adsorption models could be fitted using the pseudo-second-order kinetic model. This is consistent with numerous published studies

that have identified pseudo-second order kinetics as the best model for adsorption studies (Konicki *et al*., 2017; Maguana *et al.,* 2020 ; Lin *et al*., 2020). In their research finding, Gurav *et al*., (2021) reported that the adsorption data fitted best to pseudo-second order kinetics model with R^2>0.99. A similar research finding by Taher *et al*. (2018) reported the fitness of adsorption data to Pseudo-second order kinetics model in their research finding. In contrast to this finding, some researchers have reported the use of kinetic model to describe some scientific researches not necessarily adsorption. For example, Bilehal *et al*. (2001) have reported the use of Pseudo-first order kinetic model to show the reaction dependence on the concentration of permanganate and ruthenium (III) in their research.

Chemisorption is the name given to the rate-controlling phase of the second order reaction, which is connected to chemical reaction. In other words, the reaction's mechanism is chemically controlled. Adsorption kinetics are dominated by two competing reversible 2nd order processes at higher adsorbate or adsorbent ratios (Shukor & Shukor, 2015; Venkata and Lakshminarayanan, 2020).

4.5 Determination of Adsorption Isotherm models for Reactive red-120 Dye

The isotherm investigation provides important physicochemical data for future evaluation of the adsorption process in the laboratory as a single operation. As a result, isothermal studies and isothermal modelling are critical in optimizing the design for any adsorption parameters (Karmakar *et al*., 2019). To select an acceptable model for the process design, accurate equilibrium data that fits appropriately into several isotherm models is required. The variable derived from various models provides critical information about the adsorption process's mechanism, surface properties, and adsorbent affinities that is not available from other sources, such as laboratory experiments. When designing an adsorption system for industrial use, it is critical to have this knowledge. To be most informative about intrinsic kinetics, which is chemical kinetics that occur on the adsorbent surface when there are no transport constraints, the kinetic isotherm should be able to shed light on it (Vijayaraghavan *et al*., 2008; Limbikai et al., 2016; Moldovan *et al*., 2019).

Before any progress can be made in understanding adsorption mechanism pathways and the practical design of systems, adsorption isotherms must be thoroughly understood. When developing the best adsorption process plan, it is critical to determine the most appropriate correlation between the equilibrium curve and the data obtained from measurements (Monte *et al.*, 2017). The adsorption capacity must be precisely defined mathematically in order to generate accurate models about equilibrium adsorption variables and to make quantitative comparisons of the biosorption behaviour of various adsorbent systems feasible (Hu *et al.*, 2018).

Table 4.8: Error function analysis for fitting the isotherm of reactive red-120 dye adsorption

Model	*p*	RMSE	adR2	AICc	BIC	HQC	BF	AF
Henry	1	2.40	-0.41	24.15	18.74	18.10	0.35	3.27
Langmuir	2	0.05	1.00	-49.65	-59.05	-60.31	0.99	1.02
Freundlich	2	0.04	1.00	-51.54	-60.93	-62.20	0.98	1.02
BET	3	0.05	1.00	-41.71	-56.80	-58.70	1.00	1.01
Toth	3	1.15	0.06	21.17	6.08	4.17	0.53	1.94
Sips	3	0.06	1.00	-37.01	-52.10	-54.00	0.68	1.48
F4	4	0.07	1.00	-24.95	-48.74	-51.27	0.61	1.66
F5	5	0.08	1.00	-8.15	-46.63	-49.80	0.68	1.48

Note:

RMSE	Root mean Square Error
p	no of parameters
adR^2	Adjusted Coefficient of determination
BF	Bias factor
AF	Accuracy factor
AICc	Adjusted Akaike Information Criterion
BIC	Bayesian Information Criterion
HQC	Hannan–Quinn information criterion

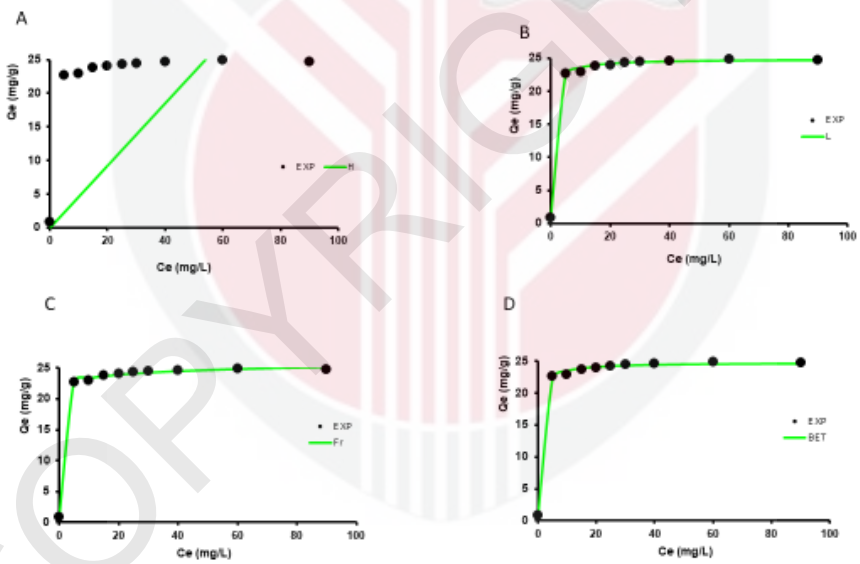

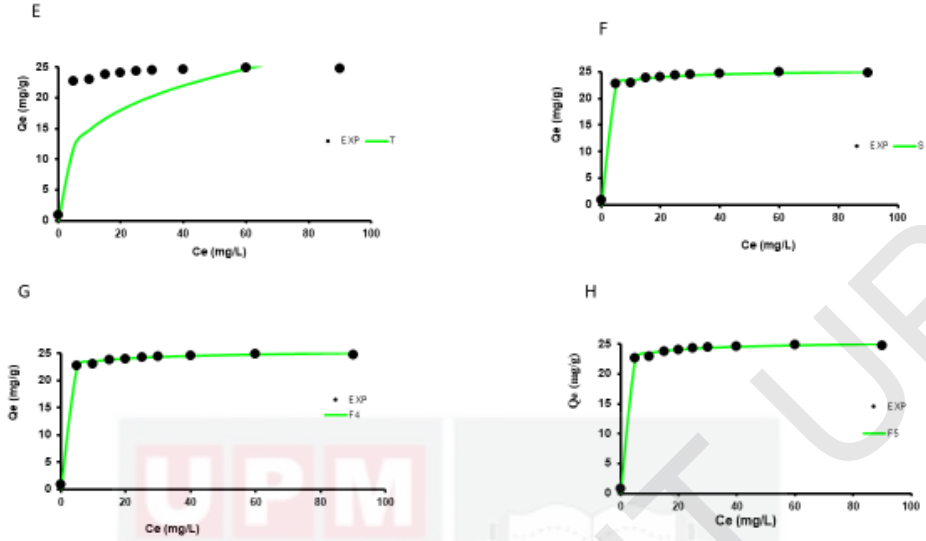

Figure 4.12: Equilibrium biosorption isotherm data of Reactive red-120 dye by *Enterobacter* sp. MM05 modelled using (A) Henry, (B) Langmuir, (C) Freundlich, (D) BET, (E) Toth, (F) Sips, (G) Fritz-Schlunder IV, and (H) Fritz-Schlunder V.

Eight different isotherm models, including Henry, Langmuir, Freundlich, BET, Toth, Sips, Fritz-Schlunder IV, and Fritz-Schlunder V, were used to analyze and fit the equilibrium data from the batch adsorption studies. As shown in **Figure 4.12**, only Henry isotherm model fails to fit the data. The Feundlich model was found to be the best isotherm model through statistical analysis using the corrected Akaike Information Criterion (AICc), root-mean-square error (RMSE), adjusted coefficient of determination (adjR2), accuracy factor (AF), and bias factor (BF). The best isotherm model, as shown in **Table 4.8** above was found to be the Feundlich model after statistical analysis using the corrected Akaike Information Criterion (AICc), root-mean-square error (RMSE), adjusted coefficient of determination (adjR2), accuracy factor (AF), and bias factor (BF). Several researchers have reported Freundlich as the best isotherm model in the adsorption of dyes using different adsorbents. For example, Muthukumaran *et al*. (2016) have reported the fitting of adsorption data to Freundlich isotherm model with the R^2 value of 0.957 in their research finding. Also, Felista *et al*. (2020), have reported Freundlich isotherm as the best model in the adsorption of reactive black 5 using macademia seed husk (a plant adsorbent). Furthermore, Ali *et al*. (2020) reported the fitting of adsorption data to Freundlich isotherm model.

In contrast, many researchers have reported the fitting of adsorption data to other isotherm models such as Langmuir, Toth, BET, etc. For example, Canizo *et al*. (2019) have reported the fiiting of adsorption data to Langmuir isotherm model in their research finding. Similarly, Horciu *et al*. (2020) have reported the fitting

of adsorption data to Langmuir isotherm model in their finding. Research conducted by Rusu *et al*., (2022) reported the fitting of adsorption data to Toth's isotherm model.

4.6 Thermodynamic studies of Reactive-red 120 Dye Adsorption

Establishing the adsorption processes is essential for adsorption research, whether they include chemical or physical adsorption. Van der Waals forces and other relatively weak interactions cause physisorption, whereas stronger chemical bonds and consequent electron transfer between the adsorbent and adsorbate cause chemisorption to occur (Salem *et al*., 2016; Elsherif *et al*., 2021). The thermodynamic characteristics of an adsorption process determine its feasibility and spontaneity. The equilibrium *Kc* constant is essential for calculating these thermodynamic parameters. Gibbs free energy and other thermodynamic properties are calculated using constants derived from various isothermal models, partition constants, and distribution coefficients (Değermenci *et al*., 2019).

In this study, the Langmuir constant, *Kc*, and nonlinear regression of the van't Hoff plot were used to calculate the thermodynamic parameter according to the Nguyen et al. (2020) and Chen *et al.* (2021) methods. Despite the linearized variant frequently being used, the nonlinear van't Hoff plot was used in this study. Models of linearized kinetics, isotherms, and thermodynamics may experience significant error deviations due to the peculiar error distribution described by Lima et al. (2019). In nonlinear regression, the 95% confidence interval is frequently smaller (Moussout *et al*., 2018; Lima *et al*., 2019). Five temperature data points (30, 35, 40, 45, and 50°C) were used in the thermodynamics research to maximize the effectiveness of nonlinear regression, which performs better when more data points are used. The kinetic and Langmuir equilibrium isotherms of reactive red-120 dye were processed at various temperature points for different concentrations (10, 20, 30, 40, 50, 100, and 150 mg/L). According to the kinetic determination, a pseudo-second-order kinetic reaction (PSO) was used. In order to compute the Langmuir constant, K_L, the Langmuir isotherm model was plotted using the q_e constants from the PSO model. The Langmuir constant, K_L, is a dimensionless thermodynamic equilibrium constant that needs to be transformed (to form dimensionless, K_C) in order to be used in standard thermodynamic calculations (Zhou & Zhou, 2014; Tran *et al*., 2016; Lima *et al*., 2019; Tran, 2022). The region containing the actual information for adsorption equilibrium may be the Langmuir isotherms zone, which is distinguished by saturation at high concentrations. In order to estimate thermodynamic parameters, the Langmuir constant (K_L) is used in place of the thermodynamic equilibrium constant (K_C).

Table 4.9: Thermodynamics parameters of *ΔG*, *ΔH* and *ΔS* determined from the plot of van't Hoff and the dimensionless Langmuir constant for Reactive red-120 dye adsorption

Temp (*K*)	K_C	*ΔG°* *(kJ/mol)*	95% CI Lower	95% CI Upper	*ΔH°* (KJ/mol)	*ΔS°*(kJ/(mol.K)
303.15	4,678,667	-38.4139	-40.18	-36.65		
308.15	5,718,370	-39.6608	-40.86	-38.46		
313.15	8,094,836	-41.2799	-42.05	-40.51	52.91	301.30
318.15	10,916,889	-42.7485	-43.41	-42.09		
323.15	15,595,556	-44.4169	-44.83	-44.01		

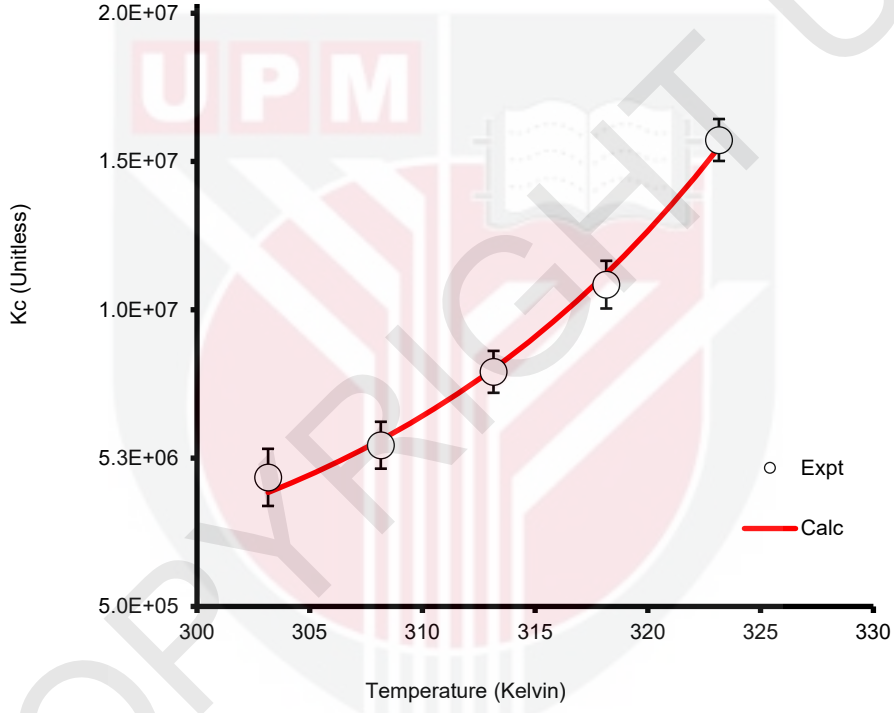

Figure 4.13: The non-linear van't Hoff plot of dimensionless constant, K_C against temperature, K of RR-120 dye adsorption process. Error bars are mean +/- standard error (n=3)

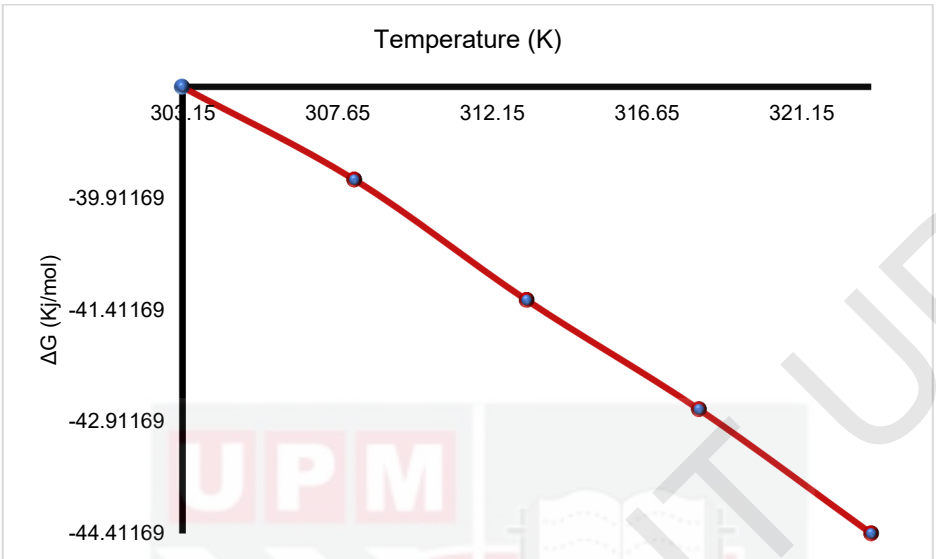

Figure 4.14: Plot of Gibb's free energy change (*ΔG*°) versus temperature of RR-120 dye adsorption process indicating the spontaneous reaction process

The determining performance of the thermodynamic parameters throughout the entire adsorption process for reactive red-120 dye is summarized in **Table 4.9.** The van't Hoff plot in **Figure 4.14** with a negative - *ΔG*° value (Tran *et al*., 2016), demonstrates that the dye adsorption onto bacterial biomass biosorbent occurred spontaneously without or with little demand for energy and heat. Since chemisorption corresponds to adsorption with a – *ΔG* °of -400 to -80 KJ/mol, the adsorption took place through chemisorption.

The entropy change (ΔS°) and enthalpy change (ΔH°), were obtained from the non-linear plot of dimensionless K_C versus temperature (**Figure 4.13**). As the solution temperature increased from 303.15 to 321.15 Kelvin, the maximum adsorption capacity of reactive red-120 dye decreased. This could either be as a result of continuous increase in the broadening sorption site on bacterial biomass which is unfavourable to the adsorbed dye molecule, or due to desorption mechanisms caused by poor adsorption contact throughout the adsorption phase (Silva *et al*., 2020). In essence, as heat is transferred out of the system, an exothermic process results in $\Delta H < 0$, and as a result, the environment experiences a positive change in entropy. On the other hand, endothermic reactions have $\Delta H > 0$. As a result, as heat is introduced into the system, the environment's entropy changes negatively (Tran *et al*., 2016; Tan & Hameed, 2017). The reactive red-120 dye adsorption was endothermic with the positive ***ΔH***° value (52.91 kJ/mol).

Numerous studies have demonstrated that raising the temperature slows the biosorption process. This is known as an exothermic (-***Δ****H*) reaction because heat in the form of energy is released into the environment during the process (Cherif *et al.*, 2021). On the other hand, endothermic reactions are those that absorb energy from the environment in the form of heat (Hamdani *et al*., 2020). The amount of energy consumed during the bond formation between the sorbate and the adsorbent between the two components during the endothermic process is less than the amount of energy released during the bond breaking (Tran *et al*., 2016). To calculate the Gibbs free energy of the biosorption process, the spontaneity of the process must be determined (Yahuza *et al*., 2020). In the presence of a specific temperature, a larger negative value (-***Δ***G) indicates a favorable spontaneous biosorption process, whereas a positive Gibbs free energy change (+***Δ***G) indicates a non-spontaneous, undesirable reaction process in the absence of a temperature. The type of reaction process, either physisorption or chemisorption, is also depicted in this manner (Srivastava *et al.*, 2015). The entropy change (*ΔS*) in the reaction solution reflects how random the sorbate (dye) is in the reaction solution. In other word, the ΔS value indicates whether a particular reaction proceeds faster or slower than another individual reaction (Subbaiah & Kim, 2016).

4.7 Bacterial Biomass Characterization using FTIR and SEM Techniques

The characterization of surface chemistry and biosorbent structure is required for the development of dye adsorption processes. Dried microbial biomass contains roughly 50% carbon, almost all of which is present as one of the numerous reduced organic cell constituents. FTIR and SEM instruments were used to investigate the physicochemical properties of bacterial biomass biosorbent (Velkova *et al*., 2018).

4.7.1 FTIR Analysis of Reactive red-120 dye Adsorption

The information provided by FTIR analysis helps identify unknown materials. It determines the infrared wavelength range that the object being studied absorbs (Asfaram *et al*., 2016). The Fourier transform, a mathematical technique that modifies a function by comparing amplitude against frequency, can be used to transform non-periodic functions. For each study, a spectrum plot was created, with the x-axis representing wave numbers and the y-axis representing compound transmittances. The intensity of IR radiation is expressed as a percentage of the radiation that can pass through in comparison to a standard (Ahmad *et al*., 2021). For example, a transmittance of 100% indicates that the sample has absorbed the same amount of radiation as the reference. When the sample had a transmittance value of 0%, the radiation was completely absorbed.

The biosorption of dyes using bacterial biomass is based on the characteristics of bacterial cell walls, which are composed of various polysaccharides, proteins,

and lipids that provide a variety of functional groups (carboxylic, hydroxyl, phosphate, amino, thio, and so on) that can interact with dyes via various chemical forces (Zaharia, 2015; Blaga *et al*., 2021). By observing changes in the functional group, FTIR analysis can validate the biosorption process by identifying the adsorption binding site (Nouri *et al*., 2021).

Unknown material information is provided and identified by Fourier Transform Infrared (FTIR) analysis. It determines the wavelength range in the infrared region absorbed by the substance under consideration (Seo *et al*., 2017). The Fourier transform, a mathematical approach that uses amplitude against frequency to change a function, can be used to transform non-periodic functions. For each study, a spectrum plot was created with the x-axis representing wavenumbers and the y-axis representing the transmittances emitted by the compound. The intensity of infrared (IR) radiation is defined as the percentage of radiation that can pass through in comparison to a standard (Alslaibi *et al*., 2013). For example, a transmittance of 100% indicates that the sample absorbed the same amount of radiation as the reference. When the sample had a transmittance of 0%, the radiation was completely absorbed. Bacterial biomass has a lot of potential as a dye adsorbent material due to its high carbon content and lignocellulosic component (Singh *et al*., 2020). The characteristics of binding sites and the attachment of dyes to the surface of proteins are determined by active functional groups such as amino, hydroxyl, sulphonate, carboxyl, and carbonyl (Ahmad *et al*., 2013; Ahmed *et al*., 2021). By observing changes in the functional group, FTIR analysis can validate the biosorption process by identifying the adsorption binding site (Wei *et al*., 2016). Low transmittance values indicate the presence of a greater number of light-absorbing bonds in the sample, whereas high transmittance values indicate the presence of fewer bonds with vibrational frequencies that correspond to the incoming light (Mona *et al*., 2011). Polysaccharides, proteins, nucleic acids, lipids, and humic compounds are the most abundant chemical constituents in bacterial biomass. They created various functional groups on the surface site, such as carboxyl, hydroxyl, and amino, that were capable of attaching the sorbate ion and molecules to the surface (Gupta & Devi, 2020).

FTIR was used to detect the presence of various functional groups on the surface of the bacterial biomass. **Figure 4.15 (a-c)** below depicts several notable peaks for the RR-120 dye in the 4000-500 cm^{-1} wavenumber region. All peaks in the vicinity of the current peak were divided into two sections: one for determining the presence of an active group (1500 cm^{-1} to 4000 cm^{-1}) and another for fingerprinting the molecule (peaks less than 1500 cm^{-1}). **Also 4.16 (d)** compares the FTIR spectrum of *Enterobacter* sp. MM05 biomass before and after treatment with 30 and 100 mg/L RR-120 dye, respectively.

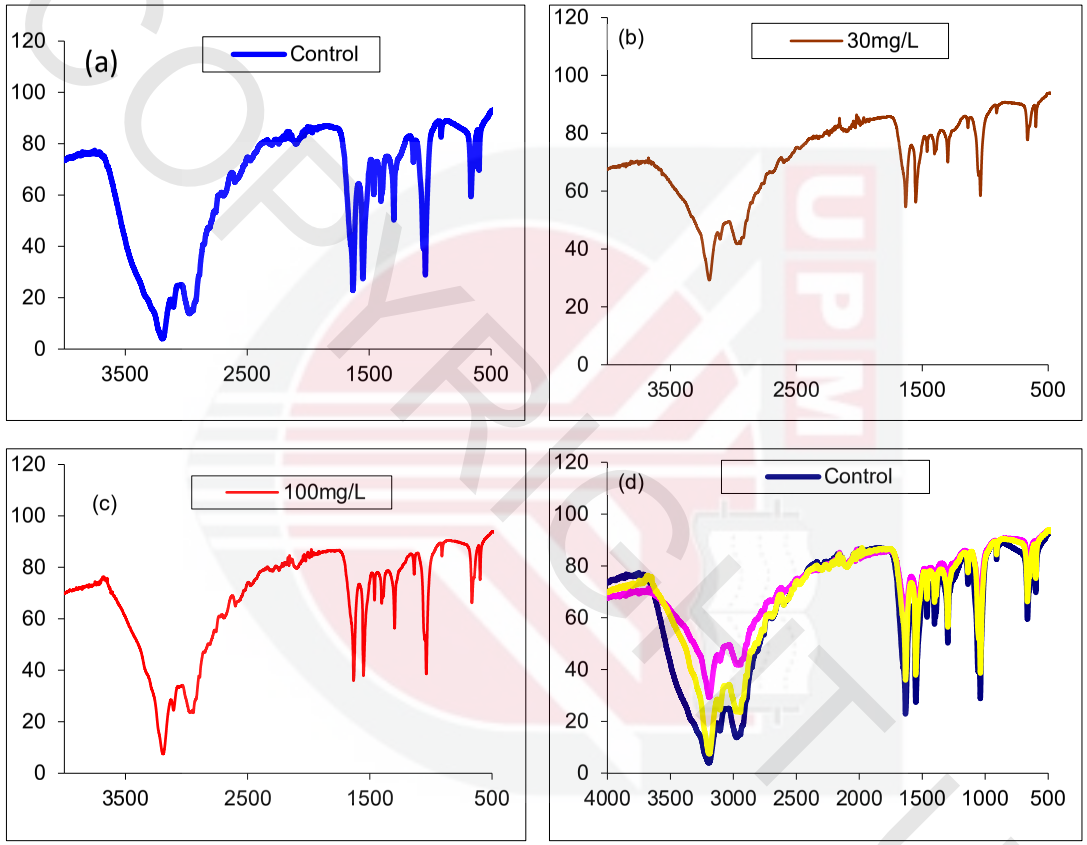

Figure 4.15: FTIR spectra of *Enterobacter* sp. MM05 biomass treated with RR-120 dye. (a) Non-treated CONTROL, (b) 30mg/L, (c) 100 mg/L, (d) superimposed spectra

Table 4.10 below contain a peak position and probable FTIR Analysis of Inter-atomic bond of isolated compounds. The FTIR analysis of raw bacterial biosorbent revealed numerous essential bands ranging from 4000 to 500 cm^{-1}. Strong and broad absorption band of hydroxyl occurred at 3191.23 cm^{-1} indicating the presence of –OH stretching depicting the presence of alcohols and phenols (hydrogen bonded), N-H stretching of amines. The FTIR Peaks obtained at 2970.07 cm^{-1} indicated the presence of C=O stretching of carboxylic acids, ketone and C=C stretching of alkenes. Peak obtained at 2104.05 cm^{-1} indicated the presence of C≡N / C≡C stretching of aldehyde/amines/nitriles (Bankole *et al*., 2017).

The peak at 1632.98 cm^{-1} showed C=O stretching of aldehyde/ketone/ester/ amides and C=O/C=C stretching of aromatic hydrocarbons, -NH stretching of amines, amides. The presence of aromatic hydrocarbon C-H/C=C bonding was indicated by the peak at 1448.5cm^{-1} (Aravind *et al*., 2016). The presence of -C-H bending /C=C stretch and -the peak indicated C-H deformation /CH(CH3) alkyl group at 1461.84 cm^{-1} (Aravind *et al*., 2016). The presence of -C-H bending /C=C stretch and -C-H deformation /CH (CH3) alkyl group was indicated by the peak at 1461.84 cm^{-1}. The presence of C-O stretching of aryl ether and phenol, as well as C-H stretching of aromatic hydrocarbons, was indicated by the peak at 1296.95 cm^{-1}. Finally, the existence of C-O stretching of aldehyde was indicated by the presence of a peak at 1038.20 cm^{-1} (Jayapal *et al*., 2018; Thanavel *et al*., 2019).

Table 4.10: Peak position and probable FTIR Analysis of Inter-atomic bond of Isolated Compounds from RR-120 Dye

IR-absorption (cm^{-1})	Functional group
3191.23	O-H Stretching vibration of alcohol and phenols
2970.7	C-H (Stretching), C=O Stretching of Carboxylic acid and ketone
2104.05	C≡N / C≡C stretching of aldehyde/amines/ nitriles.
1632.98	C=C Stretching, N-H bending of primary amines, C=O Stretching of amide
1461.84	C-N stretching of aromatic amines,C-H bending
1296.95	C-O stretching of aryl ether and phenol, and C-H stretching of aromatic hydrocarbons
1038.20	C-H stretching of aromatic hydrocarbon, C-O Stretching

4.7.2 Scanning Electron Microscopy (SEM) Analysis

Scanning Electron Microscopy (SEM) is becoming increasingly useful and essential as the size of materials decreases to accommodate more applications. Unlike a light microscope, which uses visible light, a SEM uses electrons for imaging. Using a focused beam of electrons, scanning electron microscopy (SEM) scans the surface of a sample or specimen to produce images (Amiri *et al*., 2017; Zhou *et al*., 2018; Li et al., 2020). Different signals are sent when electrons interact with the atoms in the specimen, and these signals reveal information about the surface composition and structure of the specimen. These

methods, along with numerous others, such as Atomic Force Microscopy (AFM), are used to describe dye biosorption by bacterial biomass (Zaib *et al*., 2014; Guo *et al*., 2020). The samples were washed, dried, and grounded. They were then examined with a SEM/EDX analyzer at an appropriate resolution (x5000 magnification) and micrographs were taken, as shown in Figure 4.14 below (Zhuang *et al*., 2011). An adsorption study conducted by Nguyen *et al*. (2016), employed SEM to examine the surface morphology of the bacterial biomass samples both before and after adsorption. The samples were first dried at 65°C to a stable weight before being scanned with a scanning electron microscope. The surface morphology of the biomass was discovered to be heterogeneous, non-porous, smooth, and tight based on scanning images. The images demonstrated the presence of an adhesive binding of the bacterial biomass surface and that of the dye. Similarly, our finding show that the surface morphology of the biomass of *Enterobacter* sp. strain MM05 is heterogeneous, non-porous, smooth, and tightly packed. After treatment, the images (**Figure 4.17**) revealed the presence of adhesive binding between the surface of the bacterial biomass and the dye. In a related study, adhesive interactions and the presence of phosphodiesters, carboxyl, and amino groups on the surface of Gram-negative cells were also noted (Nguyen *et al*., 2016; Tran *et al*., 2016). The micrographs also show a clear difference between the surface appearance of the untreated and treated bacterial biomass.

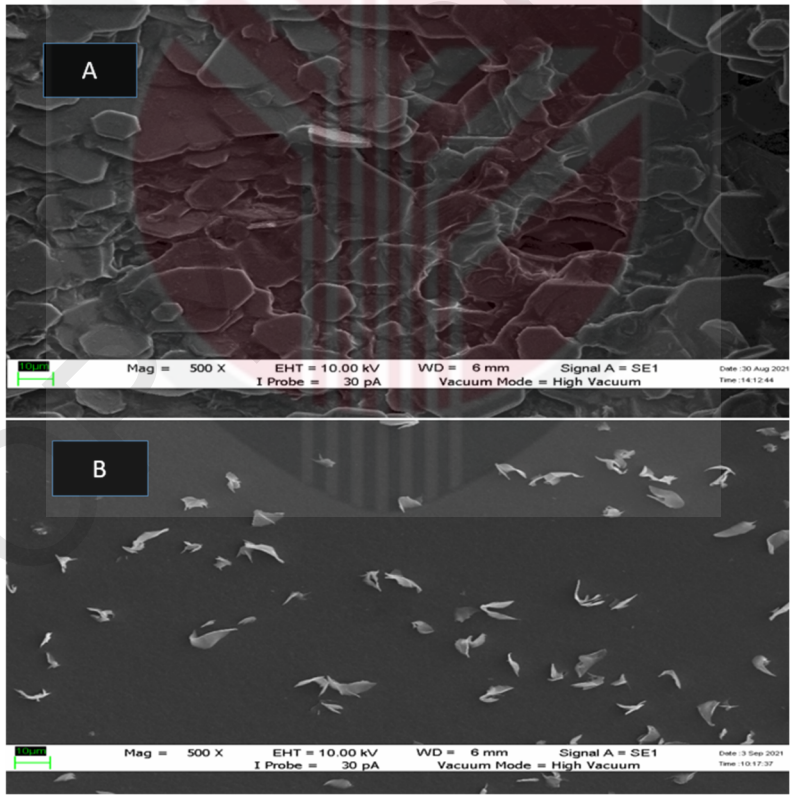

Figure 4.16: Scanning electron micrograph of *Enterobacter* sp. MM05 biomass (A) before adsorption (B) after RR-120 dye adsorption (Magnification: x5,000)

CHAPTER 5

CONCLUSION AND RECOMMENDATIONS

Twelve (12) different bacterial isolates were screened for the adsorption of Reactive red-120 dye, and it was found that *Enterobacter sp.* strain MM05 biomass had a higher percentage of dye removal (67.85%). One-Factor-at-a-Time (OFAT) and Response Surface Methodology (RSM) optimization methods were used to improve the adsorption process. These optimization methods (OFAT and RSM) improve the dye percentage removal. It was discovered that the RSM optimization provided the most optimal conditions for dye removal.

The kinetics of bacterial biomass adsorption on RR-120 dye was investigated, and the dye was discovered to follow a pseudo-second-order reaction. In addition, of all the eight (8) isotherm models employed (Henry, Langmuir, Freundlich, BET, Toth, Sips, Fritz-Schlunder IV, and Fritz-Schlunder) in the isotherm studies, it was only the Henry model that showed the poor fitting result. The Freundlich model was determined to be the best isotherm model with the lowest AICc value after statistical analysis using the corrected Akaike Information Criterion (AICc), root-mean-square error (RMSE), adjusted coefficient of determination (adjR2), accuracy factor (AF), and bias factor (BF).

The thermodynamic parameters for the adsorption of RR-120 dye were investigated at various temperatures (30, 35, 40, 45, and 50 °C), beginning with the rate constants derived using the pseudo-second-order model and progressing to the isotherm constant (K_L) determined using the Langmuir model. The dimensionless thermodynamic constant K_C was obtained by converting the constant K_L, and the van't Hoff plot's non-linear regression was used to calculate thermodynamic parameters such as standard Gibbs free energy (ΔG), enthalpy (ΔH), and entropy (ΔS). The RR-120 dye thermodynamic results revealed that it was an endothermic reaction because the enthalpy was positive, $\Delta H° = 52.91$ kJ/mol. However, the adsorption process was found to be spontaneous and feasible having the negative Gibb's free energy value for all the temperatures.

The presence of several functional groups such as hydroxyl, alkyl, and carbonyl, which are crucial for the adsorption of reactive red-120 dye, is revealed by Fourier transform infrared (FTIR) analysis. The heterogeneous, non-porous, smooth, and densely packed surfaces of the *Enterobacter sp.* strain MM05 biomass are revealed through an analysis of the SEM data. The finding has demonstrated the potentiality of *Enterobacter sp.* MM05 biomass in the adsorption of dyes such as reactive red-120 dye (an azo dye). Bacterial biomass is eco-friendly and cost-effective. Furthermore, research on the processes of dye adsorption by inactive bacterial biomass may greatly advance our knowledge of microbial biodiversity and its role in the environment.

The following recommendations are made:

1. This study was performed using a laboratory research method, and it is uncertain how effectively it would operate in the real world when implemented. For this reason, a field experiment in naturally dyed locations should be carried out to determine the bacterial strain's competence in response to environmental conditions during ex situ application.

2. To improve the efficiency of dye removal from an environment, studies on bacterial biomass consortium using the strain of *Enterobacter* sp. MM05 biomass with other biomass of bacterial strains need to be conducted.

3. A column study is required to collect data demonstrating how well the biosorbent behaves in a column setting as well as possible scale up limitations in the future. Furthermore, column desorption studies will demonstrate whether or not the biosorbent can be reused.

4. Future innovation that can further enhance the findings is the transformation of high-potential bacterial biomass into activated carbon using both the conventional method and hydrothermal conversion.

5. Future research should focus on investigating the dye multisorption because a dye effluent frequently contains a variety of pollutants such as heavy metals, salts, microplastic debris, and so on.

6. There is a need for an improvement in the adsorption capacity of bacteria through immobolization.

REFERENCES

Abdullah, M. I., Öztürk, A., & Bayol, E. (2021). Biosorption of astrazon red dye by the bacterium Rhodopseudomonas sp. strain 51ATA. *Environmental Earth Sciences*, *80*(2), 1–8. https://doi.org/10.1007/s12665-020-09314-7

Abel, A. (2012). The history of dyes and pigments. In *Colour Design* (Second Edi). Elsevier Ltd. https://doi.org/10.1016/b978-0-08-101270-3.00024-2

Ahammad, S. Z.; Gomes, J.; Sreekrishnan, T. R. (2008). Wastewater treatment forproductionofH2S-free biogas. *Journal of Chemical Technology & Biotechnology*, *83*(May), 1163–1169. https://doi.org/10.1002/jctb

Ahmad, A. A., Ahmad, M. A., Yahaya, N. K. E. M., & Karim, J. (2021). Adsorption of malachite green by activated carbon derived from gasified Hevea brasiliensis root. *Arabian Journal of Chemistry*, *14*(4), 103104. https://doi.org/10.1016/j.arabjc.2021.103104

Ahmad, F., Daud, W. M. A. W., Ahmad, M. A., & Radzi, R. (2013). The effects of acid leaching on porosity and surface functional groups of cocoa (Theobroma cacao)-shell based activated carbon. *Chemical Engineering Research and Design*, *91*(6), 1028–1038. https://doi.org/10.1016/j.cherd.2013.01.003

Ahmad, M. A., Eusoff, M. A., Oladoye, P. O., Adegoke, K. A., & Bello, O. S. (2020). Statistical optimization of Remazol Brilliant Blue R dye adsorption onto activated carbon prepared from pomegranate fruit peel. *Chemical Data Collections*, *28*, 100426. https://doi.org/10.1016/j.cdc.2020.100426

Ahmed, W., Azmat, R., Mehmood, A., Qayyum, A., Ahmed, R., Khan, S. U., Liaquat, M., Naz, S., & Ahmad, S. (2021). The analysis of new higher operative bioactive compounds and chemical functional group from herbal plants through UF-HPLC-DAD and Fourier transform infrared spectroscopy methods and their biological activity with antioxidant potential process as future gr. *Arabian Journal of Chemistry*, *14*(2), 102935. https://doi.org/10.1016/j.arabjc.2020.102935

Akaike, H. (1974). A New Look at the Statistical Model Identification. *IEEE Transactions on Automatic Control*, *19*(6), 716–723. https://doi.org/10.1109/TAC.1974.1100705

Aksu, Z. (2005). Application of biosorption for the removal of organic pollutants: A review. *Process Biochemistry*, *40*(3–4), 997–1026. https://doi.org/10.1016/j.procbio.2004.04.008

Ali, F., Ali, N., Bibi, I., Said, A., Nawaz, S., Ali, Z., Muhammad, S., Iqbal, M. N., & Bilal, M. (2020). *Case Studies in Chemical and Environmental Engineering Adsorption isotherm , kinetics and thermodynamic of acid blue and basic blue dyes onto activated charcoal*. *2*(July), 1–6. https://doi.org/10.1016/j.cscee.2020.100040

Aljeboree, A. M., Alshirifi, A. N., & Alkaim, A. F. (2017). Kinetics and equilibrium study for the adsorption of textile dyes on coconut shell activated carbon. *Arabian Journal of Chemistry*, *10*, S3381–S3393. https://doi.org/10.1016/j.arabjc.2014.01.020

Almeida, E. J. R., & Corso, C. R. (2019). Decolorization and removal of toxicity of textile azo dyes using fungal biomass pelletized. *International Journal of Environmental Science and Technology*, *16*(3), 1319–1328. https://doi.org/10.1007/s13762-018-1728-5

Alqaragully, M. B. (2014). Removal of Textile Dyes (Maxilon Blue , and Methyl Orange) by Date Stones Activated Carbon. *International Journal of Advanced Research in Chemical Science*, *1*(1), 48–59.

Alslaibi, T. M., Abustan, I., Ahmad, M. A., & Foul, A. A. (2013). Cadmium removal from aqueous solution using microwaved olive stone activated carbon. *Journal of Environmental Chemical Engineering*, *1*(3), 589–599. https://doi.org/10.1016/j.jece.2013.06.028

Ameenudeen, S., Unnikrishnan, S., & Ramalingam, K. (2021). Statistical optimization for the efficacious degradation of reactive azo dyes using Acinetobacter baumannii JC359. *Journal of Environmental Management*, *279*(October), 111512. https://doi.org/10.1016/j.jenvman.2020.111512

Amiri, M., Salavati-Niasari, M., Akbari, A., & Gholami, T. (2017). Removal of malachite green (a toxic dye) from water by cobalt ferrite silica magnetic nanocomposite: Herbal and green sol-gel autocombustion synthesis. *International Journal of Hydrogen Energy*, *42*(39), 24846–24860. https://doi.org/10.1016/j.ijhydene.2017.08.077

Antoniadis, A., Takavakoglou, V., Zalidis, G., Darakas, E., & Poulios, I. (2010). Municipal wastewater treatment by sequential combination of photocatalytic oxidation with constructed wetlands. *Catalysis Today*, *151*(1–2), 114–118. https://doi.org/10.1016/j.cattod.2010.03.058

Aplin, R., & Waite, T. D. (2000). Comparison of three advanced oxidation processes for degradation of textile dyes. *Water Science and Technology*, *42*(5–6), 345–354. https://doi.org/10.2166/wst.2000.0534

Aravind, P., Selvaraj, H., Ferro, S., & Sundaram, M. (2016). An integrated (electro- and bio-oxidation) approach for remediation of industrial wastewater containing azo-dyes: Understanding the degradation mechanism and toxicity assessment. *Journal of Hazardous Materials*, *318*, 203–215. https://doi.org/10.1016/j.jhazmat.2016.07.028

Argun, Y., Karacali, A., Calisir, U., Kilinc, N., & Irak, H. (2017). Biosorption Method and Biosorbents for Dye Removal From Industrial Wastewater: a Review. *International Journal of Advanced Research*, *5*(8), 707–714. https://doi.org/10.21474/ijar01/5110

Asfaram, A., Ghaedi, M., Ghezelbash, G. R., Dil, E. A., Tyagi, I., Agarwal, S., & Gupta, V. K. (2016). Biosorption of malachite green by novel biosorbent Yarrowia lipolytica isf7: Application of response surface methodology. *Journal of Molecular Liquids*, *214*, 249–258. https://doi.org/10.1016/j.molliq.2015.12.075

Asgher, M. (2012). Biosorption of reactive dyes: A review. *Water, Air, and Soil Pollution*, *223*(5), 2417–2435. https://doi.org/10.1007/s11270-011-1034-z

Ashrafi, S. D., Kamani, H., Soheil Arezomand, H., Yousefi, N., & Mahvi, A. H. (2016). Optimization and modeling of process variables for adsorption of Basic Blue 41 on NaOH-modified rice husk using response surface methodology. *Desalination and Water Treatment*, *57*(30), 14051–14059. https://doi.org/10.1080/19443994.2015.1060903

Atar, N., Olgun, A., & Çolak, F. (2008). Thermodynamic, equilibrium and kinetic study of the biosorption of basic blue 41 using Bacillus macerans. *Engineering in Life Sciences*, *8*(5), 499–506. https://doi.org/10.1002/elsc.200800036

Ayawei, N., Ebelegi, A. N., & Wankasi, D. (2017). Modelling and Interpretation of Adsorption Isotherms. *Journal of Chemistry*, *2017*. https://doi.org/10.1155/2017/3039817

Ayeni, A. O., Daramola, M. O., Adetayo, A. E., Sekoai, P. T., Nwinyi, O. C., & Ejekwu, O. (2020). Biological and Non-Biological Methods for Lignocellulosic Biomass Deconstruction. In *Green Energy and Technology*. https://doi.org/10.1007/978-3-030-38032-8_7

Baldikova, E., Mullerova, S., Prochazkova, J., Rouskova, M., Solcova, O., Safarik, I., & Pospiskova, K. (2019). Use of waste Japonochytrium sp. biomass after lipid extraction as an efficient adsorbent for triphenylmethane dye applied in aquaculture. *Biomass Conversion and Biorefinery*, *9*(3), 479–488. https://doi.org/10.1007/s13399-018-0362-2

Bankole, P. O., Adekunle, A. A., & Obidi, O. F. (2017). Mycodecolorization of Reactive Red HE7B dye by Achaetomium strumarium and Aspergillus flavus and shelf life determination. *Cogent Environmental Science*, *3*(1), 1–14. https://doi.org/10.1080/23311843.2017.1278646

Basirun, A. A., & Shukor, M. Y. (2021). Kinetic Analysis of the Adsorption of Cibacron Blue onto Bean Peel. *Bulletin of Environmental Science and Sustainable Management (e-ISSN 2716-5353)*, *5*(2), 14–18. https://doi.org/10.54987/bessm.v5i2.649

Bayramoglu, G., & Yilmaz, M. (2018). Azo dye removal using free and immobilized fungal biomasses: Isotherms, Kinetics and thermodynamic studies. *Fibers and Polymers*, *19*(4), 877–886. https://doi.org/10.1007/s12221-018-7875-y

Bazrafshan, E., Mostafapour, F. K., Hosseini, A. R., Raksh Khorshid, A., & Mahvi, A. H. (2013). Decolorisation of reactive red 120 dye by using single-walled carbon nanotubes in aqueous solutions. *Journal of Chemistry*, *2013*. https://doi.org/10.1155/2013/938374

Benkhaya, S., M' rabet, S., & El Harfi, A. (2020). A review on classifications, recent synthesis and applications of textile dyes. *Inorganic Chemistry Communications*, *115*(March). https://doi.org/10.1016/j.inoche.2020.107891

Benkhaya, S., Mrabet, S., & Harfi, A. El. (2020). A REVIEW ON CLASSIFICATIONS , RECENT SYNTHESIS. *INORGANIC CHEMISTRY COMMUNICATIONS*, 107891. https://doi.org/10.1016/j.inoche.2020.107891

Bhatia, D., Sharma, N. R., Singh, J., & Kanwar, R. S. (2017). Biological methods for textile dye removal from wastewater: A review. *Critical Reviews in Environmental Science and Technology*, *47*(19), 1836–1876. https://doi.org/10.1080/10643389.2017.1393263

Bilehal, D. C., Kulkarni, R. M., & Nandibewoor, S. T. (2001). Kinetics and mechanistic study of the ruthenium(III) catalyzed oxidative deamination and decarboxylation of L-valine by alkaline permanganate. *Canadian Journal of Chemistry*, *79*(12), 1926–1933. https://doi.org/10.1139/cjc-79-12-1926

Biswas, S., & Mishra, U. (2015). Effective remediation of lead ions from aqueous solution by chemically carbonized rubber wood sawdust: Equilibrium, kinetics, and thermodynamic study. *Journal of Chemistry*, *2015*. https://doi.org/10.1155/2015/842707

Blaga, A. C., Zaharia, C., & Suteu, D. (2021). Polysaccharides as support for microbial biomass-based adsorbents with applications in removal of heavy metals and dyes. *Polymers*, *13*(17). https://doi.org/10.3390/polym13172893

Blanchard, G., Maunaye, M., & Martin, G. (1984). Removal of heavy metals from waters by means of natural zeolites. *Water Research*, *18*(12), 1501–1507. https://doi.org/10.1016/0043-1354(84)90124-6

Bouras, H. D., Yeddou, A. R., Bouras, N., Hellel, D., Holtz, M. D., Sabaou, N., Chergui, A., & Nadjemi, B. (2017). Biosorption of Congo red dye by Aspergillus carbonarius M333 and Penicillium glabrum Pg1: Kinetics, equilibrium and thermodynamic studies. *Journal of the Taiwan Institute of Chemical Engineers*, *80*, 915–923. https://doi.org/10.1016/j.jtice.2017.08.002

Brunauer, S., Emmett, P. H., & Teller, E. (1938). Adsorption of Gases in Multimolecular Layers. *Journal of the American Chemical Society*, *60*(2), 309–319. https://doi.org/10.1021/ja01269a023

Canizo, B. V., Agostini, E., Wevar Oller, A. L., Dotto, G. L., Vega, I. A., & Escudero, L. B. (2019). Removal of Crystal Violet from Natural Water and Effluents Through Biosorption on Bacterial Biomass Isolated from Rhizospheric Soil. *Water, Air, and Soil Pollution*, *230*(8). https://doi.org/10.1007/s11270-019-4235-5

Çelekli, A., Al-Nuaimi, A. I., & Bozkurt, H. (2019). Adsorption kinetic and isotherms of Reactive Red 120 on Moringa oleifera seed as an eco-friendly process. *Journal of Molecular Structure*, *1195*, 168–178. https://doi.org/10.1016/j.molstruc.2019.05.106

Çelekli, A., Ilgün, G., & Bozkurt, H. (2012). Sorption equilibrium, kinetic, thermodynamic, and desorption studies of Reactive Red 120 on Chara contraria. *Chemical Engineering Journal*, *191*(May), 228–235. https://doi.org/10.1016/j.cej.2012.03.007

Chatterjee, S., Lee, M. W., & Wooa, S. H. (2010). Adsorption of congo red by chitosan hydrogel beads impregnated with carbon nanotubes. *Bioresource Technology*, *101*(6), 1800–1806. https://doi.org/10.1016/j.biortech.2009.10.051

Chaudhary, B. (2020). Chemistry of synthetic dyes: A review. *Journal of Interdisciplinary Cycle Research*, *11*(390), 390–396.

Chen, F., Ma, W., He, J., & Zhao, J. (2002). Fenton degradation of malachite green catalyzed by aromatic additives. *Journal of Physical Chemistry A*, *106*(41), 9485–9490. https://doi.org/10.1021/jp0144350

Chen, S. H., Cheow, Y. L., Ng, S. L., & Ting, A. S. Y. (2020). Removal of triphenylmethane dyes in single-dye and dye-metal mixtures by live and dead cells of metal-tolerant Penicillium simplicissimum. *Separation Science and Technology (Philadelphia)*, *55*(13), 2410–2420. https://doi.org/10.1080/01496395.2019.1626422

Chen, T., Da, T., & Ma, Y. (2021). Reasonable calculation of the thermodynamic parameters from adsorption equilibrium constant. *Journal of Molecular Liquids*, *322*, 114980. https://doi.org/10.1016/j.molliq.2020.114980

Cheng, Z., Feng, K., Su, Y., Ye, J., Chen, D., Zhang, S., Zhang, X., & Dionysiou, D. D. (2020). Novel biosorbents synthesized from fungal and bacterial biomass and their applications in the adsorption of volatile organic compounds. *Bioresource Technology*, *300*, 122705. https://doi.org/10.1016/j.biortech.2019.122705

Cherdchoo, W., Nithettham, S., & Charoenpanich, J. (2019). Removal of Cr(VI) from synthetic wastewater by adsorption onto coffee ground and mixed waste tea. *Chemosphere*, *221*, 758–767. https://doi.org/10.1016/j.chemosphere.2019.01.100

Cherfi Abdelhamid, A. M. (2014). Kinetic and Equilibrium Studies of Coomassie Blue G-250 Adsorption on Apricot Stone Activated Carbon. *Journal of Environmental & Analytical Toxicology*, *05*(02). https://doi.org/10.4172/2161-0525.1000264

Cherif, M., Rodrigues, N., Veloso, A. C. A., Zaghdoudi, K., Pereira, J. A., & Peres, A. M. (2021). Kinetic-thermodynamic study of the oxidative stability of Arbequina olive oils flavored with lemon verbena essential oil. *Lwt*, *140*, 110711. https://doi.org/10.1016/j.lwt.2020.110711

Cheruiyot, G. K., Wanyonyi, W. C., Kiplimo, J. J., & Maina, E. N. (2019). Adsorption of toxic crystal violet dye using coffee husks: Equilibrium, kinetics and thermodynamics study. *Scientific African*, *5*, 1–11. https://doi.org/10.1016/j.sciaf.2019.e00116

Chinoune, K., Bentaleb, K., Bouberka, Z., Nadim, A., & Maschke, U. (2016). Adsorption of reactive dyes from aqueous solution by dirty bentonite. *Applied Clay Science*, *123*, 64–75. https://doi.org/10.1016/j.clay.2016.01.006

Choy, K. K. H., McKay, G., & Porter, J. F. (1999). Sorption of acid dyes from effluents using activated carbon. *Resources, Conservation and Recycling*, *27*(1–2), 57–71. https://doi.org/10.1016/S0921-3449(98)00085-8

Çolak, F., Atar, N., & Olgun, A. (2009). Biosorption of acidic dyes from aqueous solution by Paenibacillus macerans: Kinetic, thermodynamic and equilibrium studies. *Chemical Engineering Journal*, *150*(1), 122–130. https://doi.org/10.1016/j.cej.2008.12.010

Cope, F. W. (1972). Generalizations of the Roginsky-Zeldovich (or Elovich) equation for charge transport across biological surfaces. *The Bulletin of Mathematical Biophysics*, *34*(3), 419–427. https://doi.org/10.1007/BF02476452

Dahbi, S., El Moussami, H., & Ezzine, L. (2016). Multiple regression model for surface roughness using full factorial design. *Proceedings of 2015 International Conference on Industrial Engineering and Systems Management, IEEE IESM 2015*, *October*, 439–444. https://doi.org/10.1109/IESM.2015.7380194

Das, A., & Mishra, S. (2017). Removal of textile dye reactive green-19 using bacterial consortium: Process optimization using response surface methodology and kinetics study. *Journal of Environmental Chemical Engineering*, *5*(1), 612–627. https://doi.org/10.1016/j.jece.2016.10.005

Das, S. K., Shome, I., & Guha, A. K. (2012). Biotechnological Potential of Soil Isolate, Flavobacterium mizutaii for Removal of Azo Dyes: Kinetics, Isotherm, and Microscopic Study. *Separation Science and Technology (Philadelphia)*, *47*(13), 1913–1925. https://doi.org/10.1080/01496395.2012.663446

Değermenci, G. D., Değermenci, N., Ayvaoğlu, V., Durmaz, E., Çakır, D., & Akan, E. (2019). Adsorption of reactive dyes on lignocellulosic waste; characterization, equilibrium, kinetic and thermodynamic studies. *Journal of Cleaner Production*, *225*, 1220–1229. https://doi.org/10.1016/j.jclepro.2019.03.260

Demirhan, E. (2020). Response surface methodology approach for adsorptive removal of Reactive Blue 19 onto green pea pod. *Water Science and Technology*, *81*(6), 1137–1147. https://doi.org/10.2166/wst.2020.199

Dönmez, G., & Aksu, Z. (2002). Removal of chromium(VI) from saline wastewaters by Dunaliella species. *Process Biochemistry*, *38*(5), 751–762. https://doi.org/10.1016/S0032-9592(02)00204-2

E., F.-K., & A.F., M.-B. (2014). Review of challenges in the escalation of metal-biosorbing processes for wastewater treatment: Applied and commercialized technologies. *African Journal of Biotechnology*, *13*(17), 1756–1771. https://doi.org/10.5897/ajb2013.13311

Ebadi, A., Soltan Mohammadzadeh, J. S., & Khudiev, A. (2009). What is the correct form of BET isotherm for modeling liquid phase adsorption? *Adsorption*, *15*(1), 65–73. https://doi.org/10.1007/s10450-009-9151-3

Ed, E. M. (2014). *Saurashtra University*. ૦૨૭૫૨(૨૫૬૫૬૧), 363002. https://doi.org/10.13140/RG.2.1.2275.3044

El Haddad, M., Slimani, R., Mamouni, R., ElAntri, S., & Lazar, S. (2013). Removal of two textile dyes from aqueous solutions onto calcined bones. *Journal of the Association of Arab Universities for Basic and Applied Sciences*, *14*(1), 51–59. https://doi.org/10.1016/j.jaubas.2013.03.002

El Maguana, Y., Elhadiri, N., Benchanaa, M., & Chikri, R. (2020). Activated Carbon for Dyes Removal: Modeling and Understanding the Adsorption Process. *Journal of Chemistry*, *2020*. https://doi.org/10.1155/2020/2096834

Elkady, M. F., Ibrahim, A. M., & El-Latif, M. M. A. (2011). Assessment of the adsorption kinetics, equilibrium and thermodynamic for the potential removal of reactive red dye using eggshell biocomposite beads. *Desalination*, *278*(1–3), 412–423. https://doi.org/10.1016/j.desal.2011.05.063

Elsherif, K. M., El-dali, A., Alkarewi, A. A., & Mabrok, A. (2021). *Crystal violet absorption maxima*. *7*(2), 79–89.

Eris, S., & Azizian, S. (2017). Analysis of adsorption kinetics at solid/solution interface using a hyperbolic tangent model. *Journal of Molecular Liquids*, *231*, 523–527. https://doi.org/10.1016/j.molliq.2017.02.052

Evans, J. R., Davids, W. G., MacRae, J. D., & Amirbahman, A. (2002). Kinetics of cadmium uptake by chitosan-based crab shells. *Water Research*, *36*(13), 3219–3226. https://doi.org/10.1016/S0043-1354(02)00044-1

Farah, J. Y., El-Gendy, N. S., & Farahat, L. A. (2007). Biosorption of Astrazone Blue basic dye from an aqueous solution using dried biomass of Baker's yeast. *Journal of Hazardous Materials*, *148*(1–2), 402–408. https://doi.org/10.1016/j.jhazmat.2007.02.053

Farooq, S., Saeed, A., Sharif, M., Hussain, J., Mabood, F., & Iftekhar, M. (2017). Process optimization studies of crystal violet dye adsorption onto novel, mixed metal Ni0.5Co0.5Fe2O4 ferrospinel nanoparticles using factorial design. *Journal of Water Process Engineering*, *16*, 132–141. https://doi.org/10.1016/j.jwpe.2017.01.001

Fathi, M. R., & Asfaram, A. (2011). Investigation of Kinetics and Equilibrium Isotherms of Direct Red 12B Dye Adsorption on Hazelnut Shells. *J. Chemical Health Risks*, *1*(2), 1–12.

Felista, M. M., Wanyonyi, W. C., & Ongera, G. (2020). Adsorption of anionic dye (Reactive black 5) using macadamia seed Husks: Kinetics and equilibrium studies. *Scientific African*, *7*, e00283. https://doi.org/10.1016/j.sciaf.2020.e00283

Ferreira, E. S. B., Hulme, A. N., McNab, H., & Quye, A. (2004). The natural constituents of historical textile dyes. *Chemical Society Reviews*, *33*(6), 329–336. https://doi.org/10.1039/b305697j

Flores-Gallegos, A. C., Contreras-Esquivel, J. C., Morlett-Chávez, J. A., Aguilar, C. N., & Rodríguez-Herrera, R. (2015). Comparative study of fungal strains for thermostable inulinase production. *Journal of Bioscience and Bioengineering*, *119*(4), 421–426. https://doi.org/10.1016/j.jbiosc.2014.09.020

Fomina, M., & Gadd, G. M. (2014). Biosorption: Current perspectives on concept, definition and application. *Bioresource Technology*, *160*, 3–14. https://doi.org/10.1016/j.biortech.2013.12.102

Foo, K. Y., & Hameed, B. H. (2010). Insights into the modeling of adsorption isotherm systems. *Chemical Engineering Journal*, *156*(1), 2–10. https://doi.org/10.1016/j.cej.2009.09.013

Froment, G. F. (1975). Model discrimination and parameter estimation in heterogeneous catalysis. *AIChE Journal*, *21*(6), 1041–1057. https://doi.org/10.1002/aic.690210602

Gadd, G. M. (2009). Biosorption: Critical review of scientific rationale, environmental importance and significance for pollution treatment. *Journal of Chemical Technology and Biotechnology*, *84*(1), 13–28. https://doi.org/10.1002/jctb.1999

Gähr, Frank; Hermanutz, Frank; Oppermann, W. (1994). f4c6dd515f3f3279bd8ccbe3ec36ee16.pdf. *Water Science and Technology*, *30*(3), 255–263.

Galindo, C., Jacques, P., & Kalt, A. (2000). Photodegradation of the aminoazobenzene acid orange 52 by three advanced oxidation processes: UV/H2O2, UV/TiO2 and VIS/TiO2. *Journal of Photochemistry and Photobiology A: Chemistry*, *130*(1), 35–47. https://doi.org/10.1016/s1010-6030(99)00199-9

Gopalakrishnan, Y., Al-Gheethi, A., Malek, M. A., Azlan, M. M., Al-Sahari, M., Radin Mohamed, R. M. S., Alkhadher, S., & Noman, E. (2020). Removal of basic brown 16 from aqueous solution using durian shell adsorbent, optimisation and techno-economic analysis. *Sustainability (Switzerland)*, *12*(21), 1–22. https://doi.org/10.3390/su12218928

Gorman, R., & Adley, C. C. (2004). Characterization of Salmonella enterica Serotype Typhimurium Isolates from Human, Food, and Animal Sources in the Republic of Ireland. *Journal of Clinical Microbiology*, *42*(5), 2314–2316. https://doi.org/10.1128/JCM.42.5.2314-2316.2004

Guo, L., Wang, J., Gou, Y., Tan, L., Liu, H., Pan, Y., & Zhao, Y. (2020). Comparative proteomics reveals stress responses of Vibrio parahaemolyticus biofilm on different surfaces: Internal adaptation and external adjustment. *Science of the Total Environment*, *731*, 138386. https://doi.org/10.1016/j.scitotenv.2020.138386

Gupta, K. K., & Devi, D. (2020). Characteristics investigation on biofilm formation and biodegradation activities of Pseudomonas aeruginosa strain ISJ14 colonizing low density polyethylene (LDPE) surface. *Heliyon*, *6*(7), e04398. https://doi.org/10.1016/j.heliyon.2020.e04398

Gurav, R., Bhatia, S. K., Choi, T. R., Choi, Y. K., Kim, H. J., Song, H. S., Lee, S. M., Lee Park, S., Lee, H. S., Koh, J., Jeon, J. M., Yoon, J. J., & Yang, Y. H. (2021). Application of macroalgal biomass derived biochar and bioelectrochemical system with Shewanella for the adsorptive removal and biodegradation of toxic azo dye. *Chemosphere*, *264*, 128539. https://doi.org/10.1016/j.chemosphere.2020.128539

Gürses, A., Açıkyıldız, M., Güneş, K., & Gürses, M. S. (2016a). *Classification of Dye and Pigments*. 31–45. https://doi.org/10.1007/978-3-319-33892-7_3

Gürses, A., Açıkyıldız, M., Güneş, K., & Gürses, M. S. (2016b). *Dyes and Pigments: Their Structure and Properties*. 13–29. https://doi.org/10.1007/978-3-319-33892-7_2

Hamdani, A., Amrane, A., Kader Yettefti, I., Mountadar, M., & Assobhei, O. (2020). Carbon and nitrogen removal from a synthetic dairy effluent in a vertical-flow fixed bed bioreactor. *Bioresource Technology Reports*, *12*(September), 100581. https://doi.org/10.1016/j.biteb.2020.100581

Hamzeh, Y., Ashori, A., Azadeh, E., & Abdulkhani, A. (2012). Removal of Acid Orange 7 and Remazol Black 5 reactive dyes from aqueous solutions using a novel biosorbent. *Materials Science and Engineering C*, *32*(6), 1394–1400. https://doi.org/10.1016/j.msec.2012.04.015

Hassan, M. M., & Carr, C. M. (2018). A critical review on recent advancements of the removal of reactive dyes from dyehouse effluent by ion-exchange adsorbents. *Chemosphere*, *209*, 201–219. https://doi.org/10.1016/j.chemosphere.2018.06.043

Hassan, M. M., & Carr, C. M. (2021). Biomass-derived porous carbonaceous materials and their composites as adsorbents for cationic and anionic dyes: A review. *Chemosphere*, *265*, 129087. https://doi.org/10.1016/j.chemosphere.2020.129087

Hassanzadeh-Tabrizi, S. A., & Taheri-Nassaj, E. (2011). Modeling and optimization of densification of nanocrystalline Al 2O3 powder prepared by a sol-gel method using response surface methodology. *Journal of Sol-Gel Science and Technology*, *57*(2), 212–220. https://doi.org/10.1007/s10971-010-2344-0

Hasyimah, N. A. R., Furusawa, G., & Amirul, A. A. (2021). Biosorption of a dye and heavy metals using dead cells of filamentous bacterium, Aureispira sp. CCB-QB1. *International Journal of Environmental Science and Technology*, *18*(6), 1627–1636. https://doi.org/10.1007/s13762-020-02918-3

Ho, Y. S., & McKay, G. (1999). The sorption of lead(II) ions on peat. *Water Research*, *33*(2), 578–584. https://doi.org/10.1016/S0043-1354(98)00207-3

Ho, Yuh Shan. (2006a). Review of second-order models for adsorption systems. *Journal of Hazardous Materials*, *136*(3), 681–689. https://doi.org/10.1016/j.jhazmat.2005.12.043

Ho, Yuh Shan. (2006b). Second-order kinetic model for the sorption of cadmium onto tree fern: A comparison of linear and non-linear methods. *Water Research*, *40*(1), 119–125. https://doi.org/10.1016/j.watres.2005.10.040

Horciu, I. L., Blaga, A. C., Rusu, L., Zaharia, C., & Suteu, D. (2020). Biosorption of reactive dyes from aqueous media using the bacillus sp. Residual biomass. *Desalination and Water Treatment*, *195*, 353–360. https://doi.org/10.5004/dwt.2020.25901

Hosono, M., Arai, H., Aizawa, M., Yamamoto, I., Shimizu, K., & Sugiyama, M. (1993). Decoloration and degradation of azo dye in aqueous solution supersaturated with oxygen by irradiation of high-energy electron beams. *Applied Radiation and Isotopes*, *44*(9), 1199–1203. https://doi.org/10.1016/0969-8043(93)90064-H

Hu, Q., Wang, Q., Feng, C., Zhang, Z., Lei, Z., & Shimizu, K. (2018). Insights into mathematical characteristics of adsorption models and physical meaning of corresponding parameters. *Journal of Molecular Liquids*, *254*(2017), 20–25. https://doi.org/10.1016/j.molliq.2018.01.073

Hu, T. L. (1996). Removal of reactive dyes from aqueous solution by different bacterial genera. *Water Science and Technology*, *34*(10 pt 6), 89–95. https://doi.org/10.1016/S0273-1223(96)00701-9

Hu, Y., Liu, F., Sun, Y., Xu, X., Chen, X., Pan, B., Sun, D., & Qian, J. (2019). Bacterial cellulose derived paper-like purifier with multifunctionality for water decontamination. *Chemical Engineering Journal*, *371*(February), 730–737. https://doi.org/10.1016/j.cej.2019.04.091

Huang, F., Dang, Z., Guo, C. L., Lu, G. N., Gu, R. R., Liu, H. J., & Zhang, H. (2013). Biosorption of Cd(II) by live and dead cells of Bacillus cereus RC-1 isolated from cadmium-contaminated soil. *Colloids and Surfaces B: Biointerfaces*, *107*, 11–18. https://doi.org/10.1016/j.colsurfb.2013.01.062

Huang, J., Liu, D., Lu, J., Wang, H., Wei, X., & Liu, J. (2016). Biosorption of reactive black 5 by modified Aspergillus versicolor biomass: Kinetics, capacity and mechanism studies. *Colloids and Surfaces A: Physicochemical and Engineering Aspects*, *492*, 242–248. https://doi.org/10.1016/j.colsurfa.2015.11.071

Huang, R., Liu, Q., Huo, J., & Yang, B. (2017). Adsorption of methyl orange onto protonated cross-linked chitosan. *Arabian Journal of Chemistry*, *10*(1), 24–32. https://doi.org/10.1016/j.arabjc.2013.05.017

Imran Din, M., Mirza, M. L., Ata, S., Athar, M., & Mohsin, I. U. (2013). Thermodynamics of biosorption for removal of Co(II) ions by an efficient and ecofriendly biosorbent (saccharum bengalense): Kinetics and isotherm modeling. *Journal of Chemistry*, *2013*. https://doi.org/10.1155/2013/528542

Iqbal, M., & Saeed, A. (2007). Biosorption of reactive dye by loofa sponge-immobilized fungal biomass of Phanerochaete chrysosporium. *Process Biochemistry*, *42*(7), 1160–1164. https://doi.org/10.1016/j.procbio.2007.05.014

Iscen, C. F., Kiran, I., & Ilhan, S. (2007). Biosorption of Reactive Black 5 dye by Penicillium restrictum: The kinetic study. *Journal of Hazardous Materials*, *143*(1–2), 335–340. https://doi.org/10.1016/j.jhazmat.2006.09.028

Ismail, G. A., & Sakai, H. (2022). Review on effect of different type of dyes on advanced oxidation processes (AOPs) for textile color removal. *Chemosphere*, *291*, 311–320. https://doi.org/10.1016/j.chemosphere.2021.132906

Izuan, M., Halmi, E., Gunasekaran, B., Razi Othman, A., & Dahalan, F. A. (2015). A rapid inhibitive enzyme assay for monitoring heavy metals pollution in the Juru Industrial Estate. *Bioremediation Science and Technology Research*, *3*(2), 7–12. http://journal.hibiscuspublisher.com/index.php/BSTR/index

Jadhav, S. B., Surwase, S. N., Phugare, S. S., & Jadhav, J. P. (2013). Response surface methodology mediated optimization of Remazol Orange decolorization in plain distilled water by Pseudomonas aeruginosa BCH. *International Journal of Environmental Science and Technology*, *10*(1), 181–190. https://doi.org/10.1007/s13762-012-0088-9

Jayapal, M., Jagadeesan, H., Shanmugam, M., Danisha J, P., & Murugesan, S. (2018). Sequential anaerobic-aerobic treatment using plant microbe integrated system for degradation of azo dyes and their aromatic amines by-products. *Journal of Hazardous Materials*, *354*(2010), 231–243. https://doi.org/10.1016/j.jhazmat.2018.04.050

Kara, M., Yuzer, H., Sabah, E., & Celik, M. S. (2003). Adsorption of cobalt from aqueous solutions onto sepiolite. *Water Research*, *37*(1), 224–232. https://doi.org/10.1016/S0043-1354(02)00265-8

Karlapudi, A. P., Krupanidhi, S., E., R. R., M., I., Md., N. B., & T.C., V. (2018). Plackett-Burman design for screening of process components and their effects on production of lactase by newly isolated Bacillus sp. VUVD101 strain from Dairy effluent. *Beni-Suef University Journal of Basic and Applied Sciences*, *7*(4), 543–546. https://doi.org/10.1016/j.bjbas.2018.06.006

Karmakar, S., Roy, D., Janiak, C., & De, S. (2019). Insights into multi-component adsorption of reactive dyes on MIL-101-Cr metal organic framework: Experimental and modeling approach. *Separation and Purification Technology*, *215*(January), 259–275. https://doi.org/10.1016/j.seppur.2019.01.013

Karthik, V., Saravanan, K., Bharathi, P., Dharanya, V., & Meiaraj, C. (2014). An overview of treatments for the removal of textile dyes. *Journal of Chemical and Pharmaceutical Sciences*, *7*(4), 301–307.

Karthik, V., Saravanan, K., Sivarajasekar, N., & Suriyanarayanan, N. (2016a). Article-72 Bioremediation of dye bearing effluents using microbial biomass. *Copyright@ EM International*, 22.

Karthik, V., Saravanan, K., Sivarajasekar, N., & Suriyanarayanan, N. (2016b). Bioremediation of dye bearing effluents using microbial biomass. *Ecol. Environ. Conserv*, *22*, S423–S434.

Karthik, V., Sivarajasekar, N., Padmanaban, V. C., Nakkeeran, E., & Selvaraju, N. (2019). Biosorption of xenobiotic Reactive Black B onto metabolically inactive T. harzianum biomass: optimization and equilibrium studies. *International Journal of Environmental Science and Technology*, *16*(7), 3625–3636. https://doi.org/10.1007/s13762-018-1841-5

Khataee, A. R., Vatanpour, V., & Amani Ghadim, A. R. (2009). Decolorization of C.I. Acid Blue 9 solution by UV/Nano-TiO2, Fenton, Fenton-like, electro-Fenton and electrocoagulation processes: A comparative study. *Journal of Hazardous Materials*, *161*(2–3), 1225–1233. https://doi.org/10.1016/j.jhazmat.2008.04.075

Kim, S., Won, S. W., Cho, C. W., & Yun, Y. S. (2016). Valorization of Escherichia coli waste biomass as a biosorbent for removing reactive dyes from aqueous solutions. *Desalination and Water Treatment*, *57*(42), 20084–20090. https://doi.org/10.1080/19443994.2015.1108235

Kiran, I., Akar, T., Ozcan, A. S., Ozcan, A., & Tunali, S. (2006). Biosorption kinetics and isotherm studies of Acid Red 57 by dried Cephalosporium aphidicola cells from aqueous solutions. *Biochemical Engineering Journal*, *31*(3), 197–203. https://doi.org/10.1016/j.bej.2006.07.008

Konicki, W., Aleksandrzak, M., Moszyński, D., & Mijowska, E. (2017). Adsorption of anionic azo-dyes from aqueous solutions onto graphene oxide: Equilibrium, kinetic and thermodynamic studies. *Journal of Colloid and Interface Science*, *496*, 188–200. https://doi.org/10.1016/j.jcis.2017.02.031

Korner-Nievergelt, F., Roth, T., von Felten, S., Guélat, J., Almasi, B., & Korner-Nievergelt, P. (2015). Model Selection and Multimodel Inference. In *Bayesian Data Analysis in Ecology Using Linear Models with R, BUGS, and STAN* (pp. 175–196). https://doi.org/10.1016/b978-0-12-801370-0.00011-3

Kousha, M., Tavakoli, S., Daneshvar, E., Vazirzadeh, A., & Bhatnagar, A. (2015). Central composite design optimization of Acid Blue 25 dye biosorption using shrimp shell biomass. *Journal of Molecular Liquids*, *207*, 266–273. https://doi.org/10.1016/j.molliq.2015.03.046

Krei, G. A., & Hustedt, H. (1992). Extraction of enzymes by reverse micelles. *Chemical Engineering Science*, *47*(1), 99–111. https://doi.org/10.1016/0009-2509(92)80204-P

Kuipa, P. K., & Kuipa, O. (2015). Removal of Pyrethrin from Aqueous Effluents by Adsorptive Micellar Flocculation. *Journal of Chemistry*, *2015*. https://doi.org/10.1155/2015/735631

Kumar, K. V., Porkodi, K., & Rocha, F. (2008). Isotherms and thermodynamics by linear and non-linear regression analysis for the sorption of methylene blue onto activated carbon: Comparison of various error functions. *Journal of Hazardous Materials*, *151*(2–3), 794–804. https://doi.org/10.1016/j.jhazmat.2007.06.056

Kumar, P., Bhati, H., Rani, A., & Singh, R. (2015). Role of Biosorption of Dyes and Microorganisms in Environment. *Life Sciences*, *4*(2), 38–41. https://doi.org/10.13140/RG.2.2.15083.44326

Kumar, U., & Bandyopadhyay, M. (2006). Fixed bed column study for Cd(II) removal from wastewater using treated rice husk. *Journal of Hazardous Materials*, *129*(1–3), 253–259. https://doi.org/10.1016/j.jhazmat.2005.08.038

Largitte, L., & Pasquier, R. (2016). A review of the kinetics adsorption models and their application to the adsorption of lead by an activated carbon. *Chemical Engineering Research and Design*, *109*, 495–504. https://doi.org/10.1016/j.cherd.2016.02.006

Law, X. N., Cheah, W. Y., Chew, K. W., Ibrahim, M. F., Park, Y. K., Ho, S. H., & Show, P. L. (2022). Microalgal-based biochar in wastewater remediation: Its synthesis, characterization and applications. *Environmental Research*, *204*(PA), 111966. https://doi.org/10.1016/j.envres.2021.111966

Lee, J. J. (2015). Adsorption kinetics and thermodynamics of brilliant blue FCF dye onto coconut shell based activated carbon. *Korean Chemical Engineering Research*, *53*(3), 309–314. https://doi.org/10.9713/kcer.2015.53.3.309

Lellis, B., Fávaro-Polonio, C. Z., Pamphile, J. A., & Polonio, J. C. (2019). Effects of textile dyes on health and the environment and bioremediation potential of living organisms. *Biotechnology Research and Innovation*, *3*(2), 275–290. https://doi.org/10.1016/j.biori.2019.09.001

Li, Z., Sellaoui, L., Franco, D., Netto, M. S., Georgin, J., Dotto, G. L., Bajahzar, A., Belmabrouk, H., Bonilla-Petriciolet, A., & Li, Q. (2020). Adsorption of hazardous dyes on functionalized multiwalled carbon nanotubes in single and binary systems: Experimental study and physicochemical interpretation of the adsorption mechanism. *Chemical Engineering Journal*, *389*, 124467. https://doi.org/10.1016/j.cej.2020.124467

Liang, J., Xia, J., & Long, J. (2017). Biosorption of methylene blue by nonliving biomass of the brown macroalga Sargassum hemiphyllum. *Water Science and Technology*, *76*(6), 1574–1583. https://doi.org/10.2166/wst.2017.343

Lim, C. K., Aris, A., Neoh, C. H., Lam, C. Y., Abdul Majid, Z., & Ibrahim, Z. (2014). Evaluation of macrocomposite based sequencing batch biofilm reactor (MC-SBBR) for decolorization and biodegradation of azo dye Acid Orange 7. *International Biodeterioration and Biodegradation*, *87*, 9–17. https://doi.org/10.1016/j.ibiod.2013.10.022

Lim, C. K., Bay, H. H., Aris, A., Abdul Majid, Z., & Ibrahim, Z. (2013). Biosorption and biodegradation of Acid Orange 7 by Enterococcus faecalis strain ZL: Optimization by response surface methodological approach. *Environmental Science and Pollution Research*, *20*(7), 5056–5066. https://doi.org/10.1007/s11356-013-1476-5

Limbikai, S. S., Deshpande, N. A., Kulkarni, R. M., Khan, A. A. P., & Khan, A. (2016). Kinetics and adsorption studies on the removal of levofloxacin using coconut coir charcoal impregnated with Al2O3 nanoparticles. *Desalination and Water Treatment*, *57*(50), 23918–23926. https://doi.org/10.1080/19443994.2016.1138330

Lin, D., Wu, F., Hu, Y., Zhang, T., Liu, C., Hu, Q., Hu, Y., Xue, Z., Han, H., & Ko, T. H. (2020). Adsorption of Dye by Waste Black Tea Powder: Parameters, Kinetic, Equilibrium, and Thermodynamic Studies. *Journal of Chemistry*, *2020*. https://doi.org/10.1155/2020/5431046

Liu, C., Yuan, H., Yang, J., & Li, B. (2011). Effective biosorption of reactive blue 5 by pH-independent lyophilized biomass of Bacillus megaterium. *African Journal of Biotechnology*, *10*(73), 16626–16636. https://doi.org/10.5897/ajb11.1824

Liu, J., Chen, F., Li, C., Lu, L., Hu, C., Wei, Y., Raymer, P., & Huang, Q. (2019). Characterization and utilization of industrial microbial waste as novel adsorbent to remove single and mixed dyes from water. *Journal of Cleaner Production*, *208*, 552–562. https://doi.org/10.1016/j.jclepro.2018.10.136

Liu, X., Zhou, Y., Zhang, J., Luo, L., Yang, Y., Huang, H., Peng, H., Tang, L., & Mu, Y. (2018). Insight into electro-Fenton and photo-Fenton for the degradation of antibiotics: Mechanism study and research gaps. *Chemical Engineering Journal*, *347*, 379–397. https://doi.org/10.1016/j.cej.2018.04.142

Liu, Y. (2008). New insights into pseudo-second-order kinetic equation for adsorption. *Colloids and Surfaces A: Physicochemical and Engineering Aspects*, *320*(1–3), 275–278. https://doi.org/10.1016/j.colsurfa.2008.01.032

Liu, Y., & Liu, Y. J. (2008). Biosorption isotherms, kinetics and thermodynamics. *Separation and Purification Technology*, *61*(3), 229–242. https://doi.org/10.1016/j.seppur.2007.10.002

Lokesh, K. N., & R, S. K. R. (2014). Biological methods of dye removal from textile effluents - A review. *Journal of Biochemical Technology*, *3*(5), 177–180.

Long, J., Li, H., Jiang, D., Luo, D., Chen, Y., Xia, J., & Chen, D. (2017). Biosorption of strontium(II) from aqueous solutions by Bacillus cereus isolated from strontium hyperaccumulator Andropogon gayanus. *Process Safety and Environmental Protection*, *111*(li), 23–30. https://doi.org/10.1016/j.psep.2017.06.010

Lu, M. C. (2000). Oxidation of chlorophenols with hydrogen peroxide in the presence of goethite. *Chemosphere*, *40*(2), 125–130. https://doi.org/10.1016/S0045-6535(99)00213-1

Ma, J., Song, W., Chen, C., Ma, W., Zhao, J., & Tang, Y. (2005). Fenton degradation of organic compounds promoted by dyes under visible irradiation. *Environmental Science and Technology*, *39*(15), 5810–5815. https://doi.org/10.1021/es050001x

Mahmoud, M. S., Mostafa, M. K., Mohamed, S. A., Sobhy, N. A., & Nasr, M. (2017). Bioremediation of red azo dye from aqueous solutions by Aspergillus niger strain isolated from textile wastewater. *Journal of Environmental Chemical Engineering*, *5*(1), 547–554. https://doi.org/10.1016/j.jece.2016.12.030

Maier, J., Kandelbauer, A., Erlacher, A., Cavaco-Paulo, A., & Gübitz, G. M. (2004). A New Alkali-Thermostable Azoreductase from Bacillus sp. Strain SF. *Applied and Environmental Microbiology*, *70*(2), 837–844. https://doi.org/10.1128/AEM.70.2.837-844.2004

Malik, A., & Grohmann, E. (2012). Environmental protection strategies for sustainable development. *Environmental Protection Strategies for Sustainable Development*, *February 2016*, 1–605. https://doi.org/10.1007/978-94-007-1591-2

Mameri, N., Boudries, N., Addour, L., Belhocine, D., Lounici, H., Grib, H., & Pauss, A. (1999). Batch zinc biosorption by a bacterial nonliving Streptomyces rimosus biomass. *Water Research*, *33*(6), 1347–1354. https://doi.org/10.1016/S0043-1354(98)00349-2

Mane, U. V., Gurav, P. N., Deshmukh, A. M., & Govindwar, S. P. (2008). Degradation of textile dye reactive navy-blue Rx (Reactive blue?9) by an isolated Actinomycete Streptomyces krainskii SUK-5. *Malaysian Journal of Microbiology*, *4*(2), 1–5. https://doi.org/10.21161/mjm.10408

Manogaran, M., Shukor, M. Y., Yasid, N. A., Khalil, K. A., & Ahmad, S. A. (2018). Optimisation of culture composition for glyphosate degradation by Burkholderia vietnamiensis strain AQ5-12. *3 Biotech*, *8*(2). https://doi.org/10.1007/s13205-018-1123-4

Manogaran, M., Yasid, N. A., Othman, A. R., Gunasekaran, B., Halmi, M. I. E., & Shukor, M. Y. A. (2021). Biodecolourisation of reactive red 120 as a sole carbon source by a bacterial consortium—toxicity assessment and statistical optimisation. *International Journal of Environmental Research and Public Health*, *18*(5), 1–26. https://doi.org/10.3390/ijerph18052424

Manzar, M. S., Khan, G., dos Santos Lins, P. V., Zubair, M., Khan, S. U., Selvasembian, R., Meili, L., Blaisi, N. I., Nawaz, M., Abdul Aziz, H., & Kayed, T. S. (2021). RSM-CCD optimization approach for the adsorptive removal of Eriochrome Black T from aqueous system using steel slag-based adsorbent: Characterization, Isotherm, Kinetic modeling and thermodynamic analysis. *Journal of Molecular Liquids*, *339*, 116714. https://doi.org/10.1016/j.molliq.2021.116714

Manzoor, J., & Sharma, M. (2019). *Impact of Textile Dyes on Human Health and Environment*. *April*, 162–169. https://doi.org/10.4018/978-1-7998-0311-9.ch008

Marbawi, H., Saidon, M., Othman, A., Halmi, M., Gansau, J., Yasid, N., & Abd. Shukor, Y. (2019). Isothermal modelling of the adsoprtion of glyphosate onto palm oil fronds activated carbon. *Journal of Environmental Microbiology And Toxicology*, *7*(1), 21–26.

Mark J. Anderson • Patrick J. Whitcomb. (2019). *Optimizing Processes Using Response Surface Methods for Design of Experiments*.

Masomboon, N., Ratanatamskul, C., & Lu, M. C. (2011). Kinetics of 2,6-dimethylaniline oxidation by various Fenton processes. *Journal of Hazardous Materials*, *192*(1), 347–353. https://doi.org/10.1016/j.jhazmat.2011.05.034

Mawad, A. M. M., Albasri, H., & Temerk, H. A. (2021). Biosorption of malachite green by dry cells of isolated free living nitrogen fixing bacteria. *Nature Environment and Pollution Technology*, *20*(3), 1217–1223. https://doi.org/10.46488/NEPT.2021.V20I03.030

Michael F. Toney Jocelyn Richer Gary L. Borges Joseph G. Gordon Owen R. Melroy David G. Wiesler Dennis Yee & Larry B. Sorensen, J. N. H. (1994). © 19 9 1 Nature Publishing Group 그라첼꺼. *Nature*, *368*, 444–446.

Milonjić, S. K. (2007). A consideration of the correct calculation of thermodynamic parameters of adsorption. *Journal of the Serbian Chemical Society*, *72*(12), 1363–1367. https://doi.org/10.2298/JSC0712363M

Miyah, Y., Lahrichi, A., Idrissi, M., Boujraf, S., Taouda, H., & Zerrouq, F. (2017). Assessment of adsorption kinetics for removal potential of Crystal Violet dye from aqueous solutions using Moroccan pyrophyllite. *Journal of the Association of Arab Universities for Basic and Applied Sciences*, *23*, 20–28. https://doi.org/10.1016/j.jaubas.2016.06.001

Moghazy, R. M. (2019). *Activated biomass of the green microalga Chlamydomonas variabilis as an efficient biosorbent to remove methylene blue dye from aqueous solutions*. *45*(1), 20–28.

Mohammadi, N., Khani, H., Gupta, V. K., Amereh, E., & Agarwal, S. (2011). Adsorption process of methyl orange dye onto mesoporous carbon material-kinetic and thermodynamic studies. *Journal of Colloid and Interface Science*, *362*(2), 457–462. https://doi.org/10.1016/j.jcis.2011.06.067

Mohan, S. V., Bhaskar, Y. V., & Karthikeyan, J. (2004). Biological decolourisation of simulated azo dye in aqueous phase by algae Spirogyra species. *International Journal of Environment and Pollution*, *21*(3), 211–222. https://doi.org/10.1504/IJEP.2004.004190

Moldovan, A., Neag, E., Băbălău-Fuss, V., Cadar, O., Micle, V., & Roman, C. (2019). Optimized Removal of Methylene Blue from Aqueous Solution using a Commercial Natural Activated Plant-Based Carbon and Taguchi Experimental Design. *Analytical Letters*, *52*(1), 150–162. https://doi.org/10.1080/00032719.2017.1418879

Mona, S., Kaushik, A., & Kaushik, C. P. (2011). Biosorption of reactive dye by waste biomass of Nostoc linckia. *Ecological Engineering*, *37*(10), 1589–1594. https://doi.org/10.1016/j.ecoleng.2011.04.005

Monte Blanco, S. P. D., Scheufele, F. B., Módenes, A. N., Espinoza-Quiñones, F. R., Marin, P., Kroumov, A. D., & Borba, C. E. (2017). Kinetic, equilibrium and thermodynamic phenomenological modeling of reactive dye adsorption onto polymeric adsorbent. *Chemical Engineering Journal*, *307*, 466–475. https://doi.org/10.1016/j.cej.2016.08.104

Moussout, H., Ahlafi, H., Aazza, M., & Maghat, H. (2018). Critical of linear and nonlinear equations of pseudo-first order and pseudo-second order kinetic models. *Karbala International Journal of Modern Science*, *4*(2), 244–254. https://doi.org/10.1016/j.kijoms.2018.04.001

Muthukumaran, C., Sivakumar, V. M., & Thirumarimurugan, M. (2016). Adsorption isotherms and kinetic studies of crystal violet dye removal from aqueous solution using surfactant modified magnetic nanoadsorbent. *Journal of the Taiwan Institute of Chemical Engineers*, *63*, 354–362. https://doi.org/10.1016/j.jtice.2016.03.034

Muthuraman, G., Teng, T. T., Leh, C. P., & Norli, I. (2009). Extraction and recovery of methylene blue from industrial wastewater using benzoic acid as an extractant. *Journal of Hazardous Materials*, *163*(1), 363–369. https://doi.org/10.1016/j.jhazmat.2008.06.122

Nasar, A., & Mashkoor, F. (2019). Application of polyaniline-based adsorbents for dye removal from water and wastewater—a review. *Environmental Science and Pollution Research*, *26*(6), 5333–5356. https://doi.org/10.1007/s11356-018-3990-y

Naskar, A., & Majumder, R. (2017). Understanding the adsorption behaviour of acid yellow 99 on Aspergillus niger biomass. *Journal of Molecular Liquids*, *242*, 892–899. https://doi.org/10.1016/j.molliq.2017.05.155

Nath, J., Das, A., & Ray, L. (2015). Biosorption of Malachite Green from Aqueous Solution Using Resting and Immobilised Biomass of Bacillus cereus M116 (MTCC 5521). *Indian Chemical Engineer*, *57*(1), 82–100. https://doi.org/10.1080/00194506.2014.997813

Navaei, A., Yazdani, M., Alidadi, H., Dankoob, M., Bonyadi, Z., Dehghan, A., & Hosseini, A. (2019). Biosorption of reactive red 120 dye from aqueous solution using saccharomyces cerevisiae: Rsm analysis, isotherms and kinetic studies. *Desalination and Water Treatment*, *171*, 418–427. https://doi.org/10.5004/dwt.2019.24780

Neag, E., Moldovan, A., Băbălău-Fuss, V., Török, A., Cadar, O., & Roman, C. (2019). Kinetic, equilibrium and phytotoxicity studies for dyes removal by low cost natural activated plant-based carbon. *Acta Chimica Slovenica*, *66*(4), 850–858. https://doi.org/10.17344/acsi.2018.4924

Neyens, E., & Baeyens, J. (2003). A review of classic Fenton's peroxidation as an advanced oxidation technique. *Journal of Hazardous Materials*, *98*(1–3), 33–50. https://doi.org/10.1016/S0304-3894(02)00282-0

Nguyen, D. T., Tran, H. N., Juang, R. S., Dat, N. D., Tomul, F., Ivanets, A., Woo, S. H., Hosseini-Bandegharaei, A., Nguyen, V. P., & Chao, H. P. (2020). Adsorption process and mechanism of acetaminophen onto commercial activated carbon. *Journal of Environmental Chemical Engineering*, *8*(6), 104408. https://doi.org/10.1016/j.jece.2020.104408

Nguyen, T. A., Fu, C. C., & Juang, R. S. (2016). Biosorption and biodegradation of a sulfur dye in high-strength dyeing wastewater by Acidithiobacillus thiooxidans. *Journal of Environmental Management*, *182*, 265–271. https://doi.org/10.1016/j.jenvman.2016.07.083

Nigam, P., Armour, G., Banat, I. ., Singh, D., Marchant, R., McHale, A. ., & McMullan, G. (2000). Corrigendum to "Physical removal of textile dyes from effluents and solid-state fermentation of dye-adsorbed agricultural residues." *Bioresource Technology*, *74*(2), 179. https://doi.org/10.1016/s0960-8524(00)00027-4

Nouri, H., Azin, E., Kamyabi, A., & Moghimi, H. (2021). Biosorption performance and cell surface properties of a fungal-based sorbent in azo dye removal coupled with textile wastewater. *International Journal of Environmental Science and Technology*, *18*(9), 2545–2558. https://doi.org/10.1007/s13762-020-03011-5

O'Mahony, T., Guibal, E., & Tobin, J. M. (2002). Reactive dye biosorption by Rhizopus arrhizus biomass. *Enzyme and Microbial Technology*, *31*(4), 456–463. https://doi.org/10.1016/S0141-0229(02)00110-2

Olpan, D., & Güven, O. (2002). Decoloration and degradation of some textile dyes by gamma irradiation. *Radiation Physics and Chemistry*, *65*(4–5), 549–558. https://doi.org/10.1016/S0969-806X(02)00366-3

Oya, N., Keskin, S., & Sarioglu, F. (2015). *RSC Advances Removal of a reactive dye and hexavalent chromium by a reusable bacteria attached electrospun nano fi brous web †. c*, 86867–86874. https://doi.org/10.1039/C5RA15601G

Paredes-Quevedo, L. C., González-Caicedo, C., Torres-Luna, J. A., & Carriazo, J. G. (2021). Removal of a Textile Azo-Dye (Basic Red 46) in Water by Efficient Adsorption on a Natural Clay. *Water, Air, and Soil Pollution*, *232*(1). https://doi.org/10.1007/s11270-020-04968-2

Park, D., Yun, Y. S., & Park, J. M. (2010). The past, present, and future trends of biosorption. *Biotechnology and Bioprocess Engineering*, *15*(1), 86–102. https://doi.org/10.1007/s12257-009-0199-4

Patel, R., & Suresh, S. (2008). Kinetic and equilibrium studies on the biosorption of reactive black 5 dye by Aspergillus foetidus. *Bioresource Technology*, *99*(1), 51–58. https://doi.org/10.1016/j.biortech.2006.12.003

Pereira, L., & Alves, M. (2012). Dyes-environmental impact and remediation. *Environmental Protection Strategies for Sustainable Development*, 111–162. https://doi.org/10.1007/978-94-007-1591-2_4

Piasecki, W., & Rudziński, W. (2007). Application of the statistical rate theory of interfacial transport to investigate the kinetics of divalent metal ion adsorption onto the energetically heterogeneous surfaces of oxides and activated carbons. *Applied Surface Science*, *253*(13 SPEC. ISS.), 5814–5817. https://doi.org/10.1016/j.apsusc.2006.12.066

Plazinski, W., & Rudzinski, W. (2010). A novel two-resistance model for description of the adsorption kinetics onto porous particles. *Langmuir*, *26*(2), 802–808. https://doi.org/10.1021/la902211c

Plazinski, W., Rudzinski, W., & Plazinska, A. (2009). Theoretical models of sorption kinetics including a surface reaction mechanism: A review. *Advances in Colloid and Interface Science*, *152*(1–2), 2–13. https://doi.org/10.1016/j.cis.2009.07.009

Popoola, L. T. (2019). Characterization and adsorptive behaviour of snail shell-rice husk (SS-RH) calcined particles (CPs) towards cationic dye. *Heliyon*, *5*(1), e01153. https://doi.org/10.1016/j.heliyon.2019.e01153

Rani, A., & Sharma, P. K. (2021). *Biosorption : Principles , and Applications Biosorption : Principles , and Applications*. *January*. https://doi.org/10.1007/978-981-15-6463-5

Rápó, E., & Tonk, S. (2021). Factors affecting synthetic dye adsorption; desorption studies: A review of results from the last five years (2017–2021). *Molecules*, *26*(17). https://doi.org/10.3390/molecules26175419

Regti, A., Laamari, M. R., Stiriba, S. E., & El Haddad, M. (2017). Use of response factorial design for process optimization of basic dye adsorption onto activated carbon derived from Persea species. *Microchemical Journal*, *130*, 129–136. https://doi.org/10.1016/j.microc.2016.08.012

Ribas, M. C., de Franco, M. A. E., Adebayo, M. A., Lima, E. C., Parkes, G. M. B., & Feris, L. A. (2020). Adsorption of Procion Red MX-5B dye from aqueous solution using homemade peach and commercial activated carbons. *Applied Water Science*, *10*(6), 1–13. https://doi.org/10.1007/s13201-020-01237-9

Rizzi, V., Longo, A., Fini, P., Semeraro, P., Cosma, P., Franco, E., García, R., Ferrándiz, M., Núñez, E., Gabaldón, J. A., Fortea, I., Pérez, E., & Ferrándiz, M. (2014). Applicative Study (Part I): The Excellent Conditions to Remove in Batch Direct Textile Dyes (Direct Red, Direct Blue and Direct Yellow) from Aqueous Solutions by Adsorption Processes on Low-Cost Chitosan Films under Different Conditions. *Advances in Chemical Engineering and Science*, *04*(04), 454–469. https://doi.org/10.4236/aces.2014.44048

Roy, M., & Saha, R. (2021). Dyes and their removal technologies. In *Intelligent Environmental Data Monitoring for Pollution Management*. Elsevier Inc. https://doi.org/10.1016/B978-0-12-819671-7.00006-3

Roy, U., Manna, S., Sengupta, S., Das, P., Datta, S., Mukhopadhyay, A., & Bhowal, A. (2018). *Dye Removal Using Microbial Biosorbents*. 253–280. https://doi.org/10.1007/978-3-319-92162-4_8

Rudzinski, Wladyslaw, & Plazinski, W. (2007). Studies of the kinetics of solute adsorption at solid/solution interfaces: On the possibility of distinguishing between the diffusional and the surface reaction kinetic models by studying the pseudo-first-order kinetics. *Journal of Physical Chemistry C*, *111*(41), 15100–15110. https://doi.org/10.1021/jp073249c

Rudzinski, Władysław, & Plazinski, W. (2008). Kinetics of dyes adsorption at the solid-solution interfaces: A theoretical description based on the two-step kinetic model. *Environmental Science and Technology*, *42*(7), 2470–2475. https://doi.org/10.1021/es7025278

Rusu, L., Grigoraș, C.-G., Simion, A.-I., Suceveanu, E.-M., Istrate, B., & Harja, M. (2022). Biosorption Potential of Microbial and Residual Biomass of Saccharomyces pastorianus Immobilized in Calcium Alginate Matrix for Pharmaceuticals Removal from Aqueous Solutions. *Polymers*, *14*(14), 2855. https://doi.org/10.3390/polym14142855

Salar-García, M. J., de Ramón-Fernández, A., Ortiz-Martínez, V. M., Ruiz-Fernández, D., & Ieropoulos, I. (2019). Towards the optimisation of ceramic-based microbial fuel cells: A three-factor three-level response surface analysis design. *Biochemical Engineering Journal*, *144*, 119–124. https://doi.org/10.1016/j.bej.2019.01.015

Salem, I. A., El-Ghamry, H. A., & El-Ghobashy, M. A. (2014). Catalytic decolorization of Acid blue 29 dye by H2O2 and a heterogeneous catalyst. *Beni-Suef University Journal of Basic and Applied Sciences*, *3*(3), 186–192. https://doi.org/10.1016/j.bjbas.2014.10.003

Salem, M. A., Elsharkawy, R. G., & Hablas, M. F. (2016). Adsorption of brilliant green dye by polyaniline/silver nanocomposite: Kinetic, equilibrium, and thermodynamic studies. In *European Polymer Journal* (Vol. 75). Elsevier Ltd. https://doi.org/10.1016/j.eurpolymj.2015.12.027

Santhi, T., Manonmani, S., Vasantha, V. S., & Chang, Y. T. (2016). A new alternative adsorbent for the removal of cationic dyes from aqueous solution. *Arabian Journal of Chemistry*, *9*, S466–S474. https://doi.org/10.1016/j.arabjc.2011.06.004

Santos, S. C. R., & Boaventura, R. A. R. (2008). Adsorption modelling of textile dyes by sepiolite. *Applied Clay Science*, *42*(1–2), 137–145. https://doi.org/10.1016/j.clay.2008.01.002

Saravanan, A., Kumar, P. S., Govarthanan, M., George, C. S., Vaishnavi, S., Moulishwaran, B., Kumar, S. P., Jeevanantham, S., & Yaashikaa, P. R. (2021). Adsorption characteristics of magnetic nanoparticles coated mixed fungal biomass for toxic Cr(VI) ions in aquatic environment. *Chemosphere*, *267*(Vi), 129226. https://doi.org/10.1016/j.chemosphere.2020.129226

Sarim, K. M., Kukreja, K., Shah, I., & Choudhary, C. K. (2019). Biosorption of direct textile dye Congo red by Bacillus subtilis HAU-KK01. *Bioremediation Journal*, *23*(3), 185–195. https://doi.org/10.1080/10889868.2019.1641466

Sarioglu, O. F., Keskin, N. O. S., Celebioglu, A., Tekinay, T., & Uyar, T. (2017). Bacteria encapsulated electrospun nanofibrous webs for remediation of methylene blue dye in water. *Colloids and Surfaces B: Biointerfaces*, *152*, 245–251. https://doi.org/10.1016/j.colsurfb.2017.01.034

Sarkar, M., Acharya, P. K., & Bhattacharya, B. (2003). Modeling the adsorption kinetics of some priority organic pollutants in water from diffusion and activation energy parameters. *Journal of Colloid and Interface Science*, *266*(1), 28–32. https://doi.org/10.1016/S0021-9797(03)00551-4

Satheesh Babu, S., Mohandass, C., Vijayaraj, A. S., & Dhale, M. A. (2015). Detoxification and color removal of Congo red by a novel Dietzia sp. (DTS26)- A microcosm approach. *Ecotoxicology and Environmental Safety*, *114*, 52–60. https://doi.org/10.1016/j.ecoenv.2015.01.002

Seo, J., Hwang, K., Lee, S., Kim, D., & Park, S. (2017). ST AC. *Pharmaceutical Development and Technology*, *0*(0), 000. https://doi.org/10.1080/10837450.2017.1334664

Setiabudi, H. D., Jusoh, R., Suhaimi, S. F. R. M., & Masrur, S. F. (2016). Adsorption of methylene blue onto oil palm (Elaeis guineensis) leaves: Process optimization, isotherm, kinetics and thermodynamic studies. *Journal of the Taiwan Institute of Chemical Engineers*, *63*, 363–370. https://doi.org/10.1016/j.jtice.2016.03.035

Seyedi, Z. S., Zahraei, Z., & Jookar Kashi, F. (2020). Decolorization of Reactive Black 5 and Reactive Red 152 Azo Dyes by New Haloalkaliphilic Bacteria Isolated from the Textile Wastewater. *Current Microbiology*, *77*(9), 2084–2092. https://doi.org/10.1007/s00284-020-02039-7

Sharma, J., Sukriti, Anand, P., Pruthi, V., Chaddha, A. S., Bhatia, J., & Kaith, B. S. (2017). RSM-CCD optimized adsorbent for the sequestration of carcinogenic rhodamine-B: Kinetics and equilibrium studies. *Materials Chemistry and Physics*, *196*, 270–283. https://doi.org/10.1016/j.matchemphys.2017.04.042

Sharma, S. C. D., Sun, Q., Li, J., Wang, Y., Suanon, F., Yang, J., & Yu, C. P. (2016). Decolorization of azo dye methyl red by suspended and co-immobilized bacterial cells with mediators anthraquinone-2,6-disulfonate and Fe3O4 nanoparticles. *International Biodeterioration and Biodegradation*, *112*, 88–97. https://doi.org/10.1016/j.ibiod.2016.04.035

Sharma, S., & Kaur, A. (2018). Various methods for removal of dyes from industrial effluents - a review. *Indian Journal of Science and Technology*, *11*(12), 1–21. https://doi.org/10.17485/ijst/2018/v11i12/120847

Shehata, F. A., Attallah, M. F., Borai, E. H., Hilal, M. A., & Abo-Aly, M. M. (2010). Sorption reaction mechanism of some hazardous radionuclides from mixed waste by impregnated crown ether onto polymeric resin. *Applied Radiation and Isotopes*, *68*(2), 239–249. https://doi.org/10.1016/j.apradiso.2009.10.040

Shen, J., & Duvnjak, Z. (2005). Adsorption kinetics of cupric and cadmium ions on corncob particles. *Process Biochemistry*, *40*(11), 3446–3454. https://doi.org/10.1016/j.procbio.2005.02.016

Sheshdeh, R. K., Nikou, M. R. K., Badii, K., Limaee, N. Y., & Golkarnarenji, G. (2014). Equilibrium and kinetics studies for the adsorption of Basic Red 46 on nickel oxide nanoparticles-modified diatomite in aqueous solutions. *Journal of the Taiwan Institute of Chemical Engineers*, *45*(4), 1792–1802. https://doi.org/10.1016/j.jtice.2014.02.020

Shin, H., Tiwari, D., & Kim, D. J. (2020). Phosphate adsorption/desorption kinetics and P bioavailability of Mg-biochar from ground coffee waste. *Journal of Water Process Engineering*, *37*(April), 101484. https://doi.org/10.1016/j.jwpe.2020.101484

Shroff, K. A., & Vaidya, V. K. (2011). Kinetics and equilibrium studies on biosorption of nickel from aqueous solution by dead fungal biomass of Mucor hiemalis. *Chemical Engineering Journal*, *171*(3), 1234–1245. https://doi.org/10.1016/j.cej.2011.05.034

Shukor, M. S., & Shukor, M. Y. (2015). Statistical evaluation of the mathematical modelling on the molybdenum reduction kinetics of a molybdenum-reducing bacterium. *Journal of Environmental Bioremediation and Toxicology*, *2*(2), 62–66.

Shukor, M. Y. (2020). Arrhenius Plot Analysis of the Temperature Effect on the Biodegradation Rate of 2-chloro-4-nitrophenol. *Biogenesis: Jurnal Ilmiah Biologi*, *8*(2), 219. https://doi.org/10.24252/bio.v8i2.17419

Siddiqui, S. I., Fatima, B., Tara, N., Rathi, G., & Chaudhry, S. A. (2018). Recent advances in remediation of synthetic dyes from wastewaters using sustainable and low-cost adsorbents. In *The Impact and Prospects of Green Chemistry for Textile Technology*. Elsevier Ltd. https://doi.org/10.1016/B978-0-08-102491-1.00015-0

Silva, C. E. de F., Gama, B. M. V. da, Gonçalves, A. H. da S., Medeiros, J. A., & Abud, A. K. de S. (2020). Basic-dye adsorption in albedo residue: Effect of pH, contact time, temperature, dye concentration, biomass dosage, rotation and ionic strength. *Journal of King Saud University - Engineering Sciences*, *32*(6), 351–359. https://doi.org/10.1016/j.jksues.2019.04.006

Singh, K. P., Gupta, S., Singh, A. K., & Sinha, S. (2011). Optimizing adsorption of crystal violet dye from water by magnetic nanocomposite using response surface modeling approach. *Journal of Hazardous Materials*, *186*(2–3), 1462–1473. https://doi.org/10.1016/j.jhazmat.2010.12.032

Singh, P. K., & Singh, R. L. (2017). Bio-removal of Azo Dyes: A Review. *International Journal of Applied Sciences and Biotechnology*, *5*(2), 108–126. https://doi.org/10.3126/ijasbt.v5i2.16881

Singh, S., Kumar, V., Datta, S., Dhanjal, D. S., Sharma, K., Samuel, J., & Singh, J. (2020). Current advancement and future prospect of biosorbents for bioremediation. *Science of the Total Environment*, *709*, 135895. https://doi.org/10.1016/j.scitotenv.2019.135895

Sivashankar, R., Thirunavukkarasu, A., Nithya, R., Kanimozhi, J., Sathya, A. B., & Sivasubramanian, V. (2020). Sequestration of methylene blue dye from aqueous solution by magnetic biocomposite: Three level Box–Behnken experimental design optimization and kinetic studies. *Separation Science and Technology (Philadelphia)*, *55*(10), 1752–1765. https://doi.org/10.1080/01496395.2019.1607382

Slimani, R., Anouzla, A., Abrouki, Y., Ramli, Y., El Antri, S., Mamouni, R., Lazar, S., & El Haddad, M. (2011). Removal of a cationic dye -Methylene Blue- from aqueous media by the use of animal bone meal as a new low cost adsorbent. *Journal of Materials and Environmental Science*, *2*(1), 77–87.

Slokar, Y. M., & Majcen Le Marechal, A. (1998). Methods of decoloration of textile wastewaters. *Dyes and Pigments*, *37*(4), 335–356. https://doi.org/10.1016/S0143-7208(97)00075-2

Solomon, D., Kiflie, Z., & Van Hulle, S. (2020). Using Box–Behnken experimental design to optimize the degradation of Basic Blue 41 dye by Fenton reaction. *International Journal of Industrial Chemistry*, *11*(1), 43–53. https://doi.org/10.1007/s40090-020-00201-5

Srinivas, N. D., Barhate, R. S., & Raghavarao, K. S. M. S. (2002). *Aqueous two-phase extraction in combination with ultrafiltration for downstream processing of Ipomoea peroxidase*. *54*, 1–6.

Srinivasan, A., & Viraraghavan, T. (2010). Decolorization of dye wastewaters by biosorbents: A review. *Journal of Environmental Management*, *91*(10), 1915–1929. https://doi.org/10.1016/j.jenvman.2010.05.003

Srivastava, S., Agrawal, S. B., & Mondal, M. K. (2015). Biosorption isotherms and kinetics on removal of Cr(VI) using native and chemically modified Lagerstroemia speciosa bark. *Ecological Engineering*, *85*, 56–66. https://doi.org/10.1016/j.ecoleng.2015.10.011

Subbaiah, M. V., & Kim, D. S. (2016). Adsorption of methyl orange from aqueous solution by aminated pumpkin seed powder: Kinetics, isotherms, and thermodynamic studies. *Ecotoxicology and Environmental Safety*, *128*, 109–117. https://doi.org/10.1016/j.ecoenv.2016.02.016

Sudha, M., Bakiyaraj, G., Saranya, A., Sivakumar, N., & Selvakumar, G. (2018). Prospective assessment of the Enterobacter aerogenes PP002 in decolorization and degradation of azo dyes DB 71 and DG 28. *Journal of Environmental Chemical Engineering*, *6*(1), 95–109. https://doi.org/10.1016/j.jece.2017.11.050

Sulak, M. T., & Yatmaz, H. C. (2012). Removal of textile dyes from aqueous solutions with eco-friendly biosorbent. *Desalination and Water Treatment*, *37*(1–3), 169–177. https://doi.org/10.1080/19443994.2012.661269

Sylloscolus, D. (2016). *ine Onl Cop Onl*. *37*(March), 291–295.

Taher, T., Antini, R., Saputri, L. I., Dian, A. R., Said, M., & Lesbani, A. (2018). Removal of Congo red and Rhodamine B dyes from aqueous solution by raw Sarolangun bentonite: Kinetics, equilibrium and thermodynamic studies. *AIP Conference Proceedings*, *2049*. https://doi.org/10.1063/1.5082416

Tan, K. L., & Hameed, B. H. (2017a). Insight into the adsorption kinetics models for the removal of contaminants from aqueous solutions. *Journal of the Taiwan Institute of Chemical Engineers*, *74*, 25–48. https://doi.org/10.1016/j.jtice.2017.01.024

Tan, K. L., & Hameed, B. H. (2017b). Insight into the adsorption kinetics models for the removal of contaminants from aqueous solutions. *Journal of the Taiwan Institute of Chemical Engineers*, *74*, 25–48. https://doi.org/10.1016/j.jtice.2017.01.024

Teng, H., & Hsieh, C. T. (1999). Activation energy for oxygen chemisorption on carbon at low temperatures. *Industrial and Engineering Chemistry Research*, *38*(1), 292–297. https://doi.org/10.1021/ie980107j

Thanavel, M., Bankole, P. O., Kadam, S., Govindwar, S. P., & Sadasivam, S. K. (2019). Desulfonation of the textile azo dye Acid Fast Yellow MR by newly isolated Aeromonas hydrophila SK16. *Water Resources and Industry*, *22*, 100116. https://doi.org/10.1016/j.wri.2019.100116

Thao, N. T., Nga, H. T. P., Vo, N. Q., & Nguyen, H. D. K. (2017). Advanced oxidation of rhodamine B with hydrogen peroxide over Zn–Cr layered double hydroxide catalysts. *Journal of Science: Advanced Materials and Devices*, *2*(3), 317–325. https://doi.org/10.1016/j.jsamd.2017.07.005

Tosik, R. (2005). Dyes color removal by ozone and hydrogen peroxide: Some aspects and problems. *Ozone: Science and Engineering*, *27*(4), 265–271. https://doi.org/10.1080/01919510591005905

Tran, H. N. (2022). Improper Estimation of Thermodynamic Parameters in Adsorption Studies with Distribution Coefficient K D(q e/ C e) or Freundlich Constant (K F): Considerations from the Derivation of Dimensionless Thermodynamic Equilibrium Constant and Suggestions. *Adsorption Science and Technology*, *2022*. https://doi.org/10.1155/2022/5553212

Tran, H. N., You, S. J., & Chao, H. P. (2016a). Thermodynamic parameters of cadmium adsorption onto orange peel calculated from various methods: A comparison study. *Journal of Environmental Chemical Engineering*, *4*(3), 2671–2682. https://doi.org/10.1016/j.jece.2016.05.009

Tran, H. N., You, S. J., & Chao, H. P. (2016b). Thermodynamic parameters of cadmium adsorption onto orange peel calculated from various methods: A comparison study. *Journal of Environmental Chemical Engineering*, *4*(3), 2671–2682. https://doi.org/10.1016/j.jece.2016.05.009

Tran, H. N., You, S. J., & Chao, H. P. (2017). Insight into adsorption mechanism of cationic dye onto agricultural residues-derived hydrochars: Negligible role of π-π interaction. *Korean Journal of Chemical Engineering*, *34*(6), 1708–1720. https://doi.org/10.1007/s11814-017-0056-7

Tran, T. H., Le, A. H., Pham, T. H., Nguyen, D. T., Chang, S. W., Chung, W. J., & Nguyen, D. D. (2020). Adsorption isotherms and kinetic modeling of methylene blue dye onto a carbonaceous hydrochar adsorbent derived from coffee husk waste. *Science of the Total Environment*, *725*, 138325. https://doi.org/10.1016/j.scitotenv.2020.138325

Upendar, G., Dutta, S., Chakraborty, J., & Bhattacharyya, P. (2016). Removal of methylene blue dye using immobilized bacillus subtilis in batch & column reactor. *Materials Today: Proceedings*, *3*(10), 3467–3472. https://doi.org/10.1016/j.matpr.2016.10.029

Vanaja, K., & Rani, R. H. S. (2007). Design of experiments: Concept and applications of plackett burman design. *Clinical Research and Regulatory Affairs*, *24*(1), 1–23. https://doi.org/10.1080/10601330701220520

Veglio', F., & Beolchini, F. (1997). Removal of metals by biosorption: A review. *Hydrometallurgy*, *44*(3), 301–316. https://doi.org/10.1016/s0304-386x(96)00059-x

Velkova, Z., Kirova, G., Stoytcheva, M., Kostadinova, S., Todorova, K., & Gochev, V. (2018). Immobilized microbial biosorbents for heavy metals removal. *Engineering in Life Sciences*, *18*(12), 871–881. https://doi.org/10.1002/elsc.201800017

Velkova, Z. Y., Kirova, G. K., Stoytcheva, M. S., & Gochev, V. K. (2018). Biosorption of Congo Red and methylene blue by pretreated waste streptomyces fradiae biomass - Equilibrium, kinetic and thermodynamic studies. *Journal of the Serbian Chemical Society*, *83*(1), 107–120. https://doi.org/10.2298/JSC170519093V

Venkata Jagadeesh, R., & Lakshminarayanan, V. (2020). Electrochemical investigation on adsorption kinetics of long chain alkylsilanes and influence of solvents on their self-assembly and electron transfer behavior on indium tin oxide. *Journal of Applied Electrochemistry*, *50*(11), 1129–1138. https://doi.org/10.1007/s10800-020-01467-4

Venkata Mohan, S., Chandrasekhar Rao, N., & Karthikeyan, J. (2002). Adsorptive removal of direct azo dye from aqueous phase onto coal based sorbents: A kinetic and mechanistic study. *Journal of Hazardous Materials*, *90*(2), 189–204. https://doi.org/10.1016/S0304-3894(01)00348-X

Venkataraghavan, R., Thiruchelvi, R., & Sharmila, D. (2020). Statistical optimization of textile dye effluent adsorption by Gracilaria edulis using Plackett-Burman design and response surface methodology. *Heliyon*, *6*(10), e05219. https://doi.org/10.1016/j.heliyon.2020.e05219

Vijayaraghavan, K., Mao, J., & Yun, Y. S. (2008). Biosorption of methylene blue from aqueous solution using free and polysulfone-immobilized Corynebacterium glutamicum: Batch and column studies. *Bioresource Technology*, *99*(8), 2864–2871. https://doi.org/10.1016/j.biortech.2007.06.008

Vijayaraghavan, K., & Yun, Y. S. (2007). Utilization of fermentation waste (Corynebacterium glutamicum) for biosorption of Reactive Black 5 from aqueous solution. *Journal of Hazardous Materials*, *141*(1), 45–52. https://doi.org/10.1016/j.jhazmat.2006.06.081

Vincent, T., Taulemesse, J. M., Dauvergne, A., Chanut, T., Testa, F., & Guibal, E. (2014). Thallium(I) sorption using Prussian blue immobilized in alginate capsules. *Carbohydrate Polymers*, *99*, 517–526. https://doi.org/10.1016/j.carbpol.2013.08.076

Viswanathan, S., & Farooq, S. (2000). *Equilibrium, Kinetics, and Column Dynamics of Methyl Ethyl Ketone Biodegradation*. *1*, 3387–3396.

Vithanage, M., Mayakaduwa, S. S., Herath, I., Ok, Y. S., & Mohan, D. (2016). Kinetics, thermodynamics and mechanistic studies of carbofuran removal using biochars from tea waste and rice husks. *Chemosphere*, *150*, 781–789. https://doi.org/10.1016/j.chemosphere.2015.11.002

Volesky, B., & Prasetyo, I. (1994). Cadmium removal in a biosorption column. *Biotechnology and Bioengineering*, *43*(11), 1010–1015. https://doi.org/10.1002/bit.260431103

Wang, H., Zheng, X. W., Su, J. Q., Tian, Y., Xiong, X. J., & Zheng, T. L. (2009). Biological decolorization of the reactive dyes Reactive Black 5 by a novel isolated bacterial strain Enterobacter sp. EC3. *Journal of Hazardous Materials*, *171*(1–3), 654–659. https://doi.org/10.1016/j.jhazmat.2009.06.050

Warade, A. R., Gaikwad, R. W., Sapkal, R. S., & Sapkal, V. S. (2016). Study of Removal Techniques for Dyes By Adsorption : a Review. *Www.Ijariie.Com*, *2*(3), 2687–3869.

Wei, D., Li, M., Wang, X., Han, F., Li, L., Guo, J., Ai, L., Fang, L., Liu, L., Du, B., & Wei, Q. (2016). Extracellular polymeric substances for Zn (II) binding during its sorption process onto aerobic granular sludge. *Journal of Hazardous Materials*, *301*(September 2015), 407–415. https://doi.org/10.1016/j.jhazmat.2015.09.018

Yahuza, S., Sabo, I. A., Abubakar, A., Yunus, M., & Shukor, A. (2020a). *Biosorption of Lead (II) Ions by Brown Algae : A Thermodynamic Study*. *4*(2), 1–5.

Yahuza, S., Sabo, I. A., Abubakar, A., Yunus, M., & Shukor, A. (2020b). *Thermodynamic Study on the Biosorptive Removal of Lead (II) Ions from Aqueous Solutions using Acid-treated Cystoseira tricta Biomass*. *8*(2), 1–5.

Yan, G., & Viraraghavan, T. (2001). Heavy metal removal in a biosorption column by immobilized M. rouxii biomass. *Bioresource Technology*, *78*(3), 243–249. https://doi.org/10.1016/S0960-8524(01)00020-7

Yaseen, D. A., & Scholz, M. (2019). Textile dye wastewater characteristics and constituents of synthetic effluents: a critical review. In *International Journal of Environmental Science and Technology* (Vol. 16, Issue 2). Springer Berlin Heidelberg. https://doi.org/10.1007/s13762-018-2130-z

Yousef, R. I., El-Eswed, B., & Al-Muhtaseb, A. H. (2011). Adsorption characteristics of natural zeolites as solid adsorbents for phenol removal from aqueous solutions: Kinetics, mechanism, and thermodynamics studies. *Chemical Engineering Journal*, *171*(3), 1143–1149. https://doi.org/10.1016/j.cej.2011.05.012

Yuangyai, C., & Nembhard, H. B. (2014). Design of experiments: A key to innovation in nanotechnology. In *Emerging Nanotechnologies for Manufacturing* (Second Edi). Elsevier Inc. https://doi.org/10.1016/B978-0-323-28990-0.00008-7

Zabłocka-Godlewska, E., Przystaś, W., & Grabińska-Sota, E. (2018). Possibilities of Obtaining from Highly Polluted Environments: New Bacterial Strains with a Significant Decolorization Potential of Different Synthetic Dyes. *Water, Air, and Soil Pollution*, *229*(6). https://doi.org/10.1007/s11270-018-3829-7

Zaharia, C. (2015). Application of waste materials as “low cost” sorbents for industrial effluent treatment: A comparative overview. *International Journal of Materials and Product Technology*, *50*(3–4), 196–220. https://doi.org/10.1504/IJMPT.2015.068524

Zaharia, C., Rusu, L., & Ş, C. G. (2020). *BIOSORBENTS BASED ON MICROORGANISMS*. *66*(70).

Zaib, M., Saeed, A., Hussain, I., Athar, M. M., & Iqbal, M. (2014). Voltammetric detection of As(III) with Porphyridium cruentum based modified carbon paste electrode biosensor. *Biosensors and Bioelectronics*, *62*, 242–248. https://doi.org/10.1016/j.bios.2014.06.055

Zarezadeh-Mehrizi, M., & Badiei, A. (2014). Highly efficient removal of basic blue 41 with nanoporous silica. *Water Resources and Industry*, *5*, 49–57. https://doi.org/10.1016/j.wri.2014.04.002

Zhang, D. (2016). *ACCEPTED MANUSCRIPT A Coe ffi cient of Determination for Generalized Linear Models*. 1–20.

Zhang, D. H., Yang, H. M., Ou, Y. J., Xu, C., & Gu, J. C. (2017). Treatment of printing and dyeing wastewater by catalytic wet hydrogen peroxide oxidation of honeycomb cinder as carrier catalyst. *IOP Conference Series: Earth and Environmental Science*, *69*(1). https://doi.org/10.1088/1755-1315/69/1/012039

Zhou, G., Wang, K. P., Liu, H. W., Wang, L., Xiao, X. F., Dou, D. D., & Fan, Y. B. (2018). Three-dimensional polylactic acid@graphene oxide/chitosan sponge bionic filter: Highly efficient adsorption of crystal violet dye. *International Journal of Biological Macromolecules*, *113*, 792–803. https://doi.org/10.1016/j.ijbiomac.2018.02.017

Zhou, L., Pan, S., Chen, X., Zhao, Y., Zou, B., & Jin, M. (2014). Kinetics and thermodynamics studies of pentachlorophenol adsorption on covalently functionalized Fe3O4atSiO2-MWCNTs core-shell magnetic microspheres. *Chemical Engineering Journal*, *257*, 10–19. https://doi.org/10.1016/j.cej.2014.07.060

Zhou, X., & Zhou, X. (2014). the Unit Problem in the Thermodynamic Calculation of Adsorption Using the Langmuir Equation. *Chemical Engineering Communications*, *201*(11), 1459–1467. https://doi.org/10.1080/00986445.2013.818541

Zhou, Y., Yan, H., Guo, M., Zhu, J., Xiao, Q., & Zhang, L. (2013). Reactive oxygen species in vascular formation and development. *Oxidative Medicine and Cellular Longevity*, *2013*. https://doi.org/10.1155/2013/374963

Zhu, H. Y., Jiang, R., & Xiao, L. (2010). Adsorption of an anionic azo dye by chitosan/kaolin/γ-Fe2O3 composites. *Applied Clay Science*, *48*(3), 522–526. https://doi.org/10.1016/j.clay.2010.02.003

Zhuang, L., Zhou, S., Yuan, Y., Liu, T., Wu, Z., & Cheng, J. (2011). Development of Enterobacter aerogenes fuel cells: From in situ biohydrogen oxidization to direct electroactive biofilm. *Bioresource Technology*, *102*(1), 284–289. https://doi.org/10.1016/j.biortech.2010.06.038

Zur, L. S. (1898). JOURNAL OF BIOCHEMISTRY , MICROBIOLOGY Mathematical Modelling of the Growth of Yeast Candida tropicalis TL- F1 on Azo Dyes. *K Sven Vetenskapsakademiens Handl.*, *24*(4), 1–39.

APPENDIX

List of Instruments with their brands and origins

No.	Instrument	Brand /Model	Origin
1	Adjustable micropipette (10, 200 and 1000).	Eppendorf, MiniSpin Plus AG	Germany
2	Centrifuge tube (15 and 50 ml)	Eppendorf, MiniSpin Plus AG	Germany
3	Double water distiller	PLT Scientific	Malaysia
4	Drying oven	Fisher Scientific	UK
5	Oven incubator	Memmert	Germany
4	DTX 800 Microplate reader	Beckman Coulter	UK
5	Fourier transform infrared spectroscopy	Denver Instrument, AL-300	USA
9	Microcentrifuge tube	Isolab	Malaysia
10	Micropipette tips (White, yello and blue)	Isolab	Malaysia
11	Mini spin centrifuge	Fisher Scientific	UK
12	pH meter	Metler Toledo	Switzerland
13	Rotary shaker	Bio Rad, Mini-Protean® tetra cell	USA
14	Vortex mixer	Vision Scientific, KMC-1300V	Japan
15	Water deionizer	Elga, B114/B	UK
16	Waterbath	Bio Rad	USA

BIODATA OF STUDENT

Salihu Yahuza was born in Kano State, North-Western Nigeria, a lecturer at Federal University Dutse, Jigawa State, Nigeria. He held a Bachelor of Science (B.Sc.) degree in Microbiology from Bayero University Kano, Nigeria, and a Master's of Science (M.Sc.) degree in Genetics and Bioengineering from Fatih University Istanbul, Turkey. Salihu Yahuza is currently a Ph.D. student at the famous Universiti Putra Malaysia (UPM). He is happily married with a daughter and son.

LIST OF PUBLICATIONS

Salihu Yahuza and Ibrahim Alhaji Sabo (2022). Normality, Grubb's and Runs Tests for the von Bertalanffy Model Used in the Fitting of the Growth of *Bacillus cereus* strain on Malachite Green Dye, *Journal of Environmental Bioremediation and Toxicology (JEBAT)*, *Volume* 5 (1) *pp* 21-25.

Salihu Yahuza, Ibrahim Alhaji Sabo, Abdussamad Abubakar and Bilal Ibrahim Dan-Iya (2022). Mathematical Isothermal Modeling of Remazol Black B Biosorption by *Aspergillus flavus*, *Bioremediation Science and Technology Research (BSTR*), *Volume* 10 (2) pp 26-29.

Salihu Yahuza, Bilal Ibrahim Dan-Iya and Ibrahim Alhaji Sabo (2020). Modelling the Growth of *Enterobacter sp*. on Polyethylene, *Journal of Biochemistry, Microbiology and Biotechnology (JOBIMB), Volume 8 (1), pp 42-46.*

Salihu Yahuza, Ibrahim Alhaji Sabo, Bilal Ibrahim Dan-Iya, Mohd Yunus Abd. Shukor, (2020). Prediction of Cumulative Death Cases in Nigeria Due to COVID-19 Using Mathematical Models, *Bulletin of Environmental Science and Sustainable Management (BESSM), Volume 4 (1), pp 20-24.*

Salihu Yahuza, Nur Adeela Binti Yasid, Ahmad Razi Othman and Yunus Mohd. Abd. Shukor. Biosorption of Triphenylmethane (TPM) Dyes by Microbial Biomass: A Review (Draft).

Salihu Yahuza, Nur Adeela Yasid, Ahmad Razi Othman and Yunus Mohd. Abd. Shukor. Biosorption of Reactive red-120 dye by the biomass of *Enterobacter* sp. strain MM05: Kinetics and Isotherms studies (Draft).

Salihu Yahuza, Nur Adeela Yasid, Ahmad Razi Othman and Yunus Mohd. Abd. Shukor. Biosorption of Reactive red-120 dye by the biomass of *Enterobacter* sp. strain MM05: Thermodynamic study (Draft).